



SAPIENZA
UNIVERSITÀ DI ROMA

PhD Course in Molecular Medicine

XXXV cycle

Coordinator Prof. Giuseppe Giannini

The predictive role of immune profile in patients with solid tumours in treatment with immunotherapy: a network analysis of efficacy and toxicity

Candidate

**Giulia Pomati
Matricola 1679191**

Tutor and Supervisor

**Prof.ssa Giulia D'Amati
Prof.ssa Silvia Mezi**

A.A. 2021-2022

TABLE OF CONTENTS

Abstract	6
1. Introduction	8
1.1 <i>The immune system and cancer</i>	8
1.2 <i>Immunotherapy in metastatic renal cell carcinoma: state of art</i>	10
1.3 <i>Immunotherapy in Recurrent/Metastatic Head and Neck squamous cell carcinoma: state of art</i>	14
1.4 <i>Immunotherapy in metastatic non-oncogene addicted non-small cell lung cancer: state of art</i>	19
1.5 <i>Immunotherapy in advanced/metastatic uveal melanoma: state of art</i>	27
1.6 <i>Resistance mechanism to immunotherapy</i>	29
1.7 <i>Soluble immune Profile</i>	32
1.8 <i>The immunosuppressive role of IDO</i>	37
1.9 <i>Predictive Biomarker</i>	38
1.10 <i>Immune related Toxicities</i>	40
2. Study Endpoint	41
3. Methods and Materials	43
3.1 <i>Patients enrollment and samples collection</i>	43
3.2 <i>Outcomes</i>	43
3.3 <i>Toxicities</i>	44
3.4 <i>Serological evaluation of immune-related molecules</i>	44
3.5 <i>Statistical analysis</i>	44
3.6 <i>Connectivity analysis</i>	45
4. Results	46
4.1 <i>Patients</i>	46
4.2 <i>Outcomes</i>	47
4.3 <i>Toxicities</i>	48
4.4 <i>Statistical analysis of circulating molecules in responder and non-responder patients with and without toxicity</i>	49
4.5 <i>Connectivity analysis between circulating molecules in responder and non-responder patients with and without toxicity</i>	52
4.6 <i>Survival analysis: circulating molecules and connectivity map</i>	69
5. Discussion	77
6. Conclusion	82
7. References	83

INDEX OF TABLES

Table 1 Soluble immune molecules characteristics, function and possible role in autoimmunity and irAE development	33
Table 2 Baseline clinical and pathological characteristics	46
Table 3. Outcomes: best response, OS and PFS in the overall study population and in each tyoe of primary tumor	47
Table 4. Patients reporting toxicities; type and grading.	48
Table 5 Statistically significant connection in responder patiens with toxicity. The table reports all the connectivity networks for responder patients with toxicity at T0, along with the correlation values and corresponding p-values	56
Table 6 Statistically significant connections in responder patients without toxicity. The table reports all the connectivity networks for responder patients without toxicity at T0, along with the correlation values and corresponding p-values	58
Table 7 Statistically significant connection in non-responder patiens with toxicity. The table reports all the connectivity networks for responder patients at T0, along with the correlation values and corresponding p-values.	61
Table 8 Statistically significant connection in non-responder patiens without toxicity. The table reports all the connectivity networks for responder patients at T0, along with the correlation values and corresponding p-values.	64
Table 9 Molecule network connections shared among the four patient groups, connecting 13 molecules	67
Table 10. Specific connections in each subgroup.	68

INDEX OF FIGURES

Figure 1. Study endpoints.	42
Figure 2 Statistical analysis at T0. (A) Heatmap of molecules expression levels (logarithmic scale) at T0 across 53 patients grouped by therapy responder patients with toxicity (violet bars), therapy responder patients without toxicity (water blue bars), non-responder patients with toxicity (blue bars), non-responder patients without toxicity (orange bars). A z-score normalization was applying and colors represent different expression levels that increase from blue to yellow. The distribution of primary tumours in each subgroup is indicated at the bottom of the heatmap. (B) Boxplot of molecules expression level (logarithmic scale) in 7 responder patients with toxicity (violet box), 12 responder patients without toxicity (water blue box), 11 non-responder patients with toxicity (blue box), and 23 non-responder patients without toxicity (orange box) at T0. Pairwise p-values (p) were obtained by applying a Mann-Whitney test for unpaired samples, overall p-value was obtained by applying Kruskal-Wallis test. Only molecules showing an overall statistically significant difference among all groups and a pairwise statistical difference in at least one comparison are shown. Legend: * p-value \leq 0.05; ** p-value \leq 0.01; *** p-value \leq 0.001.....	50
Figure 3 Statistical analysis at T0 for immune-checkpoint molecules. Boxplot of immune-checkpoint molecules expression level (logarithmic scale) in 7 responder patients with toxicity (violet box), 12 responder patients without toxicity (water blue box), 11 non-responder patients with toxicity (blue box), and 23 non-responder patients without toxicity (orange box) at T0. Pairwise p-values (p) were obtained by applying a Mann-Whitney test for unpaired samples, overall p-value was obtained by applying Kruskal-Wallis test. Legend: * p-value \leq 0.05; ** p-value \leq 0.01; *** p-value \leq 0.001.....	51
Figure 4 Connectivity map between molecules in responder patients with toxicity (A), responder patients without toxicity (B), non-responder patients with toxicity (C), and non-responder patients without toxicity (D) at T0. Statistically significant Spearman correlations (p-value \leq 0.05) are reported. In the plot, circles are scaled and coloured according to the correlation values, increasing from red (negative correlation) to blue (positive correlation). Molecules are grouped and ordered according to the functional group reported in the legend.	53
Figure 5 Connectivity network between molecules in responder patients with toxicity (A), responder patients without toxicity (B), non-responder patients with toxicity (C), and non-responder patients without toxicity (D) at T0. In each network, nodes represent molecule and a link occurs between two nodes if the absolute value of Spearman correlation between their expression levels is statistically significant (p-value \leq 0.05) and greater than a selected threshold (i.e., the 80 th percentile of the overall distribution corresponding to 0.7). Nodes are colored according to the functional groups reported in the legend; whereas edge colour indicates positive (blue) or negative (red) correlation values.	55
Figure 6. Kaplan-Meier analysis. 53 patients were classified into four groups: first class including 7 responder patients with toxicity (cyan curve), second class including 12 responder patients with toxicity (violet curve), third class including 11 non-responder patients with toxicity (light red curve), fourth class including 23 non-responder patients without toxicity (green curve). The correlation between variable value and patient survival was examined as overall survival (OS) [panel A] and progression free survival (PFS) [panel B]. The prognosis of each group of patients was examined by Kaplan-Meier survival estimators, and the survival outcomes of the two groups were compared by log-rank tests. Log rank p-values less than or equal to 0.05 were considered as statistically significant.....	71

Figure 7 Statistical analysis at T0 for soluble molecules from groups of patients divided according to overall survival (OS) value. Boxplot of cytokines (A), chemokines (B), and soluble immune-checkpoints (C) molecules expression level (logarithmic scale) in 27 patients with a OS value greater than the median cut off (i.e., 11 months) (violet box), 26 patients with a survival value lower than the median cut off (water blue box) at T0. P-values were obtained by applying a Mann-Whitney test for unpaired samples. Legend: * p-value \leq 0.05; ** p-value \leq 0.01; *** p-value \leq 0.001.....74

Figure 8 Statistical analysis at T0 for soluble molecules from groups of patients divided according to progression-free survival (PFS) value. Boxplot of cytokines (A) and soluble immune-checkpoints (B) molecules expression level (logarithmic scale) in 34 patients with a PFS value greater than the median cutoff (i.e., 4 months) (violet box) and 19 patients with a PFS value lower than the median cutoff (water blue box) at T0. P-values were obtained by applying a Mann-Whitney test for unpaired samples. Legend: * p-value \leq 0.05; ** p-value \leq 0.01; *** p-value \leq 0.001.....74

Figure 9 Connectivity map between molecules in patients with a value of overall survival (OS) that is higher (A) and lower (B) of the selected cut-off (i.e., the median of overall survival in the entire cohort of patients) at T0. Statistically significant Spearman correlations (p-value \leq 0.05) are reported. In the plot, circles are scaled and coloured according to the correlation values, increasing from red (negative correlation) to blue (positive correlation). Molecules are grouped and ordered according to the functional group reported in the legend.75

Figure 10 Connectivity map between molecules in patients with a value of progression-free survival (PFS) that is higher (A) and lower (B) of the selected cut-off (i.e., the median of progression free survival in the entire cohort of patients) at T0. Statistically significant Spearman correlations (p-value \leq 0.05) are reported. In the plot, circles are scaled and coloured according to the correlation values, increasing from red (negative correlation) to blue (positive correlation). Molecules are grouped and ordered according to the functional group reported in the legend.76

Abstract

Background:

Despite immunotherapy has deeply changed the treatment landscape and prognosis of several cancers, only a small percentage of patients achieve long-term benefit in terms of overall survival (OS). In addition, ICIs have particular immune-related adverse events (irAEs). Soluble immune profiles, resulting from the combined evaluation of circulating checkpoints, adhesion and inflammatory molecules, rather than the evaluation of individual marker, could be considered as a portrait of the immune system fitness of each patient at the baseline, which affects the response to treatment and the development of toxicities. The aim of this study was to define an immune profile predicting outcomes to ICIs and irAE development.

Methods:

A prospective, multicenter study evaluating the immune profile of patients with advanced cancer, treated with ICIs was performed. The immune profile was studied evaluating circulating concentration of 12 cytokines, 5 chemokines, 13 soluble immune checkpoints (sIC), 3 adhesion molecules and indoleamine 2,3-dioxygenase (IDO) at the baseline (T0) through a multiplex assay. Four connectivity heat maps and networks were obtained by calculating the Spearman correlation coefficients, according to the response to immunotherapy and onset of cumulative toxicity: responder patients without toxicity, non-responder with toxicity, responder with toxicity, non-responder without toxicity. Then, connectivity heat maps were defined for OS and progression-free survival (PFS) using the median values as cut-off.

Results:

Immune profile of 53 patients with advanced solid tumours treated with ICIs was evaluated at T0. Cumulative toxicity occurred in 18 patients (34%). A subgroup of non-small cell lung cancer (NSCLC) patients with high cytokine/chemokine concentrations was identified in non-responder patients without toxicity. A statistically significant up-regulation of IL17A and all the adhesion molecules in non-responder patients with toxicity with respect to the other ones was detected. CTLA4 was significantly higher in non-responders with toxicity compared to both responders and non-responders without toxicity, as well as sCD80 compared to both non-responders without toxicity and responders with toxicity. Four connectivity maps in responder and non-responder patients with and without toxicity were defined. In patients with toxicity, we observed a clearly different connectivity patterns with a loss of connectivity of mostly of sICs and cytokines correlations. In non-responder patients with toxicity, an inversion of the correlation for some adhesion molecules was observed

(from positive or null correlation became negative). Four corresponding connectivity networks were built. Only 14 connections among the four networks were common, while connections specifically observed for each group of patients were: 26 in responder with toxicity, 38 in responder without toxicity, 80 in non-responder with toxicity, 31 in non-responder without toxicity. IL10, IL8, IL4, IL6, INFgamma, INFalpha, TNFalpha, GM-CSF, MIP-1alpha, IL13, sLAG3, sTIM3, sCD27, sCD28, sCD 137 and sPDL-2 showed a statistically significant down-regulation in patients with a longer OS. IL10, IL12p70, GM-CFS and sCD27 were statistically significant down-regulated in patients with longer PFS. No connectivity differences were instead observed when we compared the correlations maps between patients with OS and PFS above and below the respective median values.

Conclusions:

The combined evaluation of soluble molecules, rather than a single circulating factor, may be more suitable to represent the fitness of the immune system status in each patient and could allow to identify different prognostic and predictive outcome profiles. A specific connectivity model for each of the 4 clinical situation patterns, based on response to immunotherapy and irAE onset, was defined by a network analysis. Moreover, an organ-dependent immunity has also been highlighted. In patients who develop irAEs and in patients with the worst prognosis (non-responders who will develop toxicity), peculiar connectivity network of immune dysregulation was defined, which could facilitate their early and timely identification. The detection of these specific immune profiles before treatment, if confirmed in a larger patient population, could lead to the design of a personalized treatment approach fit to the peculiar characteristic of patient immune status, to improve outcomes and preventing avoidable irAEs.

Key words: soluble immune profile, immune-related toxicity, cytokine, chemokine, soluble adhesion molecules, soluble immune checkpoints, network analysis.

Introduction

1.1 The immune system and cancer

Over the years, the treatment of cancer has seen the emergence of several new therapeutic avenues overcoming many critical issues and enabling better results in terms of toxicity and efficacy.

The discovery of nitrogen mustards, folic acid antagonist drugs in the 1940s and, then, the introduction of Cisplatin in the 1970s, represented the first major revolutions in oncology followed by the introduction of molecularly targeted drugs. The real breakthrough was the understanding of the association between cancer and the immune system and the use of immune system as a weapon against the progression of malignancies [1-3].

The first to test this innovative idea was Coley at the end of the 19th century and this idea was later confirmed in 1950 by Brunet and Thomas who postulated the concept of 'cancer immunosurveillance' composed by three main, sequential steps:

- elimination, can result in the complete destruction of the tumour by the host immune system;
- equilibrium, in which tumour cells, through a selection process operated by T lymphocytes, become resistant to the control of the immune system;
- escape or evasion, in which tumor cells spread uncontrolled, giving rise to clinically detectable neoplasms [4].

The immune system is able to control the disease, especially in the early stages. However, the tumour can exert continuous antigenic stimulation, which can cause exhaustion of the immune system and promote the expression of inhibitory molecules: Cytotoxic T-Lymphocyte antigen (CTLA-4), programmed cell death protein-1 (PD-1) or its ligand, programmed death-ligand-1 (PD-L1).

These molecules expressed on cells of the immune system, together with the release of immunosuppressive molecules by the tumour, reduce the activity and proliferation of specific T-lymphocytes rendering the immune response incapable of controlling tumour growth.

The mechanisms by which tumour cells can evade the control of the immune system are manifold: reduction of antigen expression, recruitment of immunosuppressive cells (Treg) and myeloid-derived suppressor cells (MDSC), induction of T- and B-lymphocyte-mediated depletion through prolonged and ineffective stimulation, reduction of molecules of histocompatibility complex I (MHC I) required for tumour antigen recognition by lymphocytes, release of circulating factors that suppress immune activity, including adenosine, prostaglandin E2, cytokines, chemokines, soluble immune checkpoints (sICs) and the enzyme indoleamine 2,3-dioxygenase (IDO) [5, 6].

The immune system is a complex entity closely linked to the inflammatory response regulated by several circulating molecules that shape and modify the tumour microenvironment in a pro- or anti-tumour direction [7]. Since the immune system is designed to respond rapidly, specifically and comprehensively against foreign invaders and cancer cells, the cytokine/chemokine superfamily and adhesion molecules are an integral part of the signalling network between cells regulating the immune system. These interacting biological signals have remarkable capabilities, such as influencing tumor growth and development, haemopoiesis, lymphocyte recruitment, T-cell differentiation and inflammation. Improper immune responses mediated by cytokines or chemokines can cause autoimmune diseases or promote cancer progression [7].

Cytokines/chemokines are crucial in determining how an immune cell responds and acts within a specific tumour microenvironment. Tumour immune resistance mechanisms are complex and involve multiple factors, such as host-related factors (gender, age, concomitant medications, gut microbiome), genetic mutations, metabolism, inflammation, abnormal neovascularisation. The study of cytokines/chemokines and soluble adhesion molecules at baseline is a repeatable and non-invasive method to monitor the patient immune profile. Furthermore, the study of soluble factors and/or molecules of the tumour microenvironment is becoming increasingly interesting as they are involved in the dysfunctional activity of the immune system [8-13].

The ability of the entire immune network to control the growth of cancer can result in continuous molecular and phenotypic remodelling of tumour cells, which can thus survive even in a perfectly immunocompetent host.

The real breakthrough in the world of immunotherapy came when the focus was on trying to remove the inhibition induced by the cancer cells themselves, thus unlocking the anergic state of T- and B-lymphocytes. The immune checkpoint inhibitors, targeting CTLA-4 and PD-1/ PD-L1 axis, have achieved, to date, significant tumour response rates [14,15]

The first drug approved with this mechanism of action was Ipilimumab, in 2011, that blocks CTLA-4, an inhibitory control molecule that counteracts CD28 co-stimulatory signal by competitively binding to its ligands. Ipilimumab was approved, at first in monotherapy, in the treatment of metastatic melanoma [16,17]. Promising long-term results in various tumours have been made possible by the development of PD-1 inhibitors, nivolumab and pembrolizumab, and anti PD-L1 drugs such as atezolizumab and durvalumab, approved to date, in monotherapy or in combination with other agents, in several oncological diseases. Immune checkpoint inhibitors (ICIs) are a class of immunotherapeutic drugs that act by blocking the inhibitory pathways of the immune system, favouring the priming of an effective anti-cancer immune response [18,19]. Thanks to the action of

these drugs, T lymphocytes can recognise and attack tumour cells by removing the inhibitory and suppressive effect that promotes immune cell exhaustion and tumour escape [20-21].

Over the last decade, immunotherapy has revolutionised the standard treatment of many solid tumours, including non-small cell lung cancer (NSCLC), metastatic uveal melanoma (UM), recurrent/metastatic squamous cell carcinoma of the head and neck (R/M HNSCC) and renal cell carcinoma (RCC) [22-28].

1.2 Immunotherapy in metastatic renal cell carcinoma: state of art

In Italy, RCC ranks tenth in terms of frequency [29]. Twenty-five per cent of patients with renal cancer, present at diagnosis at an advanced stage, while about one third of patients undergoing excision of the primary tumour will develop distant disease recurrence during their lifetime. The choice of therapeutic strategy is complicated by many factors: 1) the number of therapeutic options available; 2) the poor comparability of the studies due to the heterogeneity of the populations. Furthermore, the lack of a validated predictive factor and homogeneity in the use of prognostic classifications.

The histological features of RCC with a prognostic value are: the histotype (clear cell 70%, papillary renal 10-15% of cases, chromophobe 5%), nucleolar grade, sarcomatoid component, tumour necrosis and renal sinus invasion [30]. The two widely used prognostic systems are the Memorial Sloan Kettering Cancer Centre (MSKCC) prognostic system and the Heng prognostic system. Both use clinical and laboratory parameters in order to stratify patients for inclusion in clinical trials and to define precise treatment indications [31].

In recent years, the treatment of metastatic RCC underwent a huge change due to the proven efficacy and market entry of new drug classes: TKIs, mTOR inhibitors and immunotherapy.

RCCs are associated with immune system dysfunction [32-35]. RCCs are rich in inflammatory infiltrates consisting of T cells, natural killer (NK) cells, dendritic cells (DC) and macrophages [36, 37]. While the function of some of these cells is still unclear, others have well-defined roles in tumour progression. Tumour-associated macrophages (TAMs) are known for their immunosuppressive action, which is associated with the secretion of inhibitory cytokines, the generation of reactive oxygen species, the development of Treg with immunosuppressive activity and the induction of angiogenesis [38, 39]. Similarly, MDSCs prevent the triggering of an effective antitumour immune response through: inhibition of effector T-cell function and induction of Treg maturation [36, 37], inhibition of DC maturation and antitumour cytotoxic T lymphocytes (CTLs). The role of the immune system in RCC is not only determined at the cellular level but also through the production of numerous inflammatory mediators (i.e. through the action of cytokines and chemokines). These

mediators contribute to angiogenesis and the survival, proliferation and progression of tumour cells [40, 41]. Therefore, modulation of immune system effectors, strategies employing immune checkpoint inhibitors and chemokine receptor antagonists have a strong rationale in the treatment of kidney tumours [42, 43].

Immunotherapy entered the therapeutic management of RCC with the CHECMATE 025 study. In the CheckMate 025 trial [44], 821 patients with metastatic renal carcinoma pre-treated with one and two lines of antiVEGFs were randomised to receive either nivolumab or everolimus. The advantage of nivolumab in overall survival (OS) was observed regardless of PDL1 expression assessed by immunohistochemistry. Nivolumab was well tolerated, with a better quality of life (QoL) and lower grade 3 and 4 toxicities compared to everolimus. In 19% and 37% Grade 3 or 4 treatment-related adverse events (AEs) occurred in nivolumab arm and everolimus arm, respectively, demonstrating a superior safety profile for nivolumab. Fatigue (34.7%) and pruritus (15.5%) were the most common treatment-related AEs of any grade with nivolumab, while fatigue (34.5%) and stomatitis (29.5%) with everolimus. Moreover, a significant increase in toxicity-free survival was observed [44, 45-47]. Based on the results of this study, nivolumab is one of the treatments of choice in patients progressing after a VEGFR inhibitor.

In April 2018, the randomised phase 3 CheckMate 214 trial [48] compared nivolumab in combination with the anti CTLA-4 ipilimumab versus sunitinib in patients with previously untreated mRCC.

A total of 1096 patients were randomised into the 2 treatment arms. After a median follow-up of 25.2 months, the OS rate at 18 months was 75% (95% CI 70-78) for the combination nivolumab plus ipilimumab, and 60% (95%CI 55-65) for sunitinib; the median OS in the immunotherapy combination arm was not achieved while it was 26 months for sunitinib (HR 0.63, $p < 0.001$). The overall response rate (ORR) was 42% vs 27% ($p < 0.001$) in the 2 arms respectively, while the complete response rate was 9% vs 1%, respectively. The median progression free survival (PFS) was 11.6 months for nivolumab plus ipilimumab and 8.4 months for sunitinib (HR 8.82 $p = 0.03$). In contrast, in the low risk class population, the sunitinib-treated group had a better performance in terms of PFS and ORR. The incidence of G3-4 AEs was 46% in the nivolumab +ipilimumab treatment arm and 63% in the sunitinib treatment arm. Discontinuation of treatment due to related AEs occurred in 22% of patients in immunotherapy arm and 12% of the patients in sunitinub arm.

At a follow up of 60 months, no deterioration of health-related QoL or new late toxic effects were observed during or after treatment with nivolumab plus ipilimumab [49].

After a median follow up of 32.4 months, the benefit of the nivolumab-ipilimumab versus sunitinib combination is maintained for both high- and intermediate-risk patients with regard to OS (median OS not reached [95% CI, 35. 6 not estimable] vs 26.6 months [22.1-33.4]; HR] 0.66[CI 95% 0.54-

0.80] , $p < 0.0001$), PFS (median 8.2 months [CI 95% 6.9-10.0] vs 8.3 months [7.0-8.8] ; HR 0.77[CI 95% 0.65-0.90], $p = 0.0014$). In January 2019, EMA authorised the use of nivolumab in combination with ipilimumab as first line therapy in patients with advanced high/intermediate risk RCC. After 4 years follow-up, OS, PFS and ORR remain higher in nivolumab-ipilimumab arm compared to sunitinib group, regardless of risk category [50]. The results reporting 5-year survival continue to favour nivolumab plus ipilimumab for both OS and PFS over sunitinib. The ORR was also higher for the combination (61% versus 23%; $P < .0001$), with more patients in complete response (23% versus 6%) and no major changes in safety and tolerability data [51].

The results of the KEYNOTE 426 trial [52], in which 861 patients with metastatic clear cell carcinoma were randomised to receive pembrolizumab and axitinib, a potent VEGFR1 receptor inhibitor, versus sunitinib as first-line treatment, were published. At a median follow-up of 12.8 months, the combination demonstrated superior OS, PFS, ORR, a 47 % reduction in the risk of death compared to sunitinib. OS at 12 and 18 months was 89.9 % vs 78.3 % and 82.3 % versus 72.1 % for the combination and sunitinib, respectively. PFS at 12 and 18 months was 59.6% and 41.1% for the combination and 46.2% and 32.9% for sunitinib, respectively. The median PFS was 15.1 months for the combination versus 11.1 months for sunitinib. The ORR was 60% for the combination (6% CR) versus 39% for sunitinib. The observed benefits were independent of PDL1 status and risk category. The toxicity of the combination does not appear to be enhanced compared to that expected for the individual drugs. High grade AEs of any cause occurred in 75.8% and in 70.6% of patients in the pembrolizumab-axitinib and sunitinib group, respectively. In the pembrolizumab-axitinib group, discontinuation of either drugs due to adverse events occurred in 30.5% of patients versus 13.9% in sunitinib group. Moreover, 4 (0.9%) patients died from treatment-related AEs in pembrolizumab-axitinib arm versus 7 patients (1.6%) in sunitinib group. Diarrhea and hypertension were the most common AE related to treatment in both groups [52]. In April 2019, the FDA approved the combination pembrolizumab and axitinib for first-line metastatic RCC. After a median follow-up of 30.6 months, pembrolizumab plus axitinib continued to show a benefit over sunitinib in both OS (median not reached v 35.7 months) and PFS (15.4 v 11.1 months) with a better ORR (60% vs 40%) [28]. After a median follow-up of 42.8 months, the median OS was 45.7 months and 40.1 months, and the median PFS was 15.7 months and 11.1 months in pembrolizumab plus axitinib and sunitinib arm, respectively [53].

The Javelin Renal 101 study [54] randomised 886 patients with clear cell carcinoma (21% low-risk, 62% intermediate-risk and 16% high-risk), 63% of whom were PDL1 positive ($\geq 1\%$), to receive the combination avelumab-axitinib versus sunitinib. At a follow-up of 13 months, the combination confirmed the benefits on PFS and ORR in the entire population regardless of risk and PDL1

expression categories. PFS was 13.8 months for the combination versus 7.2 months for sunitinib in PDL1-positive patients with a 39% reduction in the risk of disease progression or death (HR,0.61; $p < 0.0001$). AEs rates during treatment were similar in the two arms, these events were grade 3 or higher in 71.2% and 71.5% of the patients in the avelumab-axitinib and sunitinib arms, respectively. A further promising first-line therapeutic combination is atezolizumab (an anti PDL1 agent) plus bevacizumab. The results of the randomised phase III study IMmotion 151 [55], were recently published. In this study, untreated mRCC patients were randomised to receive atezolizumab plus bevacizumab or sunitinib, and were stratified according to PDL1 expression ($< 1\%$ vs $\geq 1\%$). The combination of atezolizumab + bevacizumab showed an advantage in terms of PFS 11.2 vs 7.7 months with sunitinib in PDL1 patients (HR 0.74 [95% CI; 0.57-0.96]; $p = 0.0217$). The final analysis showed a similar median OS in patients receiving atezolizumab plus bevacizumab compared to sunitinib (36.1 vs 35.3 months in the intention-to-treat populations and 38.7 vs 31.6 months in PDL1+ patients). No safety concerns were reported [56].

Some combinations have shown promising results, although not yet reimbursed. The phase 3, randomised, open-label CM9ER study compared the combination nivolumab and cabozantinib to sunitinib in patients with advanced clear cell carcinoma [57]. At a median follow-up of 18.1 months, the mPFS was 16.6 months for the combination arm and 8.3 months (HR: 0.51; LC 95%: 0.41, 0.64) for sunitinib. The OS rate at 12 months was 85.7% for the combination and 75.6% for sunitinib (HR: 0.60; LC 98.9%: 0.40, 0.89), while the ORR was 55.7% of patients receiving nivolumab plus cabozantinib and in 27.1% of those receiving sunitinib. Grade 3 or higher AEs were observed in 75.3% of patients treated with nivolumab plus cabozantinib and in 70.6% of those receiving sunitinib. Overall, 19.7% of the patients in the combination arm discontinued at least one of the drugs due to AEs. At extended follow-up, grade 3-4 treatment-related AEs occurred in 65% and 54% of patients in the nivolumab-cabozantinib and sunitinib groups, respectively. Hypertension and palmar-plantar erythrodysesthesia syndrome were the most common treatment-related grade 3-4 AEs and occurred at similar rates in both groups. Patients in nivolumab plus cabozantinib arm reported a better health-related QoL compared to sunitinib [58, 59].

The phase 3, randomised, open-label CLEAR-KN581 trial compared the combination pembrolizumab-lenvatinib to sunitinib in patients with advanced clear cell carcinoma [60]. At a median follow-up of 22.3 months, the median PFS was 23.9 months (LC95%: 20.8, 27.7) in the combination arm vs 9.2 months (LC95%: 6.0, 11.0) in the control arm with a reduction of 61% in the risk of progression compared to sunitinib. At a median follow-up of 33.7 months, the median OS is not yet estimable in both treatments under investigation, with a 28% relative reduction in the risk of death compared to sunitinib. In the combination arm there is a 15% relative increase in the risk of a

serious AE compared to sunitinib. The cumulative incidence of adverse events causing treatment discontinuation was 37.2% in the pembrolizumab-levatinib arm vs 14.4% in the sunitinib arm.

Overall, immunotherapy has proven to be safe and manageable in terms of AEs, compared to target therapy, both in monotherapy and in combination strategies. Two immunotherapeutic drugs in combination (CheckMate 214) do not lead to significant increases in the risk of serious AEs occurrence and discontinuation of therapy. Among the combinations of immunotherapy and target therapy, the pembrolizumab-levatinib study raises concerns about the risk of developing serious AEs. In contrast, the combination pembrolizumab-axitinib has been shown to be safe in clinical trials and is already currently used in clinical practice.

According to the results of the Late-Breaking Abstract of the COSMIC-313 study presented at the ESMO 2022 Congress (LBA8), the cabozantinib-nivolumab-ipilimumab (C+N+I) triplet resulted in a significant 27% reduction in the risk of progression compared to the nivolumab-ipilimumab doublet among 550 patients with untreated metastatic RCC at intermediate or poor risk with a PFS not reached in the triplet arm and 11.3 months in the doublet arm. The ORR rates were 43% and 36% with the triplet and doublet, respectively, with a higher rate of grade 3-4 treatment-related AEs (73% vs. 41%). Furthermore, treatment discontinuation for treatment-related AE was required in 12% and 5% of patients in the triplet arm and in the doublet arm, respectively [61].

Therefore, the future scenario in the treatment of RCC is destined to become even more complex due to the availability of additional and innovative strategies that will create many additional therapeutic opportunities in first-line and subsequent treatment choices. There is therefore an urgent need to define predictive factors for response or resistance that will make it possible to tailor the treatment course to the individual patient.

1.3 Immunotherapy in Recurrent/Metastatic Head and Neck squamous cell carcinoma: state of art

Head and neck squamous cell carcinoma (HNSCC) is globally the sixth most common type of cancer and is still burdened by an overall mortality ranging from 40 to 50%. ICIs, a class of drugs able to block immune suppressive pathways in order to prime an anticancer immunity, revolutionized standard of care in recurrent and/or metastatic (R/M) HNSCC both in first line and in platinum/refractory disease [26, 27, 62].

HNSCC is an immunosuppressive disease with high inflammatory component and high level of tumor-infiltrating lymphocyte (TILs) in tumor microenvironment. The PD-1/ PD-L1 axis is involved in the genesis, maintenance and progression of HNSCC and represents the target of ICIs [62]. Recent clinical trials showed that only a small subset of patients really benefits from ICIs. Therefore, the

goal is to identify possible predictive biomarker of response to immunotherapy. Although many promising biomarkers are under investigation, PD-L1 expression in tumor micro-environment has been explored in many prospective clinical trials [26, 27, 63].

KEYNOTE-012 [63], the phase I study of pembrolizumab as second line treatment of HNSCC, showed an increased response rates based on the composite positive score (CPS, the number of cells positive for PDL1 staining, divided by the total number of cells, multiplied by 100). In PDL1-positive tumors, with a CPS greater than or equal to 1, the response rate was 22% versus 4% in negative PDL1 tumors.

The phase III study KEYNOTE 048 [27] recently demonstrated a benefit in OS of pembrolizumab versus the standard first line regimen in PDL1 positive and CPS tumors > 1 and 20 . In contrast with the above results, CheckMate-141 [26] failed to demonstrate a significant association between PDL1 expression in tumor cells ($> 1\%$, $> 5\%$ or $> 10\%$), response rates and OS in platinum-refractory disease treated with nivolumab. However, in these studies, there is no homogeneity in the choice of PDL1 determination methods. Furthermore, PDL1 expression is the result of complex molecular crosstalk between different intracellular signaling pathways such as MAPK, PI3K and Aky/PKB, that play a key role in modulating and influencing the regulation of PD-L1 expression [64, 65].

The phase III KEYNOTE 048 trial [27], which evaluated pembrolizumab as first-line monotherapy or in combination with chemotherapy versus the standard first-line EXTREME regimen, recently demonstrated an OS benefit of pembrolizumab as monotherapy versus the standard first-line EXTREME regimen in PDL1-positive tumours with CPS > 1 and > 20 . At the second interim analysis in the population with CPS > 20 , OS was higher in the pembrolizumab arm compared to the EXTREME scheme (median 14.9 versus 10.7 months, HR 0.61, 95% CI 0.45-0.83). In patients with CPS ≥ 1 , the median OS was 12.3 versus 10.3 months (HR 0.78, 95% CI 0.64-0.96). No improvements in ORR or PFS were evident. The median duration of response was longer in the pembrolizumab arm compared to standard chemotherapy (20.9 vs 4.2 months in CPS ≥ 20 , 20.9 vs 4.5 months CPS ≥ 1 and 20.9 vs 4.5 months in the overall population). At final analysis, grade 3 or worse all-cause AEs occurred in 55% of patients in pembrolizumab alone group, 85% of pembrolizumab-chemotherapy group, and 83% of EXTREME chemotherapy group. Death due to AEs occurred in 8%, 12%, and 10% in the pembrolizumab alone, pembrolizumab chemotherapy, and chemotherapy-cetuximab groups, respectively. Discontinuation due to AEs occurred in 12% of 300 patients in the pembrolizumab group, 33% of 276 pembrolizumab participants with chemotherapy group and 28% of 287 participants in the cetuximab with chemotherapy group. Deaths due to treatment-related AEs occurred in 3 (1%), 11 (4%) and 8 (3%) in the pembrolizumab, pembrolizumab-chemotherapy, and cetuximab-chemotherapy group, respectively. The most common treatment-related AEs were fatigue

and hypothyroidism, while anemia and nausea was the most common AE for pembrolizumab with chemotherapy and cetuximab with chemotherapy. Pembrolizumab alone was associated with a higher risk of hypothyroidism than cetuximab with chemotherapy.

Pembrolizumab with chemotherapy has been associated with an increased risk of anemia, hypothyroidism and cough compared to cetuximab with chemotherapy, while the risks of hypokalemia, hypomagnesaemia, rash and acneiform dermatitis was greater with cetuximab with chemotherapy. Both options, pembrolizumab alone and pembrolizumab-chemotherapy maintained health-related QoL [66].

Furthermore, the results of the final KEYNOTE 048 analysis, showed a superior OS in the pembrolizumab/chemotherapy arm versus the EXTREME arm in patients with CPS ≥ 20 (14.7 vs 11 months, respectively, hazard ratio [HR] = 0.60, 95 % confidence interval [CI] = 0.45-0.82, P = .0004). Similarly, in the population with CPS ≥ 1 , OS was 13.6 versus 10.4 months (HR = 0.65, 95 % CI = 0.53-0.80, P < .0001) in the pembrolizumab/chemotherapy arm vs the EXTREME arm, respectively. Overall, the tolerability and safety profile of immunotherapy treatment, alone or in combination with chemotherapy, was confirmed and favorable compared to standard chemotherapy treatment [27, 67]. Based on these results, the FDA approved pembrolizumab as monotherapy for first-line treatment only for PD-L1 positive patients with CPS > 1 and in combination with platinum-5fluorouracil chemotherapy regardless of PD-L1 expression. EMA, on the other hand, approved pembrolizumab both as monotherapy and in combination with platinum-5fluorouracil only for patients with CPS ≥ 1 . Subsequently, AIFA also approved reimbursability for the first-line treatment of patients with relapsed or metastatic disease in potentially platinum-sensitive, with disease not amenable to locoregional treatment and with PD-L1 expression (CPS ≥ 1). In patients negative for PD-L1 expression (CPS < 1), EXTREME or TPExtreme [67] remains the treatment of choice limited to eligible patients with a good performance status.

With a 4-year follow-up, first-line pembrolizumab and pembrolizumab-chemotherapy continued to demonstrate survival benefit versus EXTREME chemotherapy in R/M HNSCC: OS improved with pembrolizumab in the PD-L1 CPS ≥ 2 and CPS ≥ 1 populations and was noninferior in the total population (HR, 0.81; 95% CI, 0.68 to 0.97), as well as pembrolizumab-chemotherapy in the PD-L1 CPS ≥ 20 and total population [68]. At an updated 5-year follow-up, pembrolizumab and pembrolizumab plus first-line chemotherapy continued to show durable efficacy and manageable safety. The 5-year OS rate for pembrolizumab versus EXTREME was 19.9% versus 7.4% in CPS ≥ 20 , 15.4% versus 5.5% in CPS ≥ 1 and 14.4% versus 6.5% in the overall population, respectively. The OS rate for the pembrolizumab plus chemotherapy versus EXTREME arm was 23.9% versus 6.4% in CPS ≥ 20 , 18.2% versus 4.3% in CPS ≥ 1 , and 16.0% versus 5.2% in the total populations,

respectively. Treatment-related grade 3-5 AEs were 17.0%, 71.7% and 69.3% in the pembrolizumab arm, in pembrolizumab plus chemotherapy and in the EXTREME arm, respectively [69].

A randomised phase III trial (CheckMate 651, NCT02741570) evaluated the combination of nivolumab and ipilimumab in first-line versus the standard first-line EXTREME regimen. Although not published in full, the presentation at the ESMO 2021 congress of the combination of nivolumab and ipilimumab showed no better survival than the EXTREME scheme in the general population and in those with CPS>20. Grade 3/4 treatment-related AEs occurred in 28.2% and 70.7% of patients treated with nivolumab plus ipilimumab and standard chemotherapy with cetuximab, respectively, demonstrating a favorable safety profile compared with EXTREME regimen [70].

The KEYNOTE-040 trial [71], a phase III study evaluating pembrolizumab in patients with metastatic and/or relapsed platinum-refractory disease not amenable to local treatment, showed an association between clinical benefit and PDL1 expression in tumour cells with tumour positive score (TPS) >50%. The authors demonstrated a median OS of 8.4 months (95% CI 6.4-9.4) with pembrolizumab and 6.9 months (5.9-8.0) with standard oncologist's choice (SOC) (HR for death was 0.80 (95% CI 0.65-0.98; nominal p = 0.0161). Serious toxicities were 13% in the pembrolizumab arm compared to 36% in the chemotherapy arm. Overall, pembrolizumab achieved a favorable safety profile; the most common treatment-related AE was hypothyroidism with pembrolizumab (13%) and fatigue with standard of care (18%). Results at a 6-year follow-up presented at ESMO 2022 showed that pembrolizumab continued to gain an OS benefit over SOC in R/M HNSCCs, regardless of PD-L1 expression. Indeed, the median OS was 8.4 months in the pembrolizumab arm versus 7.1 months in the SOC arm (HR, 0.79; 95% CI, 0.66-0.94) in the Intention-to-treat (ITT) population, 11.6 months versus 7.9 months (HR, 0.62; 95% CI, 0.43-0.90) for the TPS ≥50% population, and 8.7 months versus 7.1 months (HR, 0.72; 95% CI, 0.59-0.89) for the CPS ≥1 population. Treatment-related AEs of any grade occurred in 64.2% of patients in the pembrolizumab arm and 83.3% of patients in the SOC arm. Treatment-related AEs occurred in 13.4% and 36.8% in the pembrolizumab and SOC arms, respectively [72].

The ongoing Phase 4 study KEYNOTE-B10 (NCT04489888) is evaluating the combination pembrolizumab-carboplatin-paclitaxel in the first-line setting in HNSCC R/M. The results presented at ESMO 2022 showed good antitumor activity with a manageable safety profile, offering an alternative regimen to those containing 5-FU. With a median follow-up of 8.2 months, ORR was 43% and median OS was 12.1 months. Treatment related AEs of any grade occurred in 96% and the most common were neutropenia (57%), anemia (43%) and fatigue (40%). Grade 3-5 treatment related AEs occurred in 71% of patients [73].

The phase III Checkmate 141 trial [26] studied the use of nivolumab in patients with HNSCC

progressed after first-line platinum-based chemotherapy or after concomitant chemo/radiotherapy. Three hundred and sixty-one patients were randomised to receive nivolumab (3 mg/kg every fortnight) or SOC treatment including methotrexate, docetaxel or cetuximab. Among the 240 patients randomised to receive nivolumab, a benefit in OS with a 30% reduction in the risk of death was demonstrated (hazard ratio [HR], 0.70; 97.73% confidence interval [CI], 0.51-0.96; p 0.01). The ORR was also higher in the nivolumab arm than in the standard therapy arm (13.3% versus 5.8%, respectively). Treatment-related AEs of grade 3 or 4 occurred in 13.1% of the patients in the nivolumab group versus 35.1% of those in the standard-therapy group. At two-year follow-up, OS remained significantly higher in the nivolumab arm compared to SOC (7.7 months vs. 5.1 months, HR = 0.68 [95% CI, 0.54, 0.86]). Moreover, in the nivolumab arm safety profile was confirmed with Grade 3-4 treatment-related AE rates of 15.3% and 36.9% for nivolumab and SOC, respectively. Nivolumab was able to delay the time to deterioration of patient-reported QoL outcomes compared to SOC, supporting nivolumab as a standard of care option in this setting. Based on the results of Checkmate 141, nivolumab was approved by the FDA. CheckMate-141 [26, 74] failed to demonstrate a significant association between PDL1 expression, response rates to nivolumab, and OS. The monoclonal antibodies pembrolizumab and nivolumab showed significant activity in patients with platinum-refractory metastatic HNSCC or with loco-regional recurrence not amenable to local treatment. Therefore, they were both approved by the Food and Drug Administration FDA in 2016 and 2018, respectively. Nivolumab is currently reimbursed in Italy in the treatment of platinum-refractory disease.

In 2019, a single treatment arm phase II study evaluated durvalumab (anti PD-L1 antibody) in 112 patients with platinum refractory HNSCC and with PD-L1 expression on tumour cells (TC) >25%. The response rate was 16.2% (95% CI, 9.9-24.4). At a follow-up of 6.1 months (range, 0.2-24.3) the median OS was 7.1 months (95% CI, 4.9- 9.9). Toxicity profile was acceptable with a 57.1% of treatment-related AE of any grade occurred and no treatment related dead [75].

The randomised phase II study CONDOR enrolled 267 patients with R/M disease progressing during or after first-line treatment with platinum-based treatment for R/M disease and with absent or low PD-L1 expression. Eligible patients were randomised to receive combination therapy with durvalumab /tremelimumab versus durvalumab as monotherapy versus tremelimumab as monotherapy. The ORR was 7.8% with the combination, 9.2% with durvalumab and 16.9% with tremelimumab combination, 9.2% with durvalumab as monotherapy and only 1.6% with tremelimumab. The median OS was respectively 7.6 months with the combination, 6 months with durvalumab and 5.5 months with tremelimumab. In this phase II study, both combination therapy and monotherapy showed a safe and manageable toxicity profile with Grade 3/4 treatment-related AEs in

15.8%, 12.3% and 16.9% in patients treated with durvalumab-tremelimumab, durvalumab and with tremelimumab, respectively. Grade 3/4 immune-mediated AEs occurred only in the combination arm (6%) [76]. In 2020, the phase III Eagle study enrolled 736 patients with R/M, platinum refractory HNSCC. Eligible patients were randomised to receive durvalumab, durvalumab plus tremelimumab, or SoC. No benefit in terms of OS was observed either in the durvalumab versus SoC nor in the durvalumab versus tremelimumab versus SoC. Treatment-related AEs were consistent with previous reports. The phase 3 study confirmed the safe toxicity profile. The most common treatment-related AEs included hypothyroidism for durvalumab (11.4%) and durvalumab plus tremelimumab (12.2%). The rate of Grade ≥ 3 events was 10.1% for durvalumab, 16.3% for the combination and 24.2% for SoC [77]. The results of CheckMate 651 evaluating the combination nivolumab plus ipilimumab versus EXTREME in patients with first-line R/M HNSCC were presented at asco 2022. There were no statistically significant differences in OS in the overall population (median: 13.9 v 13.5 months; P = .4951) and in patients with CPS ≥ 20 (median: 17.6 v 14.6 months; P = .0469). In patients with CPS ≥ 20 , the PFS was 5.4 months and 7.0 months, the ORR was 34.1% and 36.0%, and the median duration of response was 32.6 and 7.0 months in the nivolumab-ipilimumab and EXTREME groups, respectively. Treatment-related Grade 3/4 AEs were 28.2% and 70.7% in the nivolumab-ipilimumab arm and EXTREME arm, respectively [78].

In a phase II, open-label, multicentre, single-arm study evaluating the tolerability and clinical benefit of pembrolizumab and cabozantinib in patients with RM HNSCC who had not received previous ICIs, with CPS > 1. At a median follow-up of 12.7 months, an overall RECIST 1.1 ORR response rate was 45.2% (CR=0; PR=14, 45.2%; SD=14, 45.2%; PD=3, 10%) with an overall clinical benefit of 90.4%; 1-year OS was 67.7% and 1-year PFS was 51.8%. The most frequent AE (all grades) was fatigue (50.0%) [79].

Immunotherapy in R/M HNSCC has become standard in I and II line, also showing an efficacy and safety profile in combination strategies with chemotherapy, a factor of considerable relevance considering the typical clinical frailty of HNSCC patients and the need to ensure a good QoL.

1.4 Immunotherapy in metastatic non-oncogene addicted non-small cell lung cancer: state of art

Lung cancer is still the leading cause of cancer-related death, with approximately 1.8 million new cases (12.9% of the total) and 1.6 million deaths (19.4% of the total) annually. More than 95% of lung carcinomas can be attributed to four main histotypes: squamous cell carcinoma (CS), adenocarcinoma (ADC), large cell carcinoma (CGC) and small cell carcinoma or microcytoma (SCLC). In Western countries, the frequency of ADC is sharply increasing (>50%), while CS and

microcytoma are significantly decreasing. In recent years, the precise histological definition of non-small cell lung cancer (NSCLC) has become critical for new histotype-related therapies [80].

In recent years, the study of the molecular characteristics of lung tumours highlighted a specific role of certain genes as important therapeutic targets, including EGFR (Epidermal Growth Factor Receptor) and ALK (Anaplastic Lymphoma Kinase) [81]. In NSCLC (particularly in 10-15% of ADCs of Caucasian patients and 40% of Asian patients) EGFR activating mutations have been identified at exons 18, 19, 20 and 21, actually, the most important predictive factor for molecularly targeted therapies with specific tyrosine kinase inhibitors of EGFR. Recently, new molecular alterations identifying other ADC subgroups have been documented: on the short arm of chromosome 2 the rearrangement of the ALK oncogene with the EML-4 oncogene (or more rarely with other fusion genes) produces a specific protein with tyrosine kinase activity involved in cell proliferation and survival processes. It is present in approximately 3-7% of lung ADCs. Determination of the ALK gene rearrangement is necessary to select patients for treatment with ALK-specific tyrosine kinase inhibitors (Crizotinib, the first to be used in clinical practice, and others such as Ceritinib and Alectinib). Other molecular alterations, particularly in ADC, with promising therapeutic choices are represented by the ROS1 gene rearrangement (about 1-2% of ADC) and the RET gene, activating mutations of BRAF (both V600E and non-V600E) and HER2 [82].

Currently, the choice of treatment for patients with advanced NSCLC (stage IIIB not amenable to locoregional treatment and stage IV) is based on:

- histology (squamous versus non-squamous)
- presence of 'driver' molecular alterations (mainly EGFR mutation or ALK rearrangement, ROS-1) identifying oncogene-addicted disease
- expression level of PD-L1
- clinical characteristics of the patient (age, performance status, comorbidities).

Before immunotherapy advent, second-line chemotherapy presented response rates <10%, median PFS of 2 months and median OS of 7-8 months. The introduction of ICIs into clinical practice has extraordinarily revolutionised patient survival and QoL. Like other tumour types, NSCLCs are characterised by an immunosuppressive tumour microenvironment capable of promoting tumour growth [83, 84]. For instance, NSCLC tumours have been shown to contain large numbers of Treg that constitutively express high levels of CTLA-4 on their surface and directly inhibit T-cell proliferation [85]. Furthermore, in NSCLCs, tumour-infiltrating CD8+ T-cells showed increased expression of PD-1 with an important impairment of immunological function [86]. PD-L1 also appears to be overexpressed on NSCLC tumour cells and correlates with suppression of DC maturation and reduced T-cell infiltration in the tumour microenvironment [87-88]. Furthermore,

tumour cells in the tumour microenvironment are able to induce a deficit in the expression of the MHC I thereby causing dysfunction in antigenic presentation mechanisms. Lung cancer cells may also be able to release immunosuppressive cytokines, including IL-10 and TGF- β [89, 90]. Given the clear role of the immune system in the genesis and progression of NSCLC, research has yielded remarkable results in the use of immunotherapy in different disease settings.

Results in terms of both efficacy and safety have recently been reported from several phase III studies investigating the role of ICIs in NSCLC [22, 23, 91-93]. Pembrolizumab can be considered a standard first-line treatment in patients with PD-L1 expression $\geq 50\%$ (KEYNOTE-024 study). The KEYNOTE-024 study, is a phase 3 randomised open-label trial, including 305 patients with metastatic NSCLC, without EGFR mutation or ALK rearrangement, with PD-L1 expression $\geq 50\%$, and with performance status of 0-1, randomised to receive first-line treatment with pembrolizumab or with a standard chemotherapy regimen (platinum-based for 4-6 cycles, with the possibility of continuing pemetrexed as maintenance therapy). Pembrolizumab demonstrated a significant increase in PFS (median 10.3 versus 6.0 months, HR 0.50, CI 95% 0.37-0.68, $P < 0.001$). At a median follow-up of 59.9 months, the median OS was 26.3 months with pembrolizumab and 13.4 months with chemotherapy (HR 0.62; 95% CI, 0.48 to 0.81, $P = 0.001$) with a 5-year OS rate of 31.9% with pembrolizumab versus 16.3% with chemotherapy. Overall, the safety profile was better for pembrolizumab compared to chemotherapy, both for the incidence of AEs of any grade (76.6% versus 90.0%), and grade 3-5 AEs (31.2% versus 53.3%). The rate of patients discontinuing treatment due to AEs was similar in the two arms (13.6% with pembrolizumab and 10.7% with chemotherapy) [94]. The multicenter, phase III trial EMPOWER-Lung 1 confirmed the cemiplimab, an anti PDL-1 agent, as a treatment option in advanced NSCLC with TPS $\geq 50\%$. Median OS was not achieved with cemiplimab compared to 14.2 months in the platinum-based chemotherapy arm. PFS was 8.2 months with cemiplimab compared to 5.7 months with chemotherapy (HR 0.54 [0.43-0.68]; $p < 0.0001$). Treatment-related grade 3-4 AEs occurred in 28% patients treated with cemiplimab versus 39% patients in the chemotherapy arm. In February 2021, FDA approved Cemiplimab in first line setting in advanced NSCLC with TPS $\geq 50\%$ [95].

Combination strategies, immunotherapy and chemotherapy, have been widely explored revolutionising the first-line setting of non-oncogene addicted disease.

The phase 2 randomised multi-cohort, open label study KEYNOTE-021 included 123 patients with metastatic NSCLC with nonsquamous histology without EGFR mutations or ALK rearrangement and with any PDL1 expression level, with performance status of 0-1, in first-line setting. Patients were randomised to receive pembrolizumab in combination with carboplatin and pemetrexed for 4 cycles, followed by maintenance pemetrexed and pembrolizumab for up to 24 months or chemotherapy alone

followed by maintenance. With a follow-up of 49.4 months, the benefit was confirmed for the combination arm with pembrolizumab in term of both ORR (58% versus 33%) and PFS (24.5 versus 9.9 months; HR 0.54; 95% CI 0.35-0.83) and OS (34.5 versus 21.1 months; HR 0.71; 95% CI 0.45-1.12), despite a 70% crossover from chemotherapy to combination arm. The incidence of severe AEs was 39% among patients treated with the combination versus 31% in patients treated with chemotherapy. Twelve per cent and 5% of the patients in the pembrolizumab plus chemotherapy group had anaemia and neutropenia as the most frequent grade 3 or higher AEs.

A further 3% of patients in the combination arm experienced acute kidney injury, decreased lymphocyte count, fatigue, neutropenia, sepsis and thrombocytopenia. In the chemotherapy group, the most common grade 3 or worse events were anaemia (15%) and decreased neutrophil count, pancytopenia and thrombocytopenia.

One (2%) of 59 patients in the pembrolizumab plus chemotherapy group experienced a treatment-related death due to sepsis, compared to two (3%) in the chemotherapy group: one due to sepsis and one due to pancytopenia [96].

The KEYNOTE-189 trial, a randomised phase 3, double-blind study, included 616 patients with metastatic NSCLC with non-squamous histology, without EGFR mutations or ALK rearrangement and with any level of PD-L1 expression, with performance status of 0-1, on first-line setting. Patients were randomised to receive pembrolizumab or placebo, up to a maximum of 35 cycles, in combination with pemetrexed and cisplatin or carboplatin for 4 cycles followed by maintenance pemetrexed. With a follow-up of 46.3 months, a benefit was observed for the combination arm with pembrolizumab in terms of both median PFS (9.0 versus 4.9 months; HR 0.50, CI 95% 0.41-0.59) and median OS (22.0 versus 10.6 months, HR 0.60, CI 95% 0.50-0.72). The benefit in OS was consistent in all subgroups analysed on the basis of levels of PD-L1 expression, including PD-L1 negative patients and those with PD-L1 expression 1-49%. Furthermore, there was no significant increase in the frequency of AEs in the pembrolizumab arm compared to chemotherapy alone (grades 3-5 52.1% versus 42.1%), and the incidence of immuno-related AEs (any grade 27.7%, grades 3-5 12.6%) was similar to that observed in studies of pembrolizumab as monotherapy, with the exception of nephritis, which occurred more frequently than expected (6.2%) [97, 98].

The 'IMpower132' study, first presented at ESMO 2018 and recently published, showed a significant benefit in terms of PFS, with a numerically, but not statistically significant OS benefit from the addition of atezolizumab to platinum-based chemotherapy and pemetrexed compared to chemotherapy alone. In the 'IMpower150' study, the addition of atezolizumab to carboplatin, paclitaxel and bevacizumab resulted in a significant increase in the primary endpoints compared to bevacizumab-chemotherapy alone: PFS, as assessed by the investigators in the wild-type population

and in the wild-type population with high tumour expression of a genetic signature of effector T cells (Teff), and OS in the wild-type population. In the same population, the "IMpower130" study demonstrated a significant increase in the primary endpoints (PFS and OS in the wild-type population) from the addition of atezolizumab to carboplatin and nab-paclitaxel compared to chemotherapy alone. None of the 3 trials, Impower 132, Impower 150 and IMpower 130, gave unexpected signals regarding safety, confirming the manageability of adding atezolizumab to chemotherapy. Grade 3 or worse treatment-related AEs were not significantly worse in the immunotherapy-chemotherapy combination arms compared with chemotherapy alone [99-102].

The 'KEYNOTE-407' study evaluated the addition of pembrolizumab to first-line chemotherapy treatment in patients with advanced, squamous histology NSCLC with any level of expression of PD-L1. Patients were randomised to receive pembrolizumab or placebo in combination with paclitaxel or nab-paclitaxel and carboplatin for 4 cycles, followed by maintenance therapy with pembrolizumab and/or placebo in case of response or disease stability, up to a maximum of 35 cycles.

The updated study results show a significant increase in OS in the group treated with pembrolizumab group (17.2 months versus 11.6 months; HR=0.71; 95% CI 0.59-0.86). PFS was also superior in the pembrolizumab arm (8.0 versus 5.1 months; HR=0.59; 95% CI 0.49-0.71), with an ORR of 62.2% for pembrolizumab compared to 38.8% in the placebo arm.

In terms of tolerability, the combination had overlapping AEs compared to the placebo-treated group: 74.5% G3-5 AEs for the pembrolizumab-treated group versus 70.0% in the placebo-treated group [103, 104].

The phase 3 study 'IMpower131' randomised patients diagnosed with squamous histology NSCLC to receive atezolizumab + carboplatin + paclitaxel, atezolizumab + carboplatin + nab-paclitaxel or carboplatin + nab-paclitaxel for 4-6 cycles, followed by maintenance with atezolizumab or placebo in patients with response or disease stability. The addition of atezolizumab to carboplatin + nab-paclitaxel chemotherapy increased the median PFS (6.3 months versus 5.6 months, HR=0.71; p=0.0001); while in terms of OS the difference was not statistically significant (median OS 14.2 versus 13.5). In terms of tolerability, the combination was more toxic compared to chemotherapy alone: 68.0% treatment-related G3/4 AEs versus 57.5%, while serious AEs occurred in 57.5% and 28.7% in combination arm and chemotherapy arm, respectively [105]. Another therapeutic strategy that has shown promising results in the first-line setting of treatment of NSCLC patients is the combination of anti-PD-1/PD-L1 and anti CTLA-4. The CheckMate 227 study demonstrated that the combination of nivolumab-ipilimumab is associated with an increase in OS compared to chemotherapy alone in untreated patients with advanced NSCLC (with both squamous and non-squamous histology) with PD-L1 expression $\geq 1\%$ or $< 1\%$. Grade 3 or 4 treatment-related AEs in

the overall population were 32.8% with nivolumab plus ipilimumab and 36.0% with chemotherapy [106]. At a 5-year follow-up, the combination of nivolumab and ipilimumab was confirmed to increase survival and long-term clinical benefit regardless of tumour PD-L1 expression [107].

The CheckMate 9LA study demonstrated an advantage in OS from the addition of nivolumab-ipilimumab (continued for up to 2 years of treatment) to 2 cycles of chemotherapy compared to chemotherapy alone for 4 cycles in patients with metastatic NSCLC with both squamous and non-squamous histology, without EGFR mutations or ALK rearrangement and with any PD-L1 expression level, with performance status of 0-1, in first-line treatment [108]. The most common AE was rash. Most immune-mediated AEs occurred within 6 months of starting treatment. Patients who discontinued nivolumab plus ipilimumab due to treatment related AE had long-term OS benefits.

The update with a minimum of 3 years follow-up confirmed that nivolumab-ipilimumab therapy with chemotherapy has durable and long-term efficacy compared with chemotherapy alone in patients with metastatic NSCLC regardless of KRAS and STK11 mutation status. The 3-year OS rates were 27% vs 19%, respectively. There were no changes in the toxicity profile with extended follow-up [109].

In the same clinical setting, the POSEIDON study demonstrated a benefit in PFS and OS from the combination of durvalumab-tremelimumab and chemotherapy compared to chemotherapy alone [110]. PFS was significantly improved in the durvalumab-chemotherapy arm compared with chemotherapy alone ($P = 0.0009$; median, 5.5 v 4.8 months) with a trend for improvement in OS without reaching statistical significance ($P = 0.0758$; median, 13.3 vs 11.7 months). Both PFS and OS were significantly better in the tremelimumab-durvalumab-chemotherapy arm compared with chemotherapy alone, with median PFS of 6.2 months versus 4.8 months and OS of 14 and 11.7 months, respectively. Treatment-related AEs were highest grade 3/4 in 51.8%, 44.6%, and 44.4% of patients treated with tremelimumab-durvalumab-chemotherapy, durvalumab-chemotherapy, and chemotherapy, respectively. After a median follow up of 4 years, the durable long-term OS benefit of tremelimumab-durvalumab and chemotherapy was confirmed, supporting the use of this regimen in first-line as well as in patients with STK11 and KRAS mutations [111].

Taken together, the results of these studies suggest that immunotherapy (alone or in combination with chemotherapy) represents a standard in the first-line treatment of a significant proportion of patients with newly diagnosed advanced NSCLC. Moreover, the combination of immunotherapy and first-line chemotherapy has never given any worrying signs of safety, and, indeed, has proved tolerable compared to chemotherapy alone.

Nivolumab is also now the standard of care in both squamous and adenocarcinoma NSCLC lung cancer, in II line setting.

The approval of nivolumab in clinical practice stems from the results of two randomised phase III trials CheckMate-017 and CheckMate-057 for squamous and non-squamous NSCLC, respectively [112]. These two multicentre, randomised, phase III trials compared nivolumab with docetaxel for stage IIIB/IV NSCLC with disease recurrence or progression during or after a previous platinum derivative-based chemotherapy regimen. In total, 272 patients with squamous and 582 with non-squamous cancer were randomised (1:1) to receive nivolumab 3 mg/kg every 2 weeks or docetaxel 75 mg/sqm every 3 weeks until disease progression and/or unacceptable toxicity. In the nivolumab arm, following initial disease progression, continuation of study treatment was allowed if clinically beneficial and well tolerated. The superiority of nivolumab over docetaxel was maintained over time, regardless of histology, with a relative reduction in the risk of death of 28% (HR 0.72, 95% CI 0.62-0.84). After a minimum follow-up of 24.2 months, the 2-year OS with nivolumab versus docetaxel was 23% versus 8% in squamous NSCLC, and 29% versus 16% in non-squamous NSCLC. Furthermore, PFS and ORR results continued to favour nivolumab for both NSCLC subtypes.

More interestingly, response to nivolumab was maintained over the long term: 10 out of 27 (37%) responders among squamous and 19 out of 56 (34%) responders among non-squamous still had ongoing response at the cut-off date, whereas no patients in the docetaxel arm demonstrated long-term benefit. Furthermore, the median response with nivolumab was 25.5 months and 17.2 months, compared to 8.4 months and 5.6 months with docetaxel in squamous and non-squamous NSCLC, respectively. In agreement with previous results, treatment with nivolumab was safe and better tolerated than docetaxel. Treatment-related AEs were lower in the nivolumab arms (regardless of grade, 68% vs 88%), mainly intermediate grade (grade 3-4, 10% vs 55%) and with a toxicity profile consistent with that expected for this drug. The most frequently observed treatment-related AEs of any grade were hypothyroidism (4% with nivolumab vs 0% with docetaxel), diarrhoea (8% vs 20%), pneumonia (5% vs 0%), creatinine elevation (3% vs 2%) and rash (4% vs 6%). In addition, no treatment-related deaths were reported in early analyses [112].

Pembrolizumab is a second-line option in patients with PD-L1 expression $\geq 1\%$ (KEYNOTE-010 study). The 'KEYNOTE-010' study, is a phase 2/3 randomised, open-label, multicentre trial, conducted in 1034 patients with a performance status of 0-1, with advanced NSCLC with PD-L1 expression $\geq 1\%$ (assessed centrally by immunohistochemistry with 22C3 antibody), and in disease progression after at least one first-line platinum-based treatment (including appropriate tyrosine kinase inhibitor therapy for patients with EGFR mutation or ALK rearrangement) [23, 113]. The median OS was significantly higher for pembrolizumab compared to docetaxel, both in the general population (10.4 months for pembrolizumab at 2 mg/kg versus 8.5 months for docetaxel; 12.7 months for pembrolizumab at 10 mg/kg versus 8.5 months for docetaxel) than in the patient population with

PD-L1 \geq 50% (14.9 months for pembrolizumab 2 mg/kg versus 8.2 months for docetaxel; 17.3 months for pembrolizumab at 10 mg/kg versus 8.2 months for docetaxel). The recent update at 42.6 months follow-up confirmed the benefit in median OS. Patients with PD-L1 TPS \geq 50% achieved a median OS of 16.9 (CI 95% = 12.3-21.4) months with pembrolizumab versus 8.2 (CI 95% = 6.4-9.8) months with docetaxel (HR = 0.53; 95% CI = 0.42-0.66; P < .00001); patients with TPS \geq 1% also had a significant benefit (HR = 0.53; 95% CI = 0.42-0.66; P < .00001) [23, 113]. The median PFS was significantly higher for pembrolizumab compared to docetaxel in the patient population with PD-L1 \geq 50%, but in the general population the pre-specified threshold of statistical significance was not reached. Grade 3-5 AEs were more frequent in the docetaxel arm (35%) than in the two pembrolizumab arms (2 mg/kg: 13%; 10 mg/kg: 16%), and the toxicity profile was consistent with that expected: the most frequent immune-related events with pembrolizumab were hypothyroidism hyperthyroidism and pneumonia, mostly grade 1-2.3

The OAK study, is an open-label randomised phase 3 trial, multicentre, conducted on 1225 patients with NSCLC, stage IIIB or IV, previously treated with one or two lines of chemotherapy (including one or more platinum derivative-based therapies, and therapy with tyrosine kinase inhibitor for patients with EGFR mutation or ALK rearrangement) and with a performance status of 0-1 [93].

The median OS was significantly higher for atezolizumab compared to docetaxel, both in the ITT population (13.8 versus 9.6 months; HR 0.73, 95% CI 0.62-0.87, P = 0.0003), in the PD-L1 positive population (5.7 versus 10.3 months; HR 0.74, CI 95% 0.58-0.93; P = 0.0102), in patients with no expression of PD-L1 on tumour cells and inflammatory infiltrate cells (TC0 and IC0; 12.6 versus 8.9 months; HR 0.75, CI 95% 0.59-0.96, P = 0.0215). In patients with high PD-L1 expression (\geq 50% of tumour cells, TC3, or \geq 10% of inflammatory infiltrate cells, IC3) the benefit is also more relevant (20.5 versus 8.9 months; HR 0.41, CI 95% 0.27-0.64, P < 0.0001). The benefit in OS in atezolizumab arm was consistent in all predefined subgroups including patients with squamous (HR 0.73, CI 95% 0.54-0.98) and non-squamous (n = 628; HR 0.73, CI 95% 0.60-0.89) disease, the non-smoking patients (HR 0.71, CI 95% 0.47-1.08) and patients with brain metastases (HR 0.54, CI 95% 0.31-0.94), with the exception of patients with EGFR mutation (HR 1.24, CI 95% 0.71-2.18). No significant difference was observed between the two arms in terms of PFS, with the exception of the subgroup of patients with high PD-L1 expression (TC3 or IC3), where there was an advantage for atezolizumab (HR for PFS 0.63, CI 95% 0.43-0.91). Even at a follow-up of 26 months the survival benefit was maintained in all subgroups [114].

Atezolizumab was better tolerated than docetaxel, with a lower incidence of grade 3- 4 related to treatment (15% versus 43%). In the atezolizumab arm the most frequently reported AEs of any grade

were fatigue (14%), nausea (9%), reduced appetite (9%) and asthenia (8%). Immune-related AEs included pneumonia (1% of any grade, <1% of grade 3), hepatitis (<1%) and colitis (<1%).

On the basis of these data, in Italy nivolumab is approved for the treatment of advanced NSCLC after prior chemotherapy, regardless of the expression of expression of PD-L1; pembrolizumab is approved for the treatment of advanced NSCLC with PD-L1 expression $\geq 1\%$ after at least one prior chemotherapy (or after molecular targeted therapy in case of patients positive for EGFR or ALK); atezolizumab is approved for the treatment of advanced NSCLC after previous chemotherapy, regardless of PD-L1 expression (or after molecular targeted therapy in case of patients positive for EGFR or ALK). Overall, immunotherapy has a well-established favourable tolerability profile compared to standard chemotherapy in the second-line setting, where patient frailty is evident and maintenance of a good QoL of paramount importance.

1.5 Immunotherapy in advanced/metastatic uveal melanoma: state of art

In the adult population, the first tumour occurring in the eye in terms of incidence is melanoma (70% of cases), followed by retinoblastoma (13% of cases). UM differs from cutaneous melanoma in histopathological features, genetic alterations, growth pattern and therapeutic strategy [115].

Choroidal or uveal melanoma has an incidence of approximately 0.7 per 100,000 person-years among female subjects and 0.5 among males, with a lower incidence among black and Hispanic subjects [116]. Generally, UM has a peak incidence between the ages of 55 and 65, while it is relatively rare before the age of 20 and after 75. UM arises from melanocytes of the iris, ciliary body or choroid. Approximately 90% of UM arise in the choroid. Even in UM, although considered a different clinical and biological entity from cutaneous melanoma, immunotherapy has become an important first line option [117]. To date, no data are available from controlled clinical trials regarding immunotherapy in UM, which in clinical practice is commonly treated in a similar fashion as cutaneous melanoma.

Recently, a single arm phase II trial evaluated the combination nivolumab-ipilimumab in 35 pre-treated metastatic UM patients. The ORR was 18%, median PFS was 5.5 months and OS 19.1 months, demonstrating a promising activity. Grade 3-4 treatment related adverse events occurred in 40% of patients [24].

A retrospective study evaluated 56 patients with metastatic UM treated with anti PD-1 (pembrolizumab or nivolumab) or anti PD-L1 (atezolizumab) according to different treatment schedules. The RR was 3.6%, stable disease for more than 6 months was recorded in 8.9%; the median PFS was 2.6 months (95%CI 2.4-2.8 months), the median of OS was 7.7 months (95% CI 0.7-14.6 months). Grade 3 AEs were reported in 12.5% of the patients. Treatment was well tolerated and discontinuation occurred only in one patient for grade 3 arthralgia. PD-1 or PD-L1 antibody therapy

was well tolerated. No AEs (AEs) were reported in 22 patients (37.9%). Grade 3 AEs included nausea, vomiting, hyperbilirubinaemia, fatigue, colitis, arthralgia and lymphopenia, whereas no grade 4 or 5 AEs occurred. The most common AEs of any grade were fatigue (19.6%), pruritus (12.5%), rash (10.7%), nausea (10.7%), hypothyroidism (7.1%) and diarrhoea (8.9%) [118]. A small prospective study, published in 2016, evaluated 10 patients with advanced UM, progressing after ipilimumab. These patients were treated with pembrolizumab. The aim of the study was to evaluate the activity, efficacy and safety of the treatment. The ORR was 33%, median PFS was 18 weeks (range 3.14-49.3). The overall tolerability of the treatment was good and the toxicity profile was low/intermediate (G1/2). However, the main limitation of this study is the small sample size [119]. Maio et al in 2013 retrospectively evaluated the subgroup of patients with advanced UM treated within the Italian Expanded Access Program (EAP) with ipilimumab (3 mg/Kg q21 for 4 doses). A total of 83 patients with advanced UM, 72% of whom received the 4 planned doses. Of the 82 evaluable for response there were 4 partial responses and 24 patients reported a stable disease, for a RR of 5% and a disease control rate (DCR) of 34%. The median PFS and OS was 3.6 months. (95% CI 2.8-4.4) and 6.0 months (95% CI 4.3-7.7). The proportion of patients alive at 1 year was 31%. Of the treated patients, 57% reported an AE of any grade, while in 42% of the patients the AEs were treatment-related. The 10% (8 patients) of patients reported a grade 3 or 4 AE, but only in 5 patients were considered treatment-related (6%). Treatment-related skin AEs of any grade (itching and rash) were the most frequent, while the most frequent grade 3 or 4 AEs considered to be related to ipilimumab were liver toxicity and diarrhoea. AEs were generally manageable and reversible with a median time to resolution of 2.1 weeks [120]. The main limitation of the study is the post-hoc nature of the analysis within the EAP; however, the data reported likely reflect a real-world case series of patients.

A retrospective multicentre analysis conducted in 25 French centres evaluated 100 patients with UM who received immunotherapy (of which 63 with ipilimumab and 37 with anti PD1; 52 of these patients received first-line treatment). The 1-year OS was 52.5% (95% CI 40.1-63.0%) in patients treated with immunotherapy; there was a DCR of 32% (95% CI 23-42.1%). Unfortunately, the study provides little safety data. There were 26 serious AEs in 20 patients treated with anti-CTLA-4 and 18 serious AEs in 14 patients treated with anti-PD1, and one patient died of ulcerative colitis [121].

These studies, despite the small number of cases due to the rarity of the disease, highlight the possible efficacy of immunotherapy in UM, with generally good tolerance to treatment. Considering that most of these studies have been conducted including a real-world population with often pre-treated patients, the safety profile of immunotherapy is favourable even in this rare tumour type with a poor prognosis. Nevertheless, the results in terms of treatment activity and efficacy were inferior to those obtained in cutaneous melanoma. There are no data comparing immunotherapy with chemotherapy (e.g.

photemustine), which could represent an additional treatment option, even if burdened by a high rate of haematological AEs. Further prospective studies are needed to better define the efficacy and safety in this particular disease.

These recent data have shown that the small proportion of patients who respond achieves significant disease control. The early identification of patients who will develop AEs, even if low/intermediate grade, would facilitate their clinical management given their poor prognosis and frequent clinical frailty. Therefore, it is crucial to identify predictive factors of response and development of toxicity.

1.6 Resistance mechanism to immunotherapy

Despite the promising results, a large proportion of patients will either never respond to immunotherapy treatment or respond only briefly, resulting in a loss of control over the disease.

We can therefore distinguish different resistance mechanisms [122]. A first classification consists of:

-Primary resistance: a clinical scenario in which a tumour will never respond to immunotherapy.

-Adaptive immune resistance: a resistance mechanism in which tumour cells are recognised by the immune system but manage to protect themselves by 'adapting' to the immune attack. It may present itself clinically as primary or acquired resistance.

-Acquired resistance: a clinical scenario in which a tumour initially responds to immunotherapy, but then develops resistance resulting in disease progression. It can occur as a result of adaptive resistance mechanisms.

The primary reason for resistance to immunotherapy is the absence of tumour antigens capable of activating T lymphocytes [123]. Alternatively, tumour cells can develop mechanisms to avoid their presentation with MHC. Intrinsic factors of tumour cells contributing to resistance include intracellular signalling pathways able to impair the infiltration or function of immune cells within the tumour microenvironment. Recently, multiple mechanisms of intrinsic resistance have been identified: 1) enhancement of the MAPK pathway and/or loss of PTEN expression, which enhances the PI3K signalling pathway; 2) the WNT/ β -catenin signalling pathway; 3) loss of the interferon-gamma (IFN γ) signalling pathway; and 4) lack of response by T cells due to loss of tumour antigen expression. Activation of the MAPK pathway results in the production of VEGF and IL-8, which have known inhibitory effects on T-cell recruitment and function [124]. Similarly, loss of PTEN enhances the PI3K signalling pathway, which is associated with resistance to checkpoint inhibitor therapy [125]. Furthermore, loss of PTEN correlates with a significant reduction in IFN γ , granzyme B and CD8⁺ T cell expression.

Furthermore, in a mouse model [126], tumours with elevated β -catenin lacked DCs due to reduced expression of CCL4, a chemokine capable of attracting CD103⁺ DCs. IFN γ produced by tumour-specific T cells is able to induce an effective anti-tumour immune response through: 1) stimulation of tumour antigen presentation by increased expression of MHC molecules; 2) recruitment of other immune cells; and 3) direct anti-proliferative and pro-apoptotic effects on tumour cells. However, continuous exposure to IFN γ can lead to immunoediting in tumour cells [127, 128] causing downregulation or mutation of molecules involved in some important intracellular signalling pathways.

The extrinsic mechanisms involved in primary and/or adaptive resistance involve different cellular components present in the tumour microenvironment, including: Tregs, MDSCs, M2 macrophages and other inhibitory immune checkpoints, which may contribute to the inhibition of anti-tumour immune responses.

Regulatory T cells (Tregs), identified by the expression of the transcription factor FoxP3, play a central role in maintaining immune tolerance to the self [129]. FOXP3⁺ Treg cells play a critical role in the establishment and maintenance of an immunosuppressive tumour microenvironment through several mechanisms. Treg cells express inhibitory immune receptors and ligands such as CTLA-4, PD-1 and PD-L1, TIM-3, LAG-3 and TIGIT, promoting immune evasion mechanisms [129-131]. Through these co-inhibitory receptor molecules, Treg thus inhibit the maturation and function of APCs. Conversely, LAG3 expressed by Treg cells can inhibit MHC II expression in DCs [132]. Furthermore, Treg cells can express the CD25 subunit of the high-affinity IL-2 receptor, which can bind IL-2 in the tumour microenvironment, inhibiting cytokine activity essential for effector cell survival [133]. Treg FOXP3⁺ cells can also secrete anti-inflammatory factors (TGF- β , IL-10 and IL-35), perforins and granzymes to inhibit or kill T cells, NK cells and antigen-presenting cells. Multiple immunosuppressive cytokines, IL-10, IL-35 and TGF- β inhibit APC and Teff cell function [134].

In turn, TGF- β , IL-10 and vascular endothelial growth factor (VEGF) produced by tumour cells promote the expansion of Treg cells in tumor microenvironment [135].

Recent studies indicate that many human tumours have an abundant infiltrate of Treg and decreasing Treg cells in the tumour microenvironment can enhance or restore antitumour immunity [136, 137]. In mouse models, the response to anti-CTLA-4 therapy has been shown to be associated with an increased ratio of Teffector/Tregs [138]. These data suggest that tumours for which immunotherapy is unable to increase Teff and/or reduce Tregs are likely to be resistant to treatment.

MDSCs are among the main regulators of immune responses in various pathological conditions including cancer. MDSCs were first defined in mouse models and have been implicated in the promotion of angiogenesis, invasion and metastatic potential of tumour cells [139]. Furthermore, the

presence of MDSCs correlates with reduced survival and reduced efficacy of immunotherapy in human cancers, including breast and colorectal cancer [140, 141]. Therefore, eradication or reprogramming of MDSCs could improve clinical responses to immunotherapy.

TAMs are another subset of cells that appear to influence responses to immunotherapy. TAMs include both M1 macrophages, involved in promoting anti-tumour immunity, and M2 macrophages, with pro-tumourigenic properties [142]. M1 and M2 macrophages can be distinguished on the basis of differential expression of transcription factors and surface molecules and disparities in cytokine secretion [143]. M1 macrophages are typically identified by the surface markers CD86 and CD64, chemokine ligand C-X-C 9, 10, 11 (CXCL9, 10, 11), and secretion of IL-6, IL-12, IL-1 α and TNF- α [144]. M1 macrophages have a pro-inflammatory action, promoting antigen presentation and interleukin production by activating type I T-cell immune responses [145]. They stimulate the secretion of pro-inflammatory cytokines and nitric oxide (NO) and are induced by type 1 T-helper cytokines including IFN- γ , IL-1 β and lipopolysaccharide (LPS) [144].

M2 macrophages typically express the surface markers CD206 and CD163 and express/secret transforming growth factor beta (TGF- β), chemokine ligands CC 14 and 22 (CCL14 and CCL22) [144]. M2 macrophages are typically anti-inflammatory in nature with low secretion of IL-12 and abundant secretion of IL-10, IL-4 and IL-13, factors that result in poor antigen-presenting activity and immunosuppressive effects [144]. These cells are T-helper type 2 activators and TH1 inhibitors resulting in a strong anti-inflammatory activity [146].

Macrophage polarisation is a dynamic phenomenon. Indeed, M2-type macrophages can switch to an M1 phenotype, or vice versa, depending on changes in the tumour microenvironment, secretion of cytokines and growth factors, inflammation, hypoxia and other conditions [144].

Clinical studies have shown an association between higher TAM frequencies and poor prognosis in human tumours [143]. In a chemically induced mouse model of lung adenocarcinoma, depletion of TAMs reduced tumour growth due to down-regulation of M2 / TAM recruitment, probably due to inactivation of CCL2 / CCR2 signalling [147]. Several studies suggest that macrophages can directly suppress T-cell responses via PD-L1 [148]. The immune response is dynamic and signals that activate anti-tumour immune responses also tend to trigger inhibitory pathways in order to limit the magnitude of the immune response. For example, initial T-cell activation leads to increased expression of the inhibitory immune checkpoint CTLA-4. Similarly, IFN γ production leads to increased expression of the PD-L1 protein on multiple cell types, tumour, T-cells and macrophages, resulting in suppression of anti-tumour immunity [149, 150]. In addition, IFN γ may also promote the expression of immunosuppressive enzymes such IDO, a tryptophan metabolising enzyme that may contribute to peripheral tolerance and may have a direct negative effect on effector T-cell function [151]. Among

the processes favouring the escape of tumour cells from the immune control, tumor microenvironment associated soluble factors and/or surface-bound molecules are mostly responsible for dysfunctional activity of the immune system [13].

1.7 Soluble immune Profile

In recent years, research focused on sampling sICs, circulating molecules of adhesion, as well as cytokines and chemokines, Table 1 [152, 153]. These circulating molecules could contribute to the understanding of patient immune status in order to identify biomarkers useful to select who could benefit most from immunotherapy, since, according to recent literature, the soluble isoforms of immune checkpoint receptors are involved in immune regulation and thus potentially associated with clinical outcomes [154, 155]. The origin of soluble receptors has yet to be fully elucidated. These circulating soluble factors could result from proteolytic cleavage of membrane-bound molecules, or from alternative splicing of mRNA. Alternatively, they could be released by exosomes or microvesicles [156, 157]. These soluble factors could hinder the efficacy of ICI antibodies by acting as a drug decoy. The soluble form of PD-L1 can inhibit the activation of infiltrating or circulating T-cells by acting directly on the membrane receptor and activating the PD-1/PDL1 pathway [157, 158]. Soluble CD-137 inhibits T-cell activation, blocking the interaction between T-cells and antigen-presenting cells (APCs) and hindering the function of the membrane counterpart [152, 159]. Recent results suggest that the concentration of these sICs is lower in patients benefitting from immunotherapy, with a potential role in predicting time to treatment failure [152, 153, 155]. In melanoma patients, instead, high serum levels of several sICs were associated with resistance to immunotherapy [160]. In a recent work in a patient population with different types of solid tumours, low levels of certain circulating immune checkpoints were associated with better outcomes in terms of PFS and OS. Furthermore, in the same work, cluster analysis identified a group of patients with a worse prognosis who tended to have elevated levels of circulating cytokines and chemokines [153]. Indeed, circulating cytokines and chemokines may also have a fundamental impact on the clinical outcome of immunotherapy both in terms of survival and toxicity occurrence. Recently, the upregulation of many cytokines in melanoma patients was associated with the development of high-grade AEs during immunotherapy treatment [161]. Indeed, some circulating molecules have been studied in the literature as being involved in the development of immune related AEs (irAEs) and thus as potential biomarkers. A subset of cytokines (GM-CSF, IFN- α 2, IL-12p70, IL-1 α , IL-1 β , IL-1RA, IL-2 and IL-13) is differentially expressed in the plasma of patients who develop severe irAEs, both before and during ICI treatment, representing a potential therapeutic targets for reducing ICI-

induced irAEs [162-165]. Indeed, the potential of some cytokine inhibitor drugs is already known: infliximab, adalimumab, etanercept (targeting TNF- α), tocilizumab (targeting IL-6) and secukinumab (targeting IL-17A). These agents are indicated for the treatment of severe irAE refractory to corticosteroid treatment [166-168]. TNF- α plays a key role in numerous systemic inflammatory diseases and anti-TNF- α drugs are effective in treating inflammation associated with several autoimmune diseases [169, 170]. The monoclonal anti-TNF- α antibody reduced the risk of hepatitis and colitis induced by dual checkpoint inhibition [171]. Moreover, etanercept and infliximab have been used in the clinic to treat severe irAE [172]. Recently, a study in NSCLC patients undergoing ICI, showed that a low IFN- γ level at baseline and a decrease in IFN- γ level after ICI treatment were associated with disease progression and immunotherapy-induced pneumonitis [173].

IL-6 signalling plays a key role in carcinogenesis and in the inhibition of antitumour immunity [174]. In addition, increased IL-6 is detected during inflammatory reactions. Therefore, the association of IL-6 with irAEs has been extensively studied. Two studies reported increased IL-6 levels associated with psoriasiform dermatitis in patients with melanoma in treatment with nivolumab [175, 176]. Moreover, in melanoma patients treated with nivolumab an increased IL-6 level was associated with a higher incidence of psoriasis [177]. In NSCLC patients treated with PD-1 inhibitors, in the group with an increased IL-6 level, AE rate was 43% compared to 0% in the group with a normal IL-6 level [178]. Thus, the increased IL-6 level after ICI treatment was an effective biomarker for irAE, while a low basal level of IL-6 can be used as a predictor of irAEs, but the cut-off of this level needs to be defined by further clinical studies.

Similarly, also some sICs appear to be potentially associated with irAE development in cancer patients. High levels of sCTLA4 in melanoma patients, at baseline, resulted in an increased risk of irAE [179], [Table 1].

To date, available data suggest that soluble molecules play a central role both in determining response to immunotherapy and in the occurrence of irAEs. Understanding the patient immune status may allow the identification of those who will have the worst clinical outcomes requiring alternative and targeted therapeutic strategies.

Table 1. Soluble immune molecules: characteristics, function and possible role in autoimmunity and irAE development.

Soluble molecules	Class of molecules	Cell source	Ligands	Main function	Type of action	Possible role in autoimmunity
sCD137	sIC	PBMCs	CD137L	Inhibits CD137/CD137L binding	Inhibitory	-Possible involvement in T cell-mediated autoimmune disease -correlates with severity of rheumatoid arthritis

							-high level in many autoimmune disease
sPD1	sIC	PBMCs	PDL1/PDL2	Blocks PD1/PDL1 interactions	Activatory		- levels correlate with autoimmune hepatitis , inflammatory bowel disease and pemphigus vulgaris
sPDL1	sIC	Mature DCs	PD1	Binds PD1 and inhibits T cells response	Inhibitory		Detected in chronic inflammatory and autoimmune disorders
sPDL2	sIC	Tumor exosomes, alternatively activated macrophages	PD1	Unknown	Unknown		-Unknown -associated with grade 3–4 irAEs in NSCLC
sCTLA-4*	sIC	Monocyte, immature DCs, regulatory T cells	CD80/CD86	Inhibits T cell responses	Inhibitory		-elevated serum levels in autoimmune disease -higher risk of irAEs in melanoma patients treated with ipilimumab
sTIM3	sIC	Activated lymphocytes	Tim3-L	Unknown	Unknown		possible correlation with ANCA related vasculitis, rheumatoid arthritis, systemic lupus erythematosus, autoimmune hepatitis
sLAG3	sIC	Activated and exhausted CD4 ⁺ , CD8 ⁺ T cells, regulatory T cells	Unknown	Unknown	Unknown		Unknown, increased level in rheumatoid arthritis
sGITR*	sIC	Macrophages and regulatory T cells	GITRL	Unknown	Unknown		- possible role in myasthenia gravis, sjogren syndrome, autoimmune thyroid disorders
sCD27	sIC	Activated lymphocytes	CD70	Unknown	Unknown		immune activation in autoimmune disease and chronic infectious disease, systemic lupus erythematosus, thyroid disorders, systemic sclerosis,
sCD28	sIC	T cells	CD80/CD86	Inhibits T cells activity and counteracts anti-PD1 activity	Inhibitory		-possible correlation with ANCA related vasculitis and with many autoimmune disease
sBTLA	sIC	T cells, B cells, dendritic cells and myeloid cell	HVEM	Unknown	Unknown		Unknown
sHVEM	sIC	T cells, B cells, natural killer cells, monocytes, neutrophils and dendritic cells	-	Unknown	Unknown		Elevated levels in sera of patients with autoimmune disease
sCD80*	sIC	Unstimulated monocytes and B cells	CTLA4/CD28	Unknown	Unknown		-circulating levels associated with autoimmune disease

sICAM-1*	Molecules of adhesion	B and T lymphocytes Endothelial cells	LFA-1	binding the transmembrane receptor, antagonises leukocyte recruitment	Inhibitory	Unknown, but sICAM circulates at increased concentrations in serum and cerebrospinal fluid of patients with active Multiple Sclerosis -predict of allograft rejection
sE-selectin*	Molecules of adhesion	Endothelial cells	Carbohydrate ligands on tumor cells, sialyl Lewis-X	-Enhance angiogenesis -Upregulation of ICAM-1 on tumor cells	unknown	-high level in sepsis, autoimmune disease, and inflammatory disease
sP-selectin*	Molecules of adhesion	Endothelial cells	PSGL-1, sialyl Lewis-X	-leukocyte recruitment -metastatisation -masking of tumour cells by binding to platelets	immune evasion	-high level in sepsis, autoimmune disease, and inflammatory disease
MCPI	chemokine	macrophage monocytes	CCR2 CCR4	-leucocyte recruitment	proinflammatory	-mediate the recruitment of macrophages and T cells in the Lupus nephritis -involved in dysregulation of angiogenic homeostasis in systemic sclerosis
MIP1 α MIP1 β	chemokine	Macrophages Hematopoietic cells	CCR1 CCR5	-granulocyte degranulation -production of pro-inflammatory cytokines -Promote chronic inflammation	proinflammatory	-associated to inflammatory lung disease -associated to rheumatoid arthritis and T cell mediated autoimmune disease
IP10	chemokine	Monocytes Endothelial cells Fibroblast	CXCR3	Leucocytes recruitment	proinflammatory	Involved in type 1 diabetes, Graves' disease and ophthalmopathy, systemic lupus erythematosus, mixed cryoglobulinemia, Sjogren syndrome, or systemic sclerosis
INFα	Cytokine	DC Macrophages NK cells Macrophages Endothelial cells Fibroblasts	INF α R1/2	-NK activation -Cells B proliferation -Possible suppression of -Treg cells -Antiviral activity -Enhances MHC expression	proinflammatory immune-activation	-regulates autoimmune responses -priming monocytes and neutrophils in systemic lupus erythematosus
INFγ	Cytokine	Lymphocytes T (th1) CD8 and NK	INF γ R1/2	-activation of macrophages -activation of Th1 responses -potential antigen presentation to T lymphocytes -induces apoptosis of tumour cells and reduces VEGF -increases expression of IDO	immunoactivating/ possible immunosuppressive activity)	-associated with immunotherapy-induced pneumonitis -associated with grade 3–4 irAEs in NSCLC
TNFα	Cytokine	Macrophages NK T cells	TNFR1 TNFR2	-pro-inflammatory activity -stimulates cell proliferation and survival -induction of apoptosis -implicated in resistance to antiPD1 drugs	Immune-activation/ pro-inflammatory	inappropriate or excessive activation of TNF- α signaling is associated with chronic inflammation and autoimmune disease -central role in rheumatoid and psoriatic arthritis, inflammatory bowel disease, uveitis
IL1α	Cytokine	DC Macrophages Neutrophils	IL1R1 IL1R2	-production of acute phase proteins -stimulates TNF α pathway	Immune activation	Pro-inflammatory marker in autoimmune disease

		Endothelial cells fibroblast		-implicated in fever, sepsis and inflammation	Pro-inflammatory	
IL1β	Cytokine	DC Macrophages Neutrophils Endothelial cells fibroblast	IL1R1	-production of acute phase protein -implicated in fever -induces differentiation of lymphocytes Th17	Immune activation Pro-inflammatory	Pro-inflammatory marker in autoimmune disease like rheumatoid arthritis
IL4	Cytokine	T cells Mast cells	IL4-R α	- activation of Th2 immune response - negative regulator of Th1 and Th17 cell differentiation	Pro/anti-inflammatory	-Associated with high grade 3-4 irAE in a study involving gastrointestinal cancer -role still unclear in autoimmunity Probably involved in inflammatory arthritis
IL6	Cytokine	Macrophages Endothelial cells T cells	IL6R α	-B lymphocyte proliferation and antibody response -production of prostaglandins and acute phase proteins -antagonises Treg anti-inflammatory action through inhibition of TNF α and induction of IL10	Pro-inflammatory/anti-inflammatory	- associated with autoimmune disease and irAE -association with psoriasisiform dermatitis
IL8	Chemokine	Macrophages Endothelial cells Platelets	CXCR1 CXCR2	- chemotaxis -powers phagocytosis -ability to mediate infiltration of MDSCs into the tumour environment	Immune activation/ Immune-evasion	involved in the onset and self-sustaining nature of several autoimmune diseases
IL10	Cytokine	Macrophages Treg cells B cells Mast cells Th2 T cells	IL10R α IL10R β	-downregulation of Th1 cytokines -inhibits CD4 T cell activity -suppresses expression of costimulatory molecules -increases survival of B lymphocytes -blocks secretion of proinflammatory cytokines	Antiinflammatory/ possible immunostimulating anti-tumour activity	Dysregulation of IL 10 producing lymphocytes is involved in many kind of autoimmune disease
IL12p70	Cytokine	Macrophages DC	IL12Rb1 IL12Rb2	-activation of Th1 responses -powers CD8 and NK T-cell activity -Increases INF α production by T cells -suppresses Treg proliferation and angiogenesis	Immune activation	-involved in some autoimmune disorders, such as MS, rheumatoid arthritis, inflammatory bowel, and graft versus-host disease. -involved in allograft rejection by promoting Cytotoxic T cell activities and IFN-mediated delayed-type hypersensitivity reactions
IL13	Cytokine	T CD4 Cells CD8 cells NK Eosinophils Mast cells	IL13R α 1 IL13R α 2	-involved in Th2 immune responses -potential expression of adhesion molecules on endothelial cells -activation of macrophages and production of TGF β -downregulation of Th17-mediated inflammation	Proinflammatory/anti-inflammatory	-Involved in inflammatory arthritis -role still unclear in autoimmunity
IL17A*	Cytokine	Lymphocytes TCD4 Th17	IL17R α	-induces IL6 and chemokines production - promotes recruitment of MDSCs into the tumour bed	proinflammatory	-implicated in pathogenesis of autoimmune disease, ankylosing spondylitis

GMCSF*	Cyto kine	lymphocytes, macrophages, fibroblasts, endothelial cells, chondrocytes, and tumor cells	GM-CSF receptor	- promoting differentiation of myeloid cells - differentiation of dendritic cells	Immune- activation myelopoiesis	critical roles in the development of autoimmune Th17 driven diseases
		<hr/>				

irAE immune related adverse events, DC dendritic cells, IL interleukin, IFN interferon, TNF tumor necrosis factor, MCP monocyte chemoattractant protein, MIP macrophage inflammatory protein, IP interferon induced protein, pd-11 = programmed death ligand 1, CTLA-4 Cytotoxic T-Lymphocyte Antigen 4, TIM3 T-cell immunoglobulin domain and mucin domain 3, LAG3 lymphocyte Activating 3, GITR glucocorticoid-induced TNFR family related gene, BTLA B- and T-lymphocyte attenuator, HVEM Herpesvirus entry mediator, ICAM-1 Intercellular Adhesion Molecule 1, ANCA antineutrophil cytoplasmic antibody.

* molecules probably involved in autoimmunity and irAE development in our study population.

1.8 The immunosuppressive role of IDO

Recently, IDO activity has been proposed as a possible mechanism of resistance to anti-PD-1 treatment that creates an immunosuppressive microenvironment. IDO is a key enzyme catalysing the first step and rate-limiting kinurenine (kyn) pathway of tryptophan (trp) metabolism outside the liver, and converts the essential amino acid into the main metabolite kynurenine. IDO has been shown to act as an immune checkpoint involved in peripheral immune tolerance as it is able to inhibit proliferating T-cells by causing trp depletion and sensitising T-cells to apoptosis [180, 181]. Furthermore, IDO promotes the differentiation of naïve T cells into Tregs with immunosuppressive properties through the production of kyn. Increased expression of IDO on both tumour cells and tumour-infiltrating immune cells, such as DCs, have been reported in a variety of malignancies, in which it is thought to mediate escape mechanisms from the immune system [180, 181]. In NSCLC, increased catabolism of trp, resulting in higher serum concentrations of kyn, has been linked to a more advanced stage at diagnosis, worse prognosis and lower likelihood of response to chemotherapy [182]. Furthermore, recent data showed that a higher kyn / trp ratio was associated with resistance to immunotherapy in advanced/metastatic NSCLC [181]. Interestingly, preclinical evidence suggests that increased IDO activity may be involved in checkpoint inhibition resistance. IDO represents one of the most relevant hallmarks of immunosuppression in cancer. Recently, a prospective study including different types of solid tumours showed that the serum kyn/trp ratio might have a prognostic and predictive value in patients treated with immunotherapy, possibly suggesting a primary mechanism of immune resistance in which IDO is implicated [183]. The availability in the near future of small molecules targeting IDO in combination with immunotherapy, will hopefully have a significant impact in clinical practice [183-187].

1.9 Predictive Biomarker

Despite the undisputed success of the use of immunotherapy in the treatment of solid tumours, only a portion of patients show long-term benefit, while the remaining shows rapid disease progression, indicative of innate or acquired resistance. Moreover, a new group of patients called hyper-progressors who have an accelerated rate of tumour growth and an average survival of only 3 months has also been described. The early detection of intrinsically resistant patients is an issue of crucial importance in clinical practice, as it could prevent immunotherapy failure and ensure personalised and safe treatment options for patients [183, 188, 189].

For this reason, clinical research in recent years has focused on the identification and validation of molecular and genetic biomarkers predictive of resistance to ICI therapy.

Microsatellite instability is a phenotypic and molecular marker of DNA Mismatch Repair (dMMR) deficiency. The functional defect in MMR causes an accumulation of genetic mutations during DNA replication, thereby increasing TMB and neo-antigenic burden, resulting in an enhanced endogenous immune response and correlated sensitivity to immunotherapy. Indeed, the FDA recently approved pembrolizumab in paediatric and adult solid tumours with MSI or mismatch repair deficiency, leading to the first approval based on the presence of a specific biomarker rather than organ-specific histology [190, 191].

Another biomarker is the tumor mutational burden (TMB), which is well known to reflect the load of neoantigens potentially recognised by the immune system. Goodman et al reviewed the patients charts with TMB evaluated by NGS-based technology, analysing those treated with immunotherapy [192]. The response rate to anti-PD-1/anti-PD-L1 therapy was 58% and 20% for TMB-high (TMB-H) and TMB-low patients, respectively. In the pivotal KEYNOTE-158 study, the ORR was 29% in TMB-H tumors compared with 6% in non-TMB-H tumors [193]. Based on these results, in 2020 the FDA approved pembrolizumab for patients with advanced/metastatic solid tumors and high TMB (> 10 mut /mb), in progression after prior treatment and without valid alternative treatment options.

To date, no other reliable predictive factors have been identified in solid tumours, although some clinical parameters seem to have a negative predictive value, such as a high tumour burden, poor performance status, rapidly progressive disease or the presence of brain metastases.

However, these factors are not directly representative of the patient's immune response and ongoing immunological mechanisms.

Until now, the most widely studied biomarker has been PD-L1, which is expressed on both tumour cells and infiltrated inflammatory cells. However, the determination of PD-L1 has several limitations: firstly, PD-L1 is an extremely dynamic marker, secondly, there are different antibodies, assays and

cut-offs for its determination, and finally, biopsies may not be representative of the entire tumour immune status [194].

Despite its controversial role, several studies have demonstrated an association between high PD-L1 expression levels on tumour cells and a greater chance of response to anti-PD-1/PD-L1 treatment, such as in the case of nivolumab, pembrolizumab, atezolizumab and durvalumab. However, there is no homogeneity in the choice of PDL1 determination methods in different studies.

Preclinical studies performed in different types of solid tumours, such as melanoma and lung, have shown an association between the expression of certain molecules such as TIM-3 (T-cell immunoglobulin and mucin domain-containing protein 3), LAG-3 (lymphocyte-activating gene 3) and TIGIT (T-cell immunoreceptor with Ig and ITIM domains) and the impairment of the T-lymphocyte-mediated immune response followed by resistance to anti-PD-1/PD-L1 therapies [8, 195-197].

In a recent study, HNSCC expressing abundant TIM-3 and LAG-3 levels were among the non-responders to anti-PD-1 therapy [9].

Furthermore, analysis of HNSCC patients continuing nivolumab beyond progression in CheckMate-141 showed that patients with low circulating levels of CD8- and Treg PD1-positive T cells were those who benefited most from continued anti-PD1 therapy [198].

The use of TIM-3 and LAG3 inhibitor molecules, especially in combination with anti-PD-1/PD-L1 agents, has a strong clinical rationale. Recently, a phase 2/3 study evaluated the combination of nivolumab and relatrinib (an anti LAG3 agent) in previously untreated melanoma, showing a benefit in PFS compared to monotherapy with nivolumab (10.1 vs. 4.6 months, respectively), with an acceptable toxicity profile, less heavy compared to the association with anti CTLA4 [199]. In the future, personalised therapeutic strategies through the integrated evaluation of new prognostic and predictive biomarkers will be of crucial importance.

Another area of research is the influence of the microbiota and microbiome in the response to immunotherapy. The microbiota is a community of microorganisms that colonise from birth different areas of the human body predominantly the intestinal, oral and nasal mucosa, vaginal tract, etc. It is a dynamic population of over a trillion microbes that includes bacteria belonging to different families, viruses and fungi that interact with each other, the habitat and the local environment. The microbiome is the incredible number of genes that can be extrapolated from this complex community of cells 100 times larger than the entire genome. The microbiota is closely associated with immunity and the development of a healthy immune system, so it is not surprising that the outcome of immunotherapeutic strategies in cancer patients may depend on the gut microbiome. The possibility that the response to ICIs, in particular anti-CTLA-4, could be associated with the composition of the

microbiome was first suggested by Zitvogel's group in 2015 in melanoma. Other groups have also confirmed and extended this knowledge by means of experimental models. Very recently, the observation has been extended to epithelial tumours. Indeed, it was shown in a cohort of 60 NSCLC patients and 40 RCC patients that an overrepresentation of Firmicutes *Akkermansia muciniphila* in the faecal microbiota was associated with increased PFS and response to immunotherapy [200]. In addition, antibiotics could impair the efficacy of PD-1 blockade. The results were further confirmed using the 'avatar mouse' model in which mice were recolonised by transplantation of faecal microbiota from non-responder and responder ICI-treated patients. The restored immunity and antitumour activity of ICI could only be achieved by transplanting faecal samples from responder patients. The immunological mechanisms underlying these findings are still being fully elucidated [155, 200].

1.10 Immune related Toxicities

ICIs have a peculiar immune-related toxicity profile due to their mechanism of action, which makes them better tolerated than chemotherapy and target therapy [201, 202]. irAEs may potentially affect any organ or body system as they are due to the action of immune-system cells against healthy tissues, interfering with self-tolerance mechanisms [203]. The most common IrAE involve the skin, endocrine glands, gastrointestinal system and liver, while cardiovascular, pulmonary, musculoskeletal, ocular and central nervous systems are less frequently affected [204, 205]. Compared to chemotherapy, irAEs are usually mild to moderate in severity, reversible and can be treated promptly with appropriate immunosuppressive agents, whereas severe and fatal irAEs are rare. Nevertheless, some of them may be associated with life-threatening declines in organ function and in QoL, temporary or permanent discontinuation of immunotherapy and, due to early onset and fulminant progression, some of them can be permanent or fatal [206, 207]. Therefore, physicians are faced with an urgent need to study and identify predictive biomarkers of immunotherapy-related toxicities, which, to date, have been poorly investigated.

The presence of sarcopenia at baseline or low muscle attenuation (qualitative muscle reduction) may be considered as patient-related predictive factors of irAE, as they are associated with an increased risk of developing severe treatment-related toxicities [208, 209]. There are no certain explanations as to why some individuals have a greater tendency to develop irAE than others. Probably some individuals have a greater predisposition to autoimmunity. Indeed, patients with pre-existing autoimmune diseases have a higher risk of irAE. Genomic profile and microbiota composition may

also play an important role in the risk of irAE [210], although these mechanisms should be further investigated. Moreover, the concomitant use of drugs such as antiarrhythmics, antibiotics, anticonvulsants or antipsychotics may play an important role in the development of severe irAE [211-215]. Furthermore, specific irAEs seem to be related to a particular type of cancer. For instance, patients with NSCLC tend to develop irAEs earlier, with a higher incidence of interstitial pneumonia than those with melanoma [216, 217]. As previously stated, several ICs and cytokines/chemokines have been associated with an increased risk of developing irAE. Therefore, the identification of a peculiar soluble immune profile could become a reliable predictor, especially when assessed in conjunction with other clinical features, in identifying patients most likely to develop irAE. In our previous work, involving 79 solid tumour patients treated with anti-PD1 drugs, a network analysis of soluble immune molecules was performed, resulting in the identification of a specific pattern of characteristic immune dysregulation in patients who developed cumulative toxicity (more than one irAEs of any grade) [179]. Randomised clinical trials evaluating new systemic agents tend to limit reporting to serious (G3-4) toxicities only, not taking into account lower-grade toxicities as well [218]. However, these toxicities, often of long duration, can have an important impact on the patient's QoL. In a recent study, it was shown that a substantial number of patients were unwilling to undergo treatment due to expected grade 1 and 2 side effects [219]. Considering that most of the irAE are mild/moderate, the simultaneous presence of multiple mild toxicities can have a major impact on the patient's QoL deserving of proper attention and management by the clinician as well as high grade AEs.

Study Endpoint

In this study a large spectrum of circulating molecules including cytokines, chemokines, sICs, molecules of adhesion as well as IDO were evaluated in serum of cancer patients before starting anti-PD1 treatment.

The purpose was to define the immune profile of both responder and non-responder patients to immunotherapy and to evaluate any peculiarities compared to patients who develop or not toxicity during treatment. An efficacy network analysis will be performed in order to assess the connectivity of molecules in responder and non-responder patients and identify any common interactions based on outcomes and the develop of irAEs.

A predictive biomarker profile of response and of irAE development represents an urgent unmet need to better treat patients by preventing ineffective treatments that could compromise QoL by causing failure of response to therapy and/or life-threatening irAE.

The aim of the study is to identify whether there is a peculiar connectivity for each of these 4 clinical situations: responder patients who develop toxicity, responder patients who do not develop toxicity, non-responder patients who develop toxicity, non-responder patients who do not develop toxicity.

Predicting the occurrence of each of these 4 clinical situations would give to the oncologist the opportunity to modulate and personalise the therapeutic strategy based on the immune characteristics of each individual patient (Figure 1).

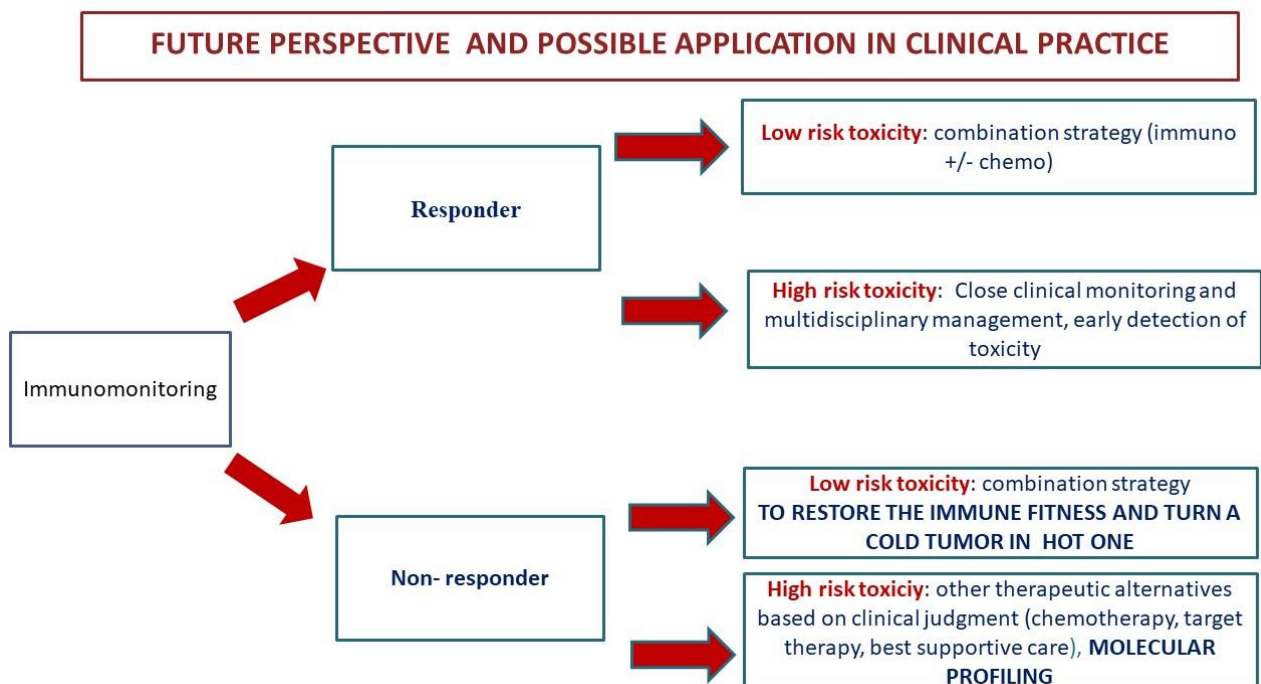


Figure 1. Study endpoints.

Methods and Materials

3.1 Patients enrollment and samples collection

From April 2017 to May 2021 53 patients with NSCLC, UM, R/M-HNSCC and RCC, who received immunotherapy, with the anti PD-1 nivolumab or pembrolizumab, were enrolled in this prospective study. ICI treatment was administered intravenously as first or second line setting, according to approved schedule, until disease progression or development of unacceptable toxicity. Patient characteristics, including Eastern Cooperative Oncology Group (ECOG) Performance Status (PS), age, gender, histology and previous treatments, were recorded. Patients were clinically staged with contrast enhanced computed tomography (CT) scan and, if clinically indicated, magnetic resonance imaging (MRI) and TC/PET at baseline (T0) and every 3 months. Patients aged 18 years or older with histologically confirmed advanced/metastatic solid tumours, fit for immunotherapy with adequate bone marrow, liver, and renal function, and ECOG PS \leq 2, were included in the study. All patients provided an informed consent to be included in the study and for blood samples to be collected. Patients who received anti-neoplastic immunotherapy for other previous or concomitant pathologies, with PS $>$ 2, with uncontrolled autoimmune or infectious diseases or not compliant with protocol requirements were excluded from the study.

Patients blood samples were collected into BD Vacutainer Plus Plastic Serum tubes (Becton Dickinson, NJ, USA) and processed within 1 hour after blood sampling.

Later, tubes were centrifuged at 1800 rpm for 10 minutes. Patients serum was collected and stored at -80°C until use. All samples were collected at T0, before starting anti-PD1 treatment.

3.2 Outcomes

Best tumor response was assessed using immune-related Response Evaluation Criteria in Solid Tumors (i-RECIST) and classified as complete response (CR), partial response (PR), stable disease (SD), and progressive disease (PD).

PFS was defined as the time from the first administration of ICIs until the first progression or in-treatment death. OS was defined as the time from patient registration, or treatment commencement, to death from any cause or last follow up available. Based on the response to immunotherapy, patients were classified as non-responders, if progression occurred at the first clinical-instrumental evaluation

after the start of immunotherapy, or responders, if the best response was stable disease (SD) or partial response (PR) for at least 4 months. Data were collected anonymously into a specific database. Protocol approval from Local Ethics Committee was obtained [CE 4421].

3.3 Toxicities

Patients were clinically evaluated with each administration of the drug. IrAEs were identified through the performance of blood chemist tests and clinical assessment. AEs were recorded at day 1 of every cycle and classified according to the National Cancer Institute Common Terminology Criteria for AEs (version 4.0). IrAEs have been distinguished into low grade (G1) and high grade (G2-G3). Cumulative toxicity was defined as the presence of at least two irAEs of any grade [220].

For each patient, the treatment of irAEs was carried out through multidisciplinary discussion with endocrinologists, rheumatologists, nephrologists and dermatologists, as suggested [221, 222].

3.4 Serological evaluation of immune-related molecules

Serum, collected at baseline (T0), was assayed to detect the concentration of 12 cytokines, 5 chemokines, 13 sICs, 3 adhesion molecules and IDO.

Levels of soluble immune related molecules were dosed through a multiplex assay using the ProcartaPlex Human Inflammation Panel (20 Plex, catalog number EPX200-12185-901; sE-Selectin; GM-CSF; ICAM-1/CD54; IFN alpha; IFN gamma; IL-1 alpha; IL-1 beta; IL-4; IL-6; IL-8; IL-10; IL-12p70; IL-13; IL-17A/CTLA-8; IP-10/CXCL10; MCP-1/CCL2; MIP-1alpha/CCL3; MIP-1 beta/CCL4; sP-Selectin; TNF alpha) (eBioscience, Vienna, Austria) and the Human Immunology Checkpoint 14-Plex ProcartaPlex Panel 1 (catalog number EPX14A-15803-901; BTLA; GITR; HVEM; IDO; LAG-3; 47; PD1; PD-L1; PD-L2; TIM-3; CD28; CD80; CD137; CD27; CD152) (eBioscience) according to manufacturer instruction. Samples were measured using Luminex 200 platform (BioPlex, Bio-Rad) and data, expressed in pg/ml of protein, were analyzed using BioPlex Manager Software.

3.5 Statistical analysis

A total of 34 molecules extracted from a cohort of 53 patients were analysed. Patients were stratified in four group, including 12 patients classified as responder to the therapy without cumulative toxicity, 7 patients classified as responder to the therapy with cumulative toxicity, 23 patients as non-responder

patients to the therapy without cumulative toxicity, and 11 patients as non-responder to the therapy with cumulative toxicity. Data were first pre-processed by applying a logarithmic transformation. Then, experimental differences of the molecules expression levels from the four patient groups were tested for statistical significance both among all groups by using the Kruskal Wallis test and between each pair of groups via the Mann-Whitney test at T0 time (i.e., basal). P-value were adjusted for multiple comparisons by using FDR correction, an adjusted p-value of 0.05 or less was considered statistically significant.

To analyze the correlation between the therapy response and the patient OS as well as PFS, for each patient group, the cumulative survival rates were computed according to the Kaplan-Meier (KM) method [223]. The survival outcomes of the four patient groups were compared by the log-rank test. A log-rank p-values equal or less than 0.05 was considered statistically significant: the lower the p-value, the better the separation between the four prognosis groups. Finally, to test statistical difference of soluble molecules expression values also in term of survival, the cohort of 53 patients were divided into two different groups according to their survival values. In particular, we set the median value of the OS (i.e., corresponding to 11 months) and the PFS (i.e., corresponding to 4 months) as cut-off and we split the patients into one group of 27 and 34 subjects showing a value higher than the median OS and PFS, respectively, and another group composed of 26 and 19 patients showing a value lower than the median OS and PFS, respectively.

3.6 Connnectivity analysis

In order to investigate the relationships between the therapy response and the toxicity, we analyzed the differences in terms of the connectivity exerted by the soluble molecules in responder patients and non-responder patients with and without toxicity. In particular, four connectivity matrices were built by calculating the Spearman correlation coefficients (and the corresponding p-values) among each pair of molecules for each group of analyzed patients: one by considering responder patients with toxicity, one for responder patients without toxicity, one for non-responder patients with toxicity, and another one for non-responder patients without toxicity. Thus, the four matrices were rendered as four connectivity maps where correlation values increase from red to blue. P-values associated to each correlation values were adjusted for multiple comparison and an adjusted p-value of 0.05 or less were considered statistically significant. Then, four corresponding networks of connectivity were then constructed, wherein nodes represent molecules and a link occurs between them if the absolute value of Spearman correlation between their expression levels is greater than a selected threshold (i.e., the 80th percentile of the overall distribution corresponding to 0.7) and statistically significant

(adjusted p-value ≤ 0.05). All the connectivity networks along with their corresponding values of correlation and statistical p-values were detailed as lists in tables.

Results

4.1. Patients

Fifty-three metastatic patients treated with anti PD-1 agent were enrolled in this study: 18 patients with UM, 8 patients with RCC, 13 with HNSCC, and 14 with NSCLC. Baseline clinical–pathological characteristics of patients are summarized in Table 2. All 8 patients in the RCC group had clear cell carcinoma and all 13 HNSCCs had squamous histology. All patients with NSCLC were non-oncogene addicted: 11 patients were squamous and 2 were adenocarcinoma. Thirty-three patients were male (63%), 20 patients were female (37%). The mean age was 71 years (50-89). All patients were treated with nivolumab and pembrolizumab: 18 patients in a first-line treated with pembrolizumab, 35 patients in a second line setting, treated with nivolumab.

Table 2. Baseline clinical and pathological characteristics

CHARACTERISICS	PATIENTS (N)	(%)
Age		
Median	71	
Range	50-89	
Gender		
Male	33	63%
Female	20	37%
Cancer type		
NSCLC	14	26.4%
UM	18	34%
R/M HNSCC	13	24.5%
RCC	8	15.1%
Previous treatment		
No treatment	18	34%
Chemotherapy	27	51%
Target therapy	8	15%
Immunotherapy		
Nivolumab	35	66%
Pembrolizumab	18	34%
Line of ICI Treatment		

First Line	18	34%
Second Line or more	35	66%

4.2 Outcomes

The outcomes of immunotherapy, in terms of best response, PFS and OS are shown in Table 3. Thirty-four patients (64.1%) experienced progressive disease as the best response, while 15 patients (28.3%) stable disease and 4 patients (7.6%) partial response. Median OS was 11 months (2-68) in overall study population: 16 months (2-35) in UM, 27.5 months (6-68) in RCC, 7 months (2-50) in HNSCC, and 5.5 months (2-36) in NSCLC. Median PFS was 4 months (2-61) in overall study population: 4 months (2-35) in UM, 12.5 months (2-61) in the RCC group, 4 months (2-38) in HNSCC, and 2 months (2-34) in NSCLC. Thirteen patients (26.4%) of the total population were alive at the last follow-up visit.

Table 3 Outcomes: best response, OS and PFS in the overall study population and in each type of primary tumor.

PARAMETER	PATIENTS (%)	UM	RCC	HNSCC	NSCLC
BEST RESPONSE					

PROGRESSIVE DISEASE	34 (64.1)	12	2	10	10
STABLE DISEASE	15 (28.3)	6	3	3	3
PARTIAL RESPONSE	4 (7.6)	-	3	.	1
SURVIVAL					
	MEDIAN (RANGE)				
OS	11 (2-68)	16 (2-35)	27.5 (6-68)	7 (2-50)	5.5 (2-36)
PFS	4 (2-61)	4 (2-35)	12.5(2-61)	4 (2-38)	2 (2-34)

4.3 Toxicities

All grade toxicities occurred in 28 patients (52.8%). Twenty-five (47%) patients reported toxicity G1 and 16 (30.2%) patients reported toxicity G2-G3. No immune related deaths as well as any unexpected toxicity was recorded. There was no discontinuation of treatment due to adverse events, as the G3 toxicities occurred in 2 patients concomitantly with disease progression.

The most common toxicity was the non-specific symptom asthenia in 20 patients (37.7%). The other toxicities were: skin toxicity in 14 patients (26.4%), endocrine toxicity in 8 (15%), gastrointestinal in 8 (15%), arthritis/arthritis in 4 (7.5%), mucositis in 3 (5.7%), neurological symptoms in 2 (3.8%), haematologic toxicity in 2 patients (3.8%) and ophthalmic toxicity in 1 (1.9%). In addition, 18 (34%) patients developed more than one toxicity during therapy, reporting the presence of at least two irAEs (Table 4).

Table 4 Patients reporting toxicities; type and grading.

CHARACTERISICS	PATIENTS (N)	(%)
Any grade Toxicities	28	52.8%
Toxicity G1	25	47 %
Toxicity G2-G3	16	30.2 %
Cumulative Toxicities	18	34 %
Asthenia	20	37.7 %
Skin Toxicity	14	26.4 %
Endocrine toxicity	8	15 %
Gastro-intestinal	8	15 %
Arthritis/arthritis	4	7.5 %
Mucositis	3	5.7 %
Neurological symptoms	2	3.8 %
Hematologic	2	3.8%
Ophthalmic	1	1.9 %

4.4 Statistical analysis of circulating molecules in responder and non-responder patients with and without toxicity

We performed an exploratory data analysis of the 34 molecules from 53 patients grouped by therapy response with or without cumulative toxicity. We analysed 4 clinical groups: 12 responder patients without cumulative toxicity (6 UM, 2 RCC, 2 HNSCC, 2 NSCLCL), 23 non-responder patients without cumulative toxicity (12 UM, 2 RCC, 1 HNSCC, 8 NSCLC), 11 non-responder patients with cumulative toxicity (9 HNSCC, 2 NSCLCL), 7 responder patients with cumulative toxicity (4 RCC, 1 HNSCC, 2 NSCLCL). Even if we did not detect a clear separation in terms of overall molecule expression levels across to the four classes (Figure 2A), in the group of non-responders without toxicity, two subgroups with different concentrations of many molecules can be identified by looking at the heatmap (Figure 2A). One of these two subgroups is characterised by a high concentration of cytokines and chemokines, and all patients in it were NSCLC.

We detected an overall statistically significant difference in the four groups for the cytokine IL17A and all the three adhesion molecules (i.e., s-ICAM-1, sP-selectin, sE-selectin) (Figure 2B). We also observed a statistically significant up-regulation of the cytokines IL17A and all the adhesion molecules in non-responder patients with toxicity with respect to the other ones (Figure 2B), regardless of primary tumor type. Furthermore, some immune-checkpoints, including sHEVM, sCTL4-1 and PDL1 showed statistical significance difference between non-responder patients with toxicity and non-responder without toxicity (Figure 3). CTLA4 was statistically significantly higher in non-responders with toxicity even compared to responders without toxicity, as well as sCD80 was significantly higher in non-responders with toxicity than both non-responders without toxicity and responders with toxicity (Figure 3).

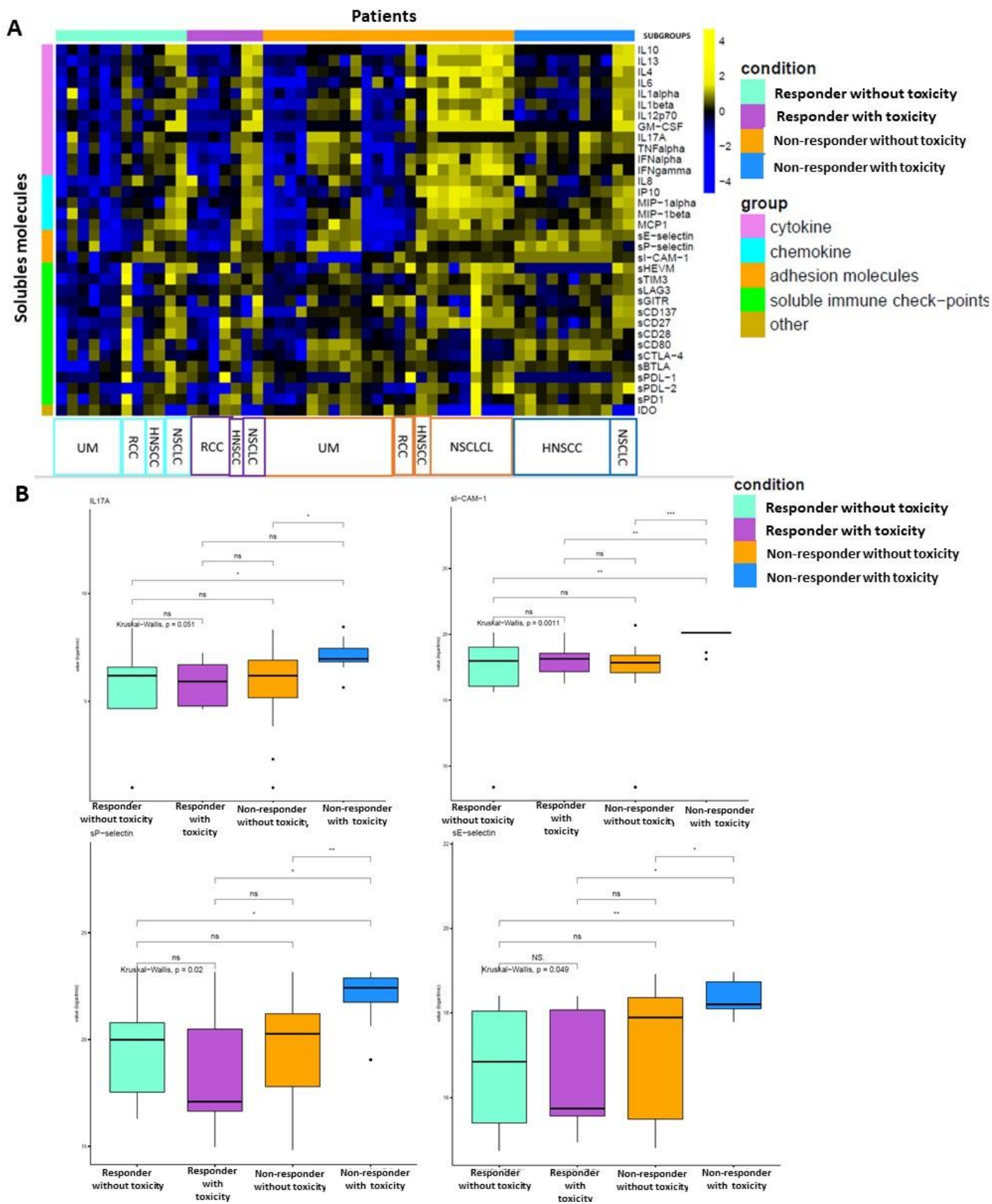


Figure 2 Statistical analysis at T0. (A) Heatmap of molecules expression levels (logarithmic scale) at T0 across 53 patients grouped by therapy responder patients with toxicity (violet bars), therapy responder patients without toxicity (water blue bars), non-responder

patients with toxicity (blue bars), non-responder patients without toxicity (orange bars). A z-score normalization was applying and colors represent different expression levels that increase from blue to yellow. The distribution of primary tumours in each subgroup is indicated at the bottom of the heatmap. (B) Boxplot of molecules expression level (logarithmic scale) in 7 responder patients with toxicity (water blue box), 12 responder patients without toxicity (water blue box), 11 non-responder patients with toxicity (blue box), and 23 non-responder patients without toxicity (orange box) at T0. Pairwise p-values (p) were obtained by applying a Mann-Whitney test for unpaired samples, overall p-value was obtained by applying Kruskal-Wallis test. Only molecules showing an overall statistically significant difference among all groups and a pairwise statistical difference in at least one comparison are shown. Legend: * p-value ≤ 0.05 ; ** p-value ≤ 0.01 ; *** p-value ≤ 0.001 .

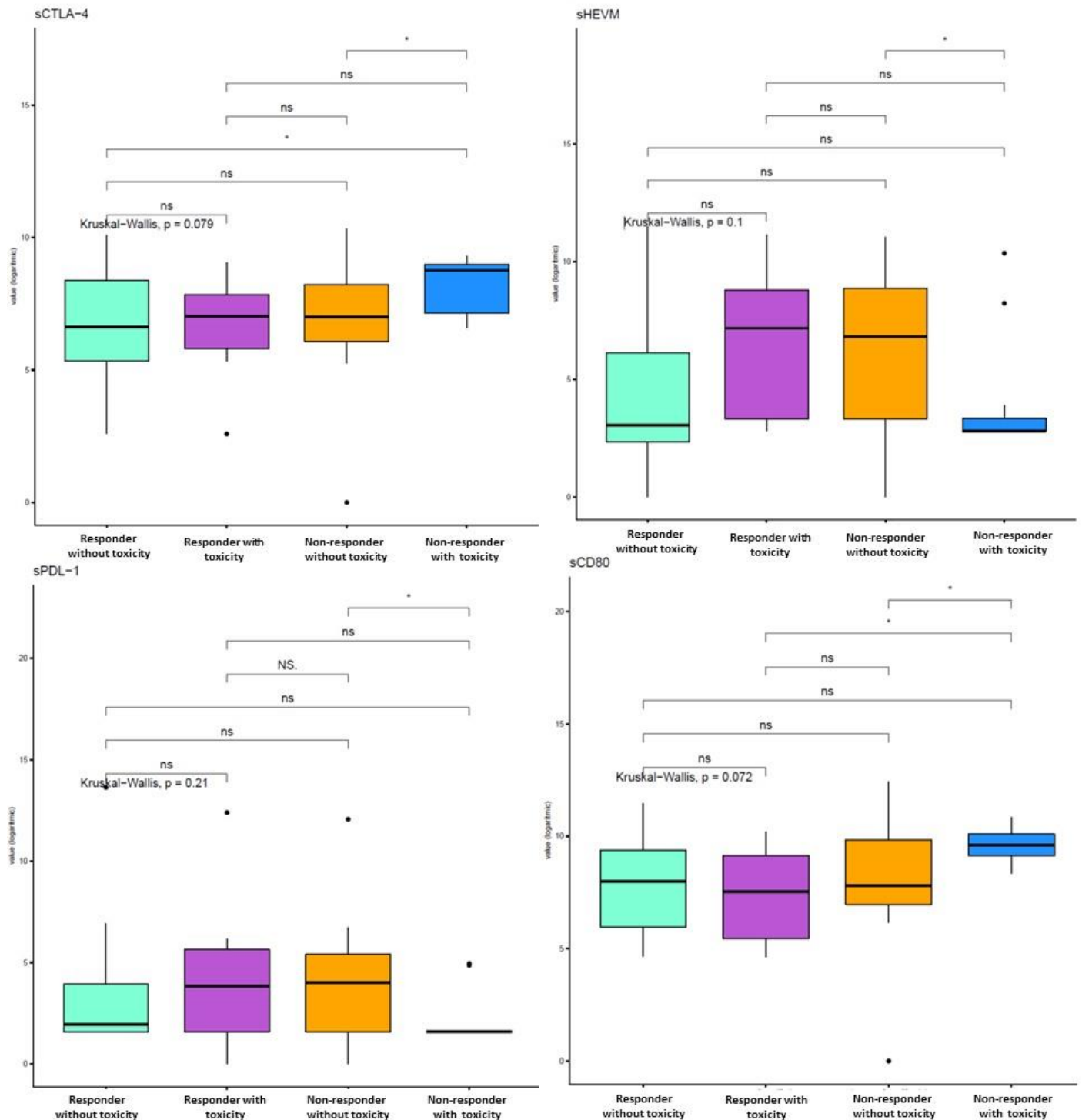


Figure 3 Statistical analysis at T0 for immune-checkpoint molecules. Boxplot of immune-checkpoint molecules expression level (logarithmic scale) in 7 responder patients with toxicity (violet box), 12 responder patients without toxicity (water blue box), 11 non-responder patients with toxicity (blue box), and 23 non-responder patients without toxicity (orange box) at T0. Pairwise p-values (p)

were obtained by applying a Mann-Whitney test for unpaired samples, overall p-value was obtained by applying Kruskal-Wallis test. Legend: * p-value ≤ 0.05 ; ** p-value ≤ 0.01 ; *** p-value ≤ 0.001 .

4.5 Connectivity analysis between circulating molecules in responder and non-responder patients with and without toxicity

To investigate the difference in the molecule connectivity patterns in terms of therapy response and toxicity, we first built four connectivity maps between each pair of the molecule expression values in responder patients with and without cumulative toxicity (Figure 4 AB) and in non-responder patients with and without cumulative toxicity considering all the different cancers type as a whole (Figure 4 CD).

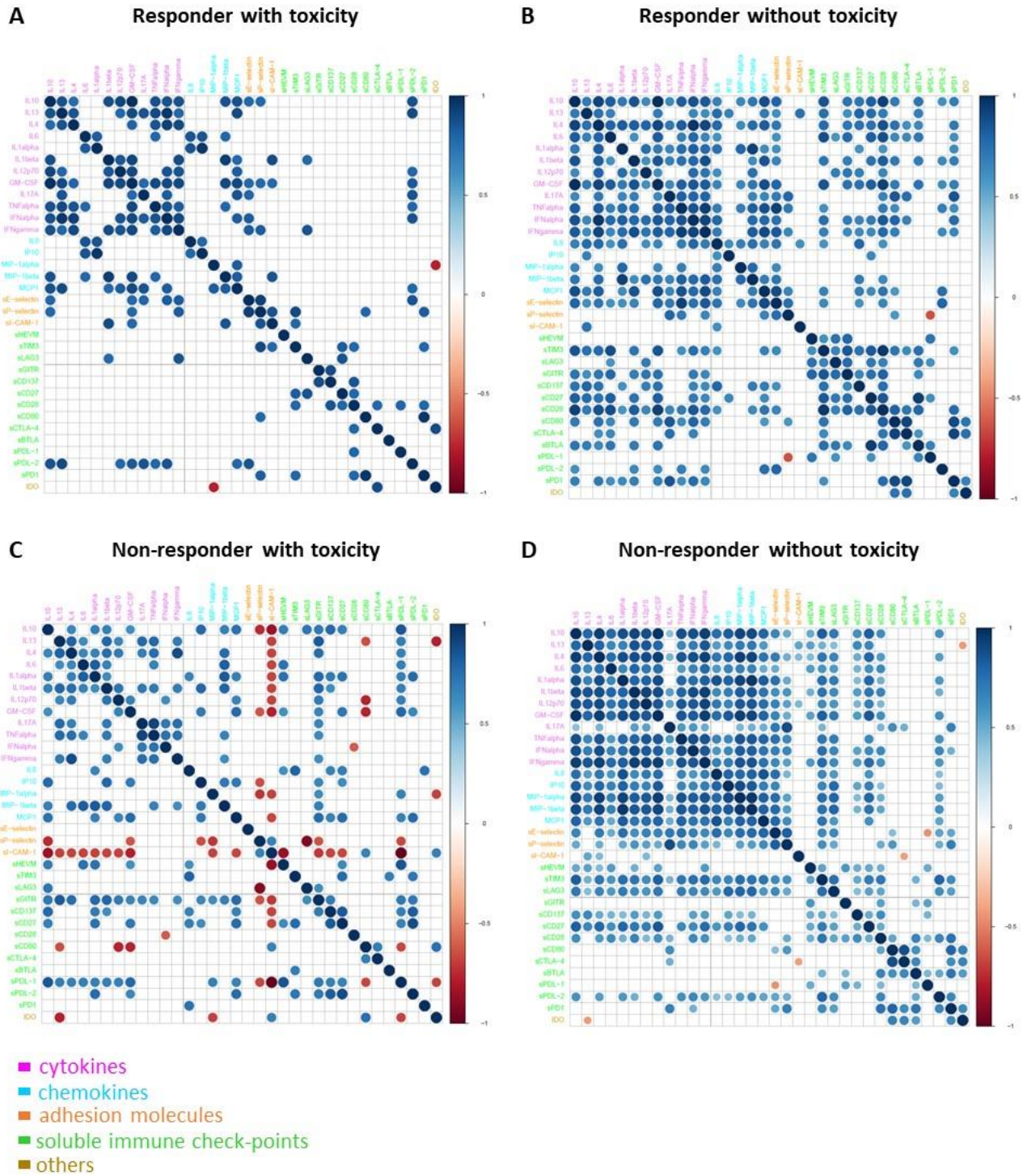


Figure 4 Connectivity map between molecules in responder patients with toxicity (A), responder patients without toxicity (B), non-responder patients with toxicity (C), and non-responder patients without toxicity (D) at T0. Statistically significant Spearman correlations ($p\text{-value} \leq 0.05$) are reported. In the plot, circles are scaled and coloured according to the correlation values, increasing from red (negative correlation) to blue (positive correlation). Molecules are grouped and ordered according to the functional group reported in the legend.

From these maps, we observed a clearly different connectivity patterns from patients with or without toxicity. In particular, by looking at the connectivity map of therapy responder patients without toxicity with respect to those ones with toxicity, we observed a loss of connectivity of mostly of soluble immune check-points and the cytokine correlations moving from one to the other group.

Also moving from non-responder patients without toxicity to those ones with toxicity, we observed a loss of connectivity of mostly of cytokines (e.g., all the connections of the pro-inflammatory cytokines IL13, IL6, IL17A, TNF alpha, or most of the connections of the other groups of chemokines including IL8, MIP-I-alpha), an inversion of the correlation for some adhesion molecules, whose correlation sign from positive became negative (e.g., the correlation of s-Pselectin with the cytokines IL10 and GM-CSF appears positive in non-responder patients without toxicity, while this correlation becomes negative in those ones with toxicity, meaning that if the cytokines value is high the other one is low and *viceversa*), or a null correlation that became negative correlation (e.g., s-ICAM-I appears with no correlation with almost all the cytokines in both responder and non-responder patients without toxicity and responder with toxicity, while it turned on with a strong negative correlation in non-responder patients with toxicity, or IDO that appears with no correlation with the chemokine MIP-1alpha in non-responder patients without toxicity, but showed a strong negative correlation in non-responder patients with toxicity). The non-responder group with toxicity is distinguished from the other 3 by the occurrence of strongly negative correlations. In particular:

- between ICAM-1 and IL-10, GM-CSF, sHVEM, sPDL-1 and many other cytokines (IL13, IL4, IL6, IL1 alpha, IL1 beta and IL12p70),
- between sP-selectin and IL10, GM-CSF, IP10, MIP1alpha, LAG3, sGITR and sPDL1,
- between sCD80 and IL13, GM-CSF, IL12p70, sPDL-1,
- between IDO and IL13, MIP-1alpha and sPDL-1.

G2-G3 toxicities are present in all patients belonging to the non-responder with toxicities group, suggesting that those with the most unfavourable clinical, prognostic and immune characteristics are concentrated in this small sample of patients.

These differences are more evident when the connectivity maps for responder and non-responder patients with and without toxicity were rendered as four corresponding connectivity networks (Figure 5), where two nodes are connected if their expression profiles are statistically significant (p -value ≤ 0.05) and exceed in absolute value a selected correlation threshold (i.e., the 80th percentile of the overall distribution corresponding to 0.7).

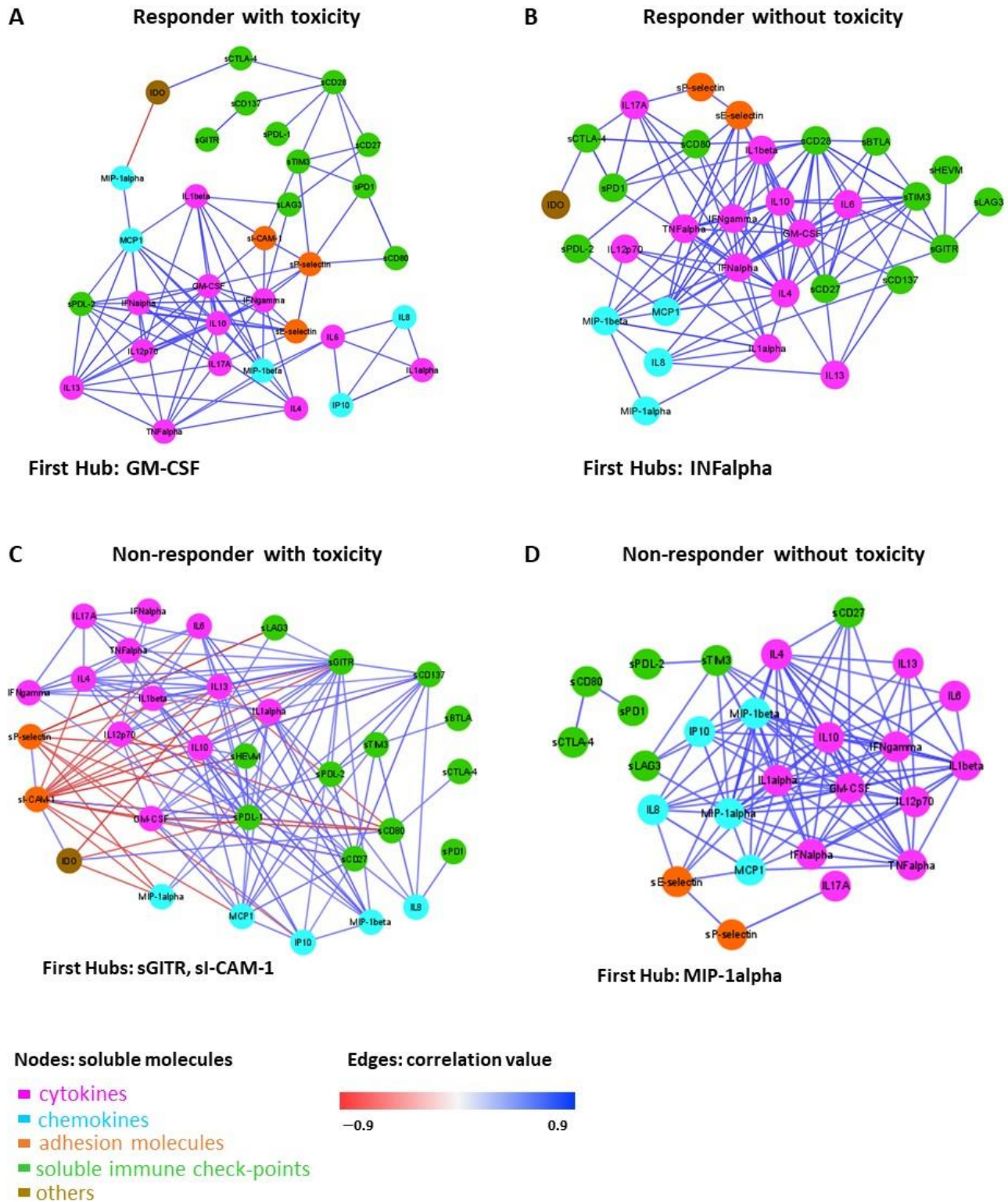


Figure 5 Connectivity network between molecules in responder patients with toxicity (A), responder patients without toxicity (B), non-responder patients with toxicity (C), and non-responder patients without toxicity (D) at T0. In each network, nodes represent molecule and a link occurs between two nodes if the absolute value of Spearman correlation between their expression levels is statistically significant ($p\text{-value} \leq 0.05$) and greater than a selected threshold (i.e., the 80th percentile of the overall distribution corresponding to 0.7). Nodes are colored according to the functional groups reported in the legend; whereas edge colour indicates positive (blue) or negative (red) correlation values.

We identified a total of 95 statistically significant connections (correlations) in responder patients with toxicity (Figure 5A and Table 5), 111 statistically significant connections in responder patients without toxicity (Figure 5B and Table 6), 143 statistically significant connections in non-responder patients with toxicity (Figure 5C and Table 7), and finally 113 statistically significant connections in non-responder patients without toxicity (Figure 5D and Table 8). Interestingly, we found only 14 common connections among the four networks connecting 13 molecules (i.e., Table 9), while a substantial number of connections specifically observed for each group of patients came up (Table 10): 26 connections in responder with toxicity, 38 in responder without toxicity, 80 in non-responder with toxicity, 31 in non-responder without toxicity.

Taken together, these findings highlight a specific signature in terms of network connectivity of the molecules characterizing the different groups of responder and non responder patients with and without toxicity regardless of primary tumor type.

Table 5. Statistically significant connection in responder patients with toxicity. The table reports all the connectivity networks for responder patients with toxicity at T0, along with the correlation values and corresponding p-values.

Source	Target	Correlation	p value
IL10	GM-CSF	0,989071	2,38E-05
IL13	IFNalpha	0,964286	0,002778
IL1alpha	IP10	0,964286	0,002778
sCD80	sPD1	0,964286	0,002778
IL1beta	MIP-1beta	0,936975	0,001851
IL4	IFNalpha	0,928571	0,006746
sE-selectin	sP-selectin	0,928571	0,006746
IL10	IL12p70	0,906327	0,004902
IL1beta	GM-CSF	0,904534	0,005134
IL13	GM-CSF	0,896421	0,006267
IL12p70	GM-CSF	0,896421	0,006267
GM-CSF	TNFalpha	0,896421	0,006267
GM-CSF	IFNalpha	0,896421	0,006267
GM-CSF	IFNgamma	0,896421	0,006267
GM-CSF	MIP-1beta	0,896421	0,006267
GM-CSF	MCP1	0,896421	0,006267
IL13	TNFalpha	0,892857	0,012302
IL4	IFNgamma	0,892857	0,012302
IFNalpha	IFNgamma	0,892857	0,012302
IL13	MCP1	0,892857	0,012302
sP-selectin	sTIM3	0,892857	0,012302
IL13	sPDL-2	0,892857	0,012302

sGITR	sCD137	0,889499	0,007339
IL1beta	IFNgamma	0,882919	0,00845
IL1beta	sI-CAM-1	0,882919	0,00845
sCTLA-4	IDO	0,882919	0,00845
IL10	IL1beta	0,874767	0,009953
IL10	IL13	0,866921	0,011536
IL10	TNFalpha	0,866921	0,011536
IL10	IFNalpha	0,866921	0,011536
IL10	IFNgamma	0,866921	0,011536
IL10	MIP-1beta	0,866921	0,011536
IL10	MCP1	0,866921	0,011536
IL10	sPDL-2	0,866921	0,011536
IL13	IL4	0,857143	0,02381
IL13	IL17A	0,857143	0,02381
IL4	TNFalpha	0,857143	0,02381
IL12p70	IFNalpha	0,857143	0,02381
TNFalpha	IFNalpha	0,857143	0,02381
IL12p70	IFNgamma	0,857143	0,02381
IL6	IL8	0,857143	0,02381
IL1alpha	IL8	0,857143	0,02381
IL6	IP10	0,857143	0,02381
IL17A	MCP1	0,857143	0,02381
MIP-1beta	sI-CAM-1	0,857143	0,02381
sP-selectin	sI-CAM-1	0,857143	0,02381
IFNgamma	sLAG3	0,857143	0,02381
sLAG3	sCD27	0,857143	0,02381
IL17A	sPDL-2	0,857143	0,02381
IFNalpha	sPDL-2	0,857143	0,02381
sE-selectin	sPDL-2	0,857143	0,02381
sCD137	sCD28	0,852437	0,014814
IL1beta	IL12p70	0,846881	0,016197
GM-CSF	sPDL-2	0,83666	0,018927
IL6	IL1alpha	0,821429	0,034127
IL17A	IFNalpha	0,821429	0,034127
TNFalpha	IFNgamma	0,821429	0,034127
IL12p70	MCP1	0,821429	0,034127
IFNalpha	MCP1	0,821429	0,034127
MIP-1alpha	MCP1	0,821429	0,034127
MIP-1beta	MCP1	0,821429	0,034127
IFNalpha	sE-selectin	0,821429	0,034127
IFNgamma	sE-selectin	0,821429	0,034127
IFNgamma	sP-selectin	0,821429	0,034127
sTIM3	sCD27	0,821429	0,034127
sP-selectin	sPD1	0,821429	0,034127
IL4	GM-CSF	0,796819	0,031928

sCD28	sPDL-1	0,792825	0,033444
IL10	sE-selectin	0,78811	0,035283
IL10	sP-selectin	0,78811	0,035283
IL13	IL12p70	0,785714	0,048016
IL6	TNFalpha	0,785714	0,048016
IL13	IFNgamma	0,785714	0,048016
IL8	IP10	0,785714	0,048016
IL6	MIP-1beta	0,785714	0,048016
TNFalpha	MIP-1beta	0,785714	0,048016
IL17A	sE-selectin	0,785714	0,048016
sI-CAM-1	sTIM3	0,785714	0,048016
sTIM3	sCD28	0,785714	0,048016
sCD27	sCD28	0,785714	0,048016
sP-selectin	sCD80	0,785714	0,048016
sCD28	sCTLA-4	0,785714	0,048016
IL12p70	sPDL-2	0,785714	0,048016
TNFalpha	sPDL-2	0,785714	0,048016
MCP1	sPDL-2	0,785714	0,048016
sTIM3	sPD1	0,785714	0,048016
sCD28	sPD1	0,785714	0,048016
GM-CSF	IL17A	0,776899	0,039877
GM-CSF	sE-selectin	0,776899	0,039877
GM-CSF	sP-selectin	0,776899	0,039877
GM-CSF	sI-CAM-1	0,776899	0,039877
IL1beta	MCP1	0,774806	0,040769
IL1beta	sLAG3	0,774806	0,040769
IL10	IL4	0,768408	0,043565
MIP-1alpha	IDO	-0,77481	0,040769

Table 6. Statistically significant connections in responder patients without toxicity. The table reports all the connectivity networks for responder patients without toxicity at T0, along with the correlation values and corresponding p-values.

Source	Target	Correlation	p value
IL10	GM-CSF	0,998045	2,24E-13
IL4	IFNalpha	0,966727	3,04E-07
sTIM3	sCD28	0,950728	2,11E-06
TNFalpha	IFNgamma	0,937063	0
sCD27	sBTLA	0,935203	8,06E-06
GM-CSF	sCD28	0,928549	1,30E-05
IL1alpha	MIP-1beta	0,923077	0
TNFalpha	sE-selectin	0,923077	0
IL10	sCD28	0,923012	1,87E-05

sCD80	sCTLA-4	0,918597	2,45E-05
IFNalpha	IFNgamma	0,914187	3,17E-05
IL10	IL4	0,912839	3,42E-05
IL4	GM-CSF	0,903518	5,59E-05
IL4	IFNgamma	0,902098	0
sCTLA-4	sPD1	0,90176	6,10E-05
IFNgamma	MCP1	0,895105	5,94E-06
sCD80	sPD1	0,892451	9,44E-05
MCP1	sE-selectin	0,888112	9,17E-05
IL1beta	IFNgamma	0,872841	0,000211
IL10	MCP1	0,872186	0,000216
IL6	sTIM3	0,871286	0,000223
IL6	sCD28	0,870339	0,000231
GM-CSF	MCP1	0,870191	0,000232
IL4	sCD28	0,866219	0,000268
IL10	IFNalpha	0,862608	0,000305
TNFalpha	MCP1	0,86014	0,000597
IL1beta	MCP1	0,858705	0,000348
IL1beta	GM-CSF	0,857011	0,000368
GM-CSF	sTIM3	0,85538	0,000389
IL10	IL1beta	0,855335	0,000389
IL17A	sPD1	0,852637	0,000425
TNFalpha	IFNalpha	0,85114	0,000446
IL10	sTIM3	0,850012	0,000462
IFNalpha	sCD28	0,846573	0,000514
GM-CSF	IFNalpha	0,845751	0,000528
sTIM3	sGITR	0,844758	0,000544
sCD27	sCD28	0,843045	0,000573
IL17A	sCD80	0,84249	0,000582
IFNgamma	sE-selectin	0,839161	0,001192
IL10	IFNgamma	0,838924	0,000647
sTIM3	sCD27	0,830124	0,000831
GM-CSF	IFNgamma	0,829459	0,000847
IL6	GM-CSF	0,829334	0,00085
IL1beta	sCD28	0,829187	0,000853
IL10	IL6	0,827713	0,000888
IL4	IL1alpha	0,825175	0,001719
IL4	TNFalpha	0,825175	0,001719
IFNgamma	MIP-1beta	0,825175	0,001719
IL4	MCP1	0,825175	0,001719
IL10	TNFalpha	0,820446	0,001078
IL4	IL1beta	0,819834	0,001095
IL6	sCD27	0,816275	0,0012
IL1alpha	IFNalpha	0,816113	0,001205
GM-CSF	sCD27	0,812366	0,001324
TNFalpha	MIP-1beta	0,811189	0,002369

GM-CSF	TNFalpha	0,810944	0,001372
IL10	sCD27	0,810778	0,001377
sCD28	sCD80	0,809948	0,001406
IL17A	TNFalpha	0,807023	0,001509
sGITR	sCD28	0,803262	0,001651
IL13	sCD137	0,798592	0,001841
IL4	IL12p70	0,797203	0,003161
sE-selectin	sPDL-2	0,797203	0,003161
IFNalpha	sCD80	0,795073	0,001995
IL10	sE-selectin	0,794576	0,002017
IL17A	IFNalpha	0,794377	0,002026
IL4	IL6	0,793682	0,002058
IL17A	IFNgamma	0,792987	0,00209
sHEVM	sGITR	0,789637	0,002251
sCD28	sBTLA	0,788752	0,002295
GM-CSF	sE-selectin	0,788727	0,002297
IL8	sCD137	0,786607	0,002405
IFNalpha	IL8	0,785965	0,002439
IL1beta	IFNalpha	0,785871	0,002443
IL17A	sP-selectin	0,783832	0,002553
IL1alpha	MIP-1alpha	0,783217	0,004115
IL6	sGITR	0,779086	0,002821
IL4	IL8	0,777584	0,00291
MIP-1alpha	MIP-1beta	0,776224	0,00466
IFNgamma	sCD28	0,774667	0,00309
IFNalpha	MIP-1beta	0,774082	0,003127
IL6	IFNalpha	0,773871	0,00314
IFNalpha	MCP1	0,770579	0,003355
IL4	MIP-1beta	0,769231	0,005253
IL12p70	IFNalpha	0,767076	0,003596
IFNalpha	sPD1	0,763574	0,00385
IL13	IL8	0,762743	0,003912
IL13	sCD27	0,762743	0,003912
IL1alpha	TNFalpha	0,762238	0,005897
IL1alpha	IFNgamma	0,762238	0,005897
IL4	sTIM3	0,762238	0,005897
sLAG3	sGITR	0,760888	0,004054
sCD28	sPD1	0,760582	0,004078
IL17A	sCTLA-4	0,758803	0,004218
sE-selectin	sP-selectin	0,756569	0,004398
IFNalpha	sTIM3	0,756569	0,004398
IL1alpha	IL12p70	0,755245	0,006597
MCP1	sPDL-2	0,755245	0,006597
IL1alpha	IL8	0,749563	0,005004

IL1beta	TNFalpha	0,749159	0,005041
sCTLA-4	IDO	0,748683	0,005084
IL12p70	MIP-1beta	0,748252	0,007353
sTIM3	sBTLA	0,748252	0,007353
sCD137	sCD28	0,744681	0,005462
IL8	MIP-1beta	0,742558	0,005671
sGITR	sCD27	0,740912	0,005836
IL13	sTIM3	0,740355	0,005893
GM-CSF	sCD137	0,738364	0,0061
IL4	sCD80	0,737242	0,006219
GM-CSF	sBTLA	0,736885	0,006258
IL13	IL4	0,733338	0,006647

Table 7. Statistically significant connection in non-responder patients with toxicity. The table reports all the connectivity networks for non-responder patients with toxicity at T0, along with the correlation values and corresponding p-values.

Source	Target	Correlation	p value
IL17A	TNFalpha	0,917808	6,80E-05
IL4	IFNgamma	0,888385	0,000258
sCD27	sPDL-2	0,883829	0,000307
sHEVM	sPDL-1	0,857493	0,000739
IL10	sPDL-1	0,840343	0,001201
IL13	sGITR	0,831497	0,00151
IL1alpha	MIP-1beta	0,831059	0,001527
sCD137	sCD27	0,83105	0,001527
sCD137	sPDL-2	0,829159	0,001601
IL6	MIP-1beta	0,819241	0,002032
IL6	IL1alpha	0,818393	0,002073
IL13	IL4	0,808632	0,002585
IL8	sTIM3	0,801824	0,002993
IL1beta	MIP-1beta	0,794529	0,003482
IL13	IL1beta	0,782375	0,004426
IL1beta	IP10	0,78083	0,004558
IL1beta	sGITR	0,780628	0,004575
GM-CSF	sPDL-1	0,777817	0,004824
IL10	sCD137	0,77645	0,004949
IL1alpha	sGITR	0,775839	0,005005
IL10	IP10	0,774683	0,005113
IL13	IL17A	0,771239	0,005445
IL13	TNFalpha	0,771239	0,005445
MCP1	sCD27	0,769934	0,005575
sTIM3	sCD27	0,769934	0,005575
IL1alpha	sPDL-2	0,767131	0,005861

IL4	MIP-1beta	0,765378	0,006046
MCP1	sPDL-2	0,763636	0,009216
MCP1	sGITR	0,76277	0,006328
GM-CSF	MCP1	0,76277	0,006328
IL4	TNFalpha	0,753425	0,00742
IL4	IL1beta	0,752862	0,00749
IL17A	IFNgamma	0,75171	0,007634
IL4	sGITR	0,750175	0,00783
TNFalpha	IFNgamma	0,742599	0,00885
sCD80	IDO	0,741967	0,008939
IL1alpha	sHEVM	0,737575	0,009578
IL8	sPD1	0,736844	0,009687
IL10	MCP1	0,734214	0,010088
IL6	sHEVM	0,733451	0,010207
IL1alpha	sCD27	0,732267	0,010393
TNFalpha	IFNalpha	0,731052	0,010586
IL1beta	IL12p70	0,725402	0,011521
sTIM3	sPDL-2	0,718182	0,016799
GM-CSF	sCD27	0,716728	0,013069
IL10	sLAG3	0,71109	0,014153
IP10	MIP-1beta	0,709091	0,018728
IP10	MCP1	0,709091	0,018728
IL17A	IFNalpha	0,708063	0,014761
sGITR	sPDL-1	0,707107	0,014956
IL1beta	TNFalpha	0,707096	0,014959
sGITR	sPDL-2	0,705562	0,015277
IL10	sGITR	0,703353	0,015743
IL1beta	IL17A	0,700231	0,01642
IL12p70	sGITR	0,697615	0,017003
sGITR	sCD137	0,697615	0,017003
IL1alpha	sCD137	0,695654	0,01745
IL4	IL12p70	0,694064	0,017818
GM-CSF	IP10	0,693909	0,017854
IL13	IFNgamma	0,690204	0,018735
IL8	sCD27	0,689498	0,018906
IL10	sHEVM	0,6875	0,019397
IL13	sPDL-1	0,684797	0,020076
sCD80	sCTLA-4	0,684212	0,020225
sTIM3	sBTLA	0,683373	0,02044
IL1beta	IFNgamma	0,680372	0,021223
IL10	sCD27	0,677945	0,021871
IL1alpha	sPDL-1	0,677285	0,02205
IL1beta	sPDL-1	0,677285	0,02205
MIP-1beta	sGITR	0,676958	0,022139
IL4	sPDL-1	0,675737	0,022473
IL12p70	sPDL-1	0,675737	0,022473

sCD137	sPDL-1	0,675737	0,022473
sI-CAM-1	IDO	0,675174	0,022629
MIP-1alpha	sPDL-1	0,6742	0,022899
IL10	IL1alpha	0,67369	0,023042
IL10	IL1beta	0,67369	0,023042
IL6	sPDL-1	0,672056	0,023503
IL1alpha	MCP1	0,67124	0,023736
IL4	IL17A	0,671233	0,023738
IL10	MIP-1beta	0,670621	0,023914
sCD27	sPDL-1	0,66898	0,024389
IL8	sCD137	0,66895	0,024398
IL12p70	GM-CSF	0,668946	0,024399
sP-selectin	sI-CAM-1	0,666806	0,02503
TNFalpha	MIP-1beta	0,66515	0,025525
MCP1	sCD137	0,66515	0,025525
IL6	TNFalpha	0,662851	0,026225
sI-CAM-1	sCD80	0,662223	0,026418
IL6	IL1beta	0,662071	0,026465
IL4	IL1alpha	0,661329	0,026695
MCP1	sPDL-1	0,660716	0,026886
IL17A	sGITR	0,654611	0,028843
IL1alpha	IL8	0,652176	0,029651
IL12p70	MCP1	0,651482	0,029884
GM-CSF	sGITR	0,65	0,030386
IL4	IL6	0,649089	0,030697
IP10	sGITR	0,648355	0,03095
GM-CSF	sPDL-2	0,646236	0,031688
IL10	IL4	0,646076	0,031744
IL13	IL12p70	0,640362	0,033797
TNFalpha	sGITR	0,635499	0,035615
sHEVM	sCD27	0,625795	0,039446
IFNgamma	sGITR	0,619751	0,041972
IP10	sCD27	0,619592	0,04204
IL1alpha	IL1beta	0,619266	0,042179
IFNgamma	MIP-1beta	0,618182	0,047817
IL13	IL6	0,61748	0,042949
IL1beta	sCD137	0,615562	0,043787
IL12p70	IFNalpha	0,611509	0,045594
MIP-1alpha	sGITR	0,610216	0,046181
sLAG3	sGITR	0,610216	0,046181
IL10	GM-CSF	0,606339	0,047972
GM-CSF	sHEVM	0,606339	0,047972
GM-CSF	sP-selectin	-0,62546	0,039582
sP-selectin	sGITR	-0,63509	0,035773

IP10	sP-selectin	-0,64223	0,033116
IL13	sCD80	-0,64737	0,03129
MCP1	sI-CAM-1	-0,66072	0,026886
sCD80	sPDL-1	-0,66222	0,026418
sP-selectin	sPDL-1	-0,66681	0,02503
sI-CAM-1	sCD27	-0,66898	0,024389
IL6	sI-CAM-1	-0,67206	0,023503
MIP-1alpha	sI-CAM-1	-0,6742	0,022899
sPDL-1	IDO	-0,67517	0,022629
IL4	sI-CAM-1	-0,67574	0,022473
IL12p70	sI-CAM-1	-0,67574	0,022473
sI-CAM-1	sCD137	-0,67574	0,022473
IL1alpha	sI-CAM-1	-0,67729	0,02205
IL1beta	sI-CAM-1	-0,67729	0,02205
IL13	sI-CAM-1	-0,6848	0,020076
MIP-1alpha	IDO	-0,6851	0,019998
sI-CAM-1	sGITR	-0,70711	0,014956
MIP-1alpha	sP-selectin	-0,71563	0,013276
IL10	sP-selectin	-0,74098	0,00908
GM-CSF	sCD80	-0,76451	0,006139
IL12p70	sCD80	-0,76712	0,005862
GM-CSF	sI-CAM-1	-0,77782	0,004824
IL13	IDO	-0,77838	0,004774
IL10	sI-CAM-1	-0,84034	0,001201
sI-CAM-1	sHEVM	-0,85749	0,000739
sP-selectin	sLAG3	-0,91747	6,92E-05
sI-CAM-1	sPDL-1	-1	2,12E-70

Table 8. Statistically significant connection in non-responder patients without toxicity. The table reports all the connectivity networks for non-responder patients without toxicity at T0, along with the correlation values and corresponding p-values.

Source	Target	Correlation	p value
IL10	GM-CSF	0,977961	9,08E-16
IL1alpha	MIP-1beta	0,963183	1,86E-13
MIP-1alpha	MIP-1beta	0,952569	2,74E-06
GM-CSF	IFNgamma	0,939151	3,27E-11
IL4	GM-CSF	0,938052	3,93E-11
IL1beta	IFNgamma	0,937281	4,46E-11
IL10	IFNgamma	0,934754	6,68E-11
IL4	MIP-1alpha	0,931785	1,05E-10

IL10	IL4	0,931139	1,16E-10
GM-CSF	MIP-1alpha	0,930296	1,31E-10
IL4	IFNgamma	0,92783	1,87E-10
IL12p70	IFNgamma	0,916234	8,47E-10
IL1beta	IL12p70	0,914099	1,09E-09
IL4	MIP-1beta	0,912506	1,32E-09
IL1alpha	MIP-1alpha	0,912281	1,35E-09
GM-CSF	MIP-1beta	0,909982	1,75E-09
IL10	MIP-1alpha	0,908265	2,12E-09
IL10	IL1beta	0,901411	4,39E-09
IL10	MIP-1beta	0,891455	1,15E-08
IL4	IL12p70	0,887763	1,61E-08
IP10	MIP-1alpha	0,887352	3,02E-06
IL1alpha	GM-CSF	0,887282	1,68E-08
IL1beta	GM-CSF	0,886809	1,75E-08
IL17A	sP-selectin	0,883032	2,43E-08
IL1beta	IFNalpha	0,881192	2,84E-08
IL10	IFNalpha	0,878856	3,44E-08
IL4	IFNalpha	0,877851	3,74E-08
IL4	IL1beta	0,877454	3,86E-08
sCD80	sCTLA-4	0,876794	4,07E-08
IL10	IL12p70	0,876389	4,21E-08
IL4	IL1alpha	0,876143	4,29E-08
TNFalpha	IFNalpha	0,872928	5,53E-08
IL10	IL1alpha	0,872058	5,92E-08
IL10	TNFalpha	0,87053	6,66E-08
IL1alpha	IL8	0,869286	7,32E-08
IFNgamma	MIP-1alpha	0,857708	2,09E-06
TNFalpha	IFNgamma	0,856931	1,79E-07
IFNgamma	MIP-1beta	0,855731	2,03E-06
IL13	IL1beta	0,853783	2,21E-07
IL8	MCP1	0,852767	1,94E-06
TNFalpha	MIP-1alpha	0,851001	2,66E-07
IL12p70	GM-CSF	0,848206	3,19E-07
IL12p70	MIP-1beta	0,848036	3,23E-07
IFNalpha	IFNgamma	0,847947	3,25E-07
IL12p70	TNFalpha	0,847257	3,39E-07
GM-CSF	sCD27	0,846983	3,45E-07
IL4	TNFalpha	0,845983	3,68E-07
IL13	IFNgamma	0,84502	3,91E-07
IL13	IL12p70	0,842496	4,58E-07
IL1beta	MIP-1beta	0,842158	4,68E-07

TNFalpha	MIP-1beta	0,841611	4,84E-07
GM-CSF	TNFalpha	0,840912	5,05E-07
IP10	MIP-1beta	0,836957	1,71E-06
IL12p70	MIP-1alpha	0,833704	7,78E-07
IL12p70	IFNalpha	0,832303	8,44E-07
GM-CSF	IP10	0,831328	8,93E-07
IFNalpha	MIP-1alpha	0,827145	1,13E-06
GM-CSF	IFNalpha	0,826602	1,17E-06
IL1beta	MIP-1alpha	0,826221	1,19E-06
IL10	sTIM3	0,824214	1,33E-06
IL1alpha	MCP1	0,82382	1,36E-06
IL10	IP10	0,820138	1,66E-06
IL1alpha	IFNgamma	0,818384	1,83E-06
GM-CSF	sTIM3	0,818306	1,83E-06
IFNalpha	MIP-1beta	0,816743	1,99E-06
sE-selectin	sP-selectin	0,815258	2,15E-06
IL10	sCD27	0,811934	2,56E-06
IL8	MIP-1beta	0,8083	4,25E-06
IL1alpha	IL12p70	0,80524	3,58E-06
IL1alpha	IP10	0,802076	4,17E-06
MIP-1alpha	MCP1	0,800395	6,35E-06
MIP-1beta	MCP1	0,800395	6,35E-06
IL1alpha	IL1beta	0,799028	4,83E-06
sTIM3	sPDL-2	0,797134	5,28E-06
TNFalpha	MCP1	0,796145	5,53E-06
sCD80	sPD1	0,795342	5,74E-06
IL6	IL1beta	0,794715	5,91E-06
GM-CSF	MCP1	0,793304	6,31E-06
IL10	MCP1	0,792631	6,51E-06
IL8	IP10	0,791502	9,94E-06
IL13	IL4	0,790765	7,09E-06
IL1beta	TNFalpha	0,790061	7,32E-06
MIP-1alpha	sCD27	0,789483	7,51E-06
IL10	IL13	0,789291	7,58E-06
MIP-1alpha	sLAG3	0,785767	8,87E-06
IL1alpha	sCD27	0,784712	9,29E-06
MCP1	sE-selectin	0,783597	1,45E-05
IL13	GM-CSF	0,78351	9,79E-06
IL1alpha	TNFalpha	0,782501	1,02E-05
IL4	sCD27	0,781429	1,07E-05
MIP-1beta	sLAG3	0,78132	1,08E-05
IL4	IP10	0,780524	1,11E-05

IL10	IL6	0,779379	1,17E-05
MIP-1beta	sE-selectin	0,77668	1,99E-05
IL6	IFNgamma	0,774164	1,46E-05
IL8	MIP-1alpha	0,773715	2,27E-05
IP10	sLAG3	0,772918	1,54E-05
IFNgamma	sTIM3	0,769763	2,70E-05
IFNgamma	sCD27	0,76565	2,07E-05
IL1alpha	IFNalpha	0,759972	2,59E-05
MIP-1alpha	sTIM3	0,757905	4,36E-05
IL12p70	MCP1	0,757598	2,83E-05
IL1alpha	sTIM3	0,757104	2,89E-05
IL6	GM-CSF	0,755581	3,06E-05
IL8	sE-selectin	0,751976	5,47E-05
MIP-1alpha	sE-selectin	0,751976	5,47E-05
GM-CSF	IL8	0,751633	3,55E-05
IL10	IL8	0,75086	3,66E-05
IL4	IL6	0,750045	3,77E-05
IL1alpha	sE-selectin	0,747714	4,11E-05
sTIM3	sLAG3	0,747714	4,11E-05
IFNalpha	sTIM3	0,74344	4,80E-05

Table 9. Molecule network connections shared among the four patient groups, connecting 13 molecules.

Source	Target	P value non-responder with tox	P value non-responder Without tox	P value responder with_tox	P value responder Without tox
GM-CSF	MCP1	0,006328	6,31E-06	0,006267	0,000232
IL10	GM-CSF	0,047972	9,08E-16	2,38E-05	2,24E-13
IL10	IL1beta	0,023042	4,39E-09	0,009953	0,000389
IL10	IL4	0,031744	1,16E-10	0,043565	3,42E-05
IL10	MCP1	0,010088	6,51E-06	0,011536	0,000216
IL12p70	IFNalpha	0,045594	8,44E-07	0,02381	0,003596
IL13	IL4	0,002585	7,09E-06	0,02381	0,006647
IL1alpha	IL8	0,029651	7,32E-08	0,02381	0,005004
IL1beta	IFNgamma	0,021223	4,46E-11	0,00845	0,000211
IL4	IFNgamma	0,000258	1,87E-10	0,012302	0
IL4	TNFalpha	0,00742	3,68E-07	0,02381	0,001719
TNFalpha	IFNalpha	0,010586	5,53E-08	0,02381	0,000446
TNFalpha	IFNgamma	0,00885	1,79E-07	0,034127	0
TNFalpha	MIP-1beta	0,025525	4,84E-07	0,048016	0,002369

Table 10. Network connections specifically present in each group of patients.

Connections	Responder with toxicity	Responder without toxicity	Non-responder with toxicity	Non-responder without toxicity
Number	26	37	80	31
Type				
	GM-CSF IL17A	GM-CSF sBTLA	GM-CSF sCD80	GM-CSF IL8
	IFNalpha sEselectin	GM-CSF sCD137	GM-CSF sGITR	GM-CSF MIP-1alpha
	IFNalpha sPDL-2	GM-CSF sCD28	GM-CSF sHEVM	IFNalpha MIP-1alpha
	IFNgamma sLAG3	IFNalpha IL8	GM-CSF sPDL-1	IFNgamma MIP-1alpha
	IFNgamma sP-selectin	IFNalpha sCD28	IFNgamma sGITR	IFNgamma sCD27
	IL10 sPDL-2	IFNalpha sCD80	IL10 sCD137	IFNgamma sTIM3
	IL12p70 sPDL-2	IFNalpha sPD1	IL10 sGITR	IL10 IL8
	IL13 IFNalpha	IFNgamma MCP1	IL10 sHEVM	IL10 MIP-1alpha
	IL13 MCP1	IFNgamma sCD28	IL10 sI-CAM-1	IL12p70 MIP-1alpha
	IL13 sPDL-2	IL10 sCD28	IL10 sLAG3	IL12p70 TNFalpha
	IL17A MCP1	IL13 IL8	IL10 sPDL-1	IL1alpha GM-CSF
	IL17A sE-selectin	IL13 sCD137	IL12p70 sCD80	IL1alpha sE-selectin
	IL17A sPDL-2	IL13 sCD27	IL12p70 sGITR	IL1alpha sTIM3
	IL1beta sLAG3	IL13 sTIM3	IL12p70 sI-CAM-1	IL1beta MIP-1alpha
	IL6 IL8	IL17A sCD80	IL12p70 sPDL-1	IL4 IP10
	IL6 IP10	IL17A sCTLA-4	IL13 IDO	IL4 MIP-1alpha
	MIP-1beta sI-CAM-1	IL17A sPD1	IL13 IL6	IL4 sCD27
	sCD28 sCTLA-4	IL1beta sCD28	IL13 sCD80	IL6 IFNgamma
	sCD28 sPDL-1	IL4 IL8	IL13 sGITR	IL8 MCP1
	sI-CAM-1 sTIM3	IL4 MCP1	IL13 sI-CAM-1	IL8 MIP-1alpha
	sLAG3 sCD27	IL4 sCD28	IL13 sPDL-1	IL8 sE-selectin
	sP-selectin sCD80	IL4 sCD80	IL17A sGITR	IP10 MIP-1alpha
	sP-selectin sPD1	IL4 sTIM3	IL1alpha sCD137	IP10 sLAG3
	sP-selectin sTIM3	IL6 IFNalpha	IL1alpha sGITR	MIP-1alpha sCD27
	sTIM3 sPD1	IL6 sCD27	IL1alpha sHEVM	MIP-1alpha sE-selectin
	TNFalpha sPDL-2	IL6 sCD28	IL1alpha sI-CAM-1	MIP-1alpha sLAG3
		IL6 sGITR	IL1alpha sPDL-1	MIP-1alpha sTIM3
		IL6 sTIM3	IL1alpha sPDL-2	MIP-1beta sE-selectin
		sCD27 sBTLA	IL1beta IL17A	MIP-1beta sLAG3
		sCD28 sBTLA	IL1beta IP10	sTIM3 sLAG3
		sCD28 sCD80	IL1beta sCD137	TNFalpha MIP-1alpha
		sCTLA-4 sPD1	IL1beta sGITR	
		sGITR sCD27	IL1beta sPDL-1	
		sGITR sCD28	IL4 IL17A	
		sHEVM sGITR	IL4 sGITR	
		sTIM3 sGITR	IL4 sI-CAM-1	
		TNFalpha sE-selectin	IL4 sPDL-1	
			IL6 sHEVM	
			IL6 sI-CAM-1	
			IL6 sPDL-1	
			IL8 sCD27	
			IL8 sPD1	
			IL8 sTIM3	
			IP10 MCP1	

			IP10	sCD27	
			IP10	sGITR	
			IP10	sP-selectin	
			MCP1	sCD137	
			MCP1	sCD27	
			MCP1	sGITR	
			MCP1	sI-CAM-1	
			MCP1	sPDL-1	
			MIP-1alpha	sGITR	
			MIP-1alpha	sI-CAM-1	
			MIP-1alpha	sP-selectin	
			MIP-1alpha	sPDL-1	
			MIP-1beta	sGITR	
			sCD137	sCD27	
			sCD137	sPDL-1	
			sCD137	sPDL-2	
			sCD27	sPDL-1	
			sCD27	sPDL-2	
			sCD80	IDO	
			sCD80	sPDL-1	
			sGITR	sPDL-1	
			sGITR	sPDL-2	
			sHEVM	sCD27	
			sHEVM	sPDL-1	
			sI-CAM-1	IDO	
			sI-CAM-1	sCD137	
			sI-CAM-1	sCD27	
			sI-CAM-1	sCD80	
			sI-CAM-1	sGITR	
			sI-CAM-1	sHEVM	
			sI-CAM-1	sPDL-1	
			sP-selectin	sGITR	
			sP-selectin	sLAG3	
			sP-selectin	sPDL-1	
			sPDL-1	IDO	
			TNFalpha	sGITR	

4.6 Survival analysis: circulating molecules and connectivity map

The Kaplan Meier analysis confirms that also in terms of the OS (Figure 6A) and PFS (Figure 6B), a statistically significance difference has been overall observed for patients belonging to the four

groups (i.e., log rank test p-value < 0.0001). In particular, we observed that patients responding to the therapy (responder patients) show a higher OS and PFS rates with respect to the non-responder ones, but no statistically distinction was shown between the two groups of responder patients with and without toxicity, suggesting that the toxicity was not determining an increasing of survival rate or PFS.

Looking at the OS values, we computed also the statistical differences of the soluble molecules by dividing the cohort of patients into patients with an OS greater and lower than a selected cut-off (i.e., median value of the OS, equal to 11 months). We observed that almost all the cytokines, two chemokines (i.e., MIP-1alpha, IL8), and most of the sICs showed a statistically significant down-regulation in patients with a greater OS value (Figure 7). Looking at the PFS values, we observed that three cytokines (i.e., IL10, IL12p70, and GM-CSF) and one most of the sIC (i.e., sCD27) were statistically significant down-regulated in patients with a PFS value higher than the selected cut-off (i.e., median value of the PFS, 4 months), (Figure 8).

No connectivity differences were instead observed when we compared the correlations maps of patients with OS (Figure 9) or PFS (Figure 10) higher and lower the selected cut-offs. Although in patients with OS below median, a loss of correlations is observed: between P-selectin and E-selectin and most cytokines/chemokines and some of the soluble checkpoints, and between sCD28 and sCD80 and cytokines/chemokines. Furthermore, in the group with PFS below the median value, a loss of correlation is observed between P-selectin and E-selectin and several cytokines/chemokines and between PDL-2 and sPD1, cytokines/chemokines and some adhesion molecules.

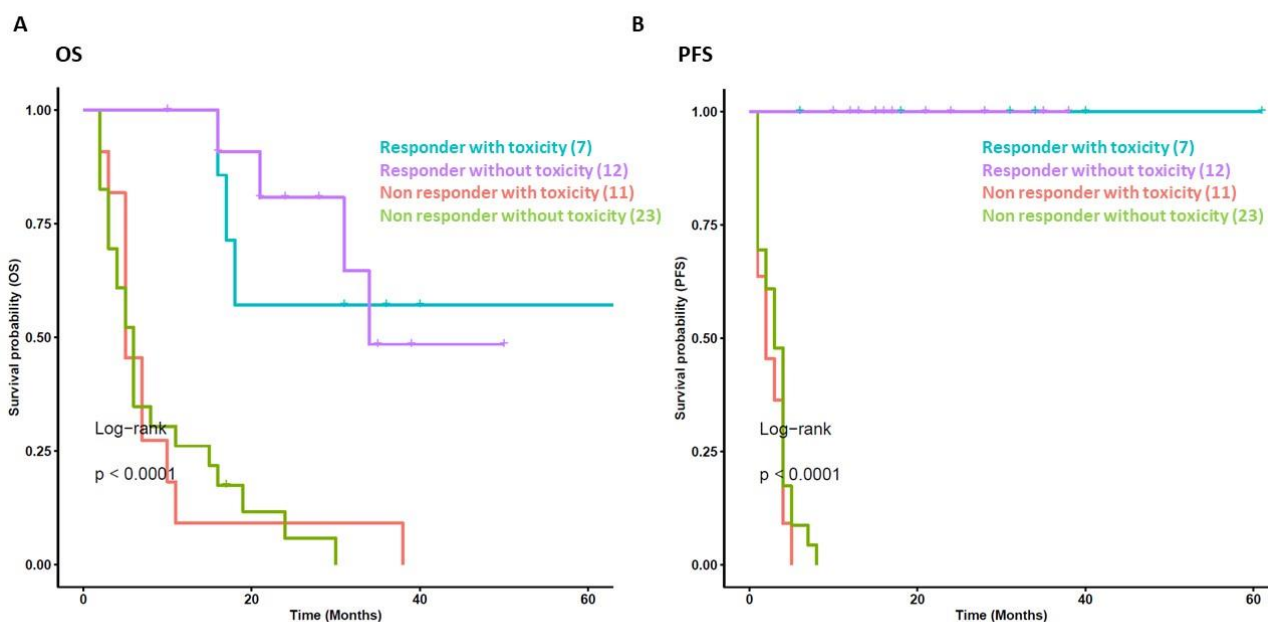
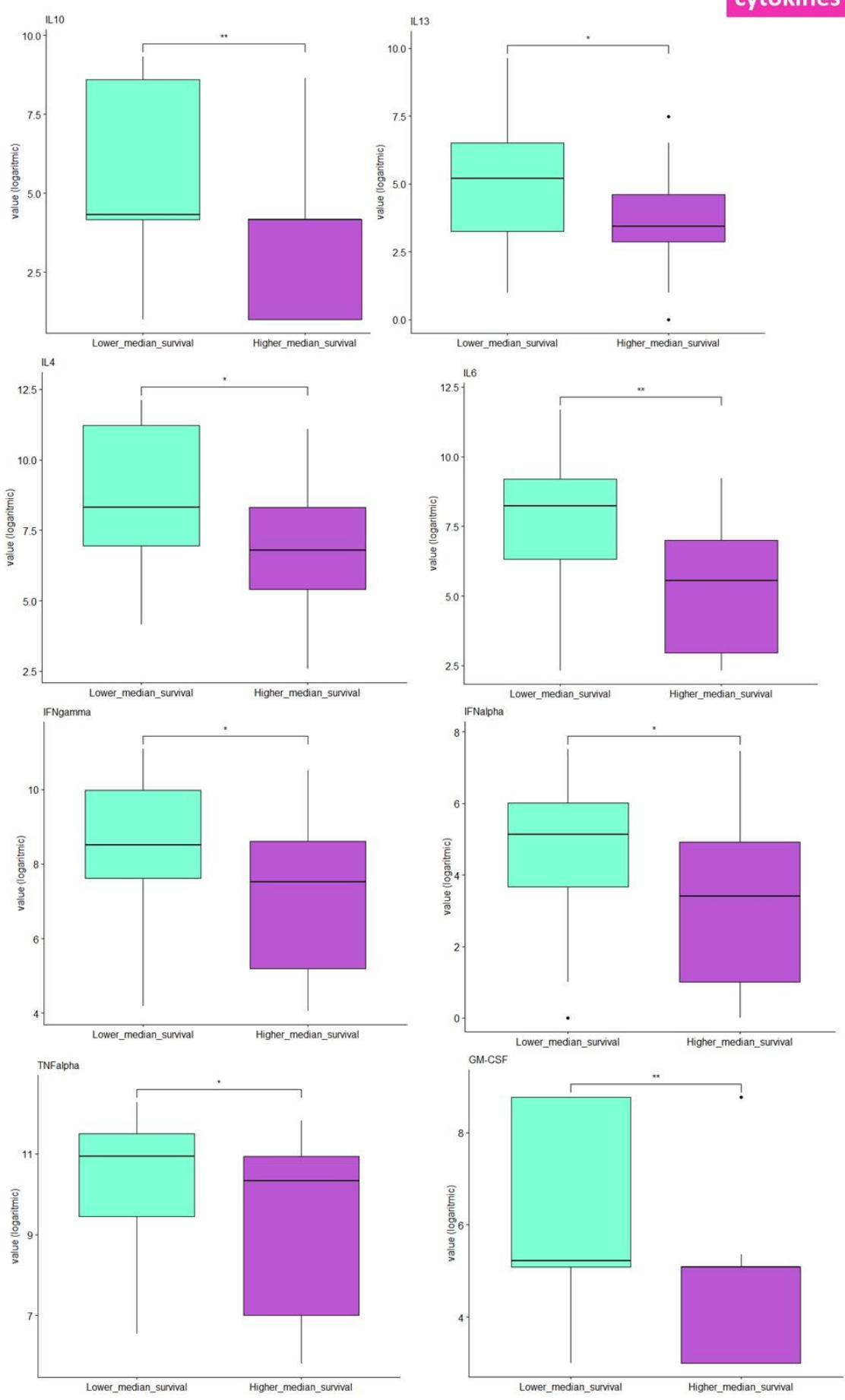


Figure 6. Kaplan-Meier analysis. 53 patients were classified into four groups: first class including 7 responder patients with toxicity (cyan curve), second class including 12 responder patients with toxicity (violet curve), third class including 11 non-responder patients with toxicity (light red curve), fourth class including 23 non-responder patients without toxicity (green curve). The correlation between variable value and patient survival was examined as overall survival (OS) [panel A] and progression free survival (PFS) [panel B]. The prognosis of each group of patients was examined by Kaplan-Meier survival estimators, and the survival outcomes of the two groups were compared by log-rank tests. Log rank p-values less than or equal to 0.05 were considered as statistically significant.

cytokines

A



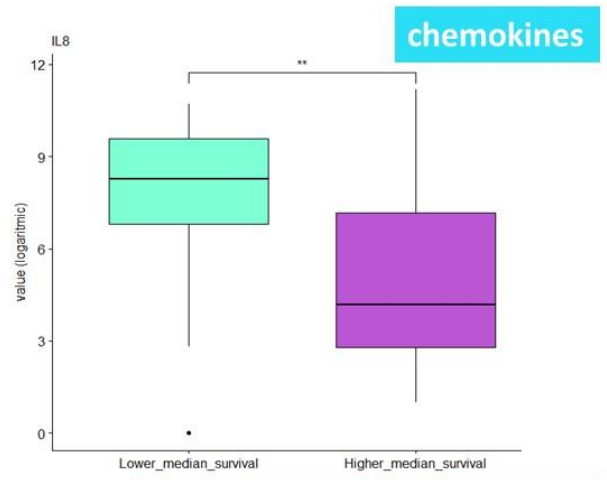
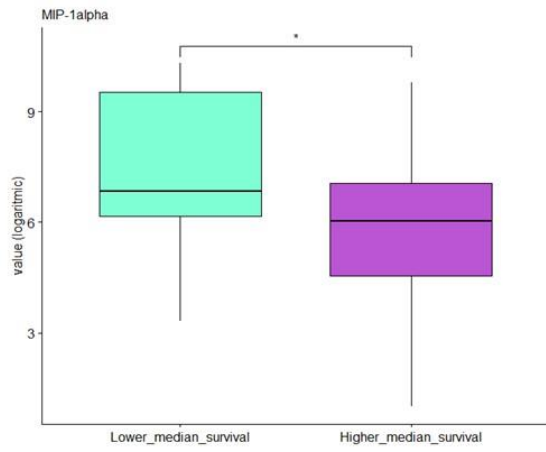
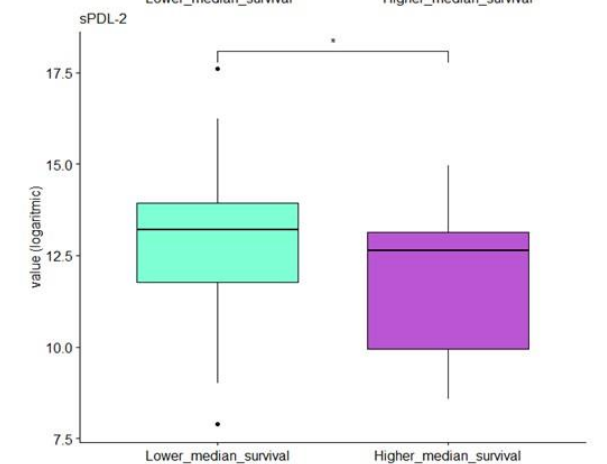
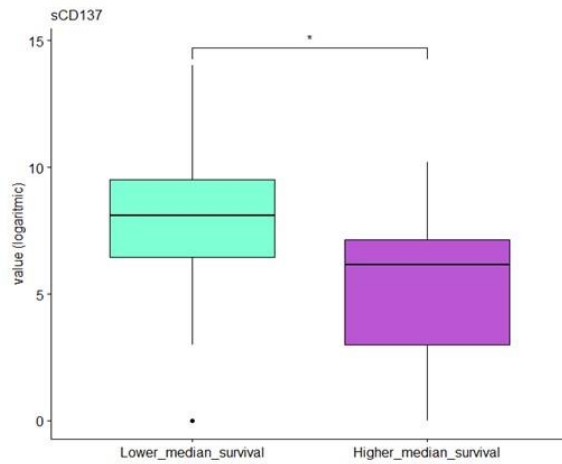
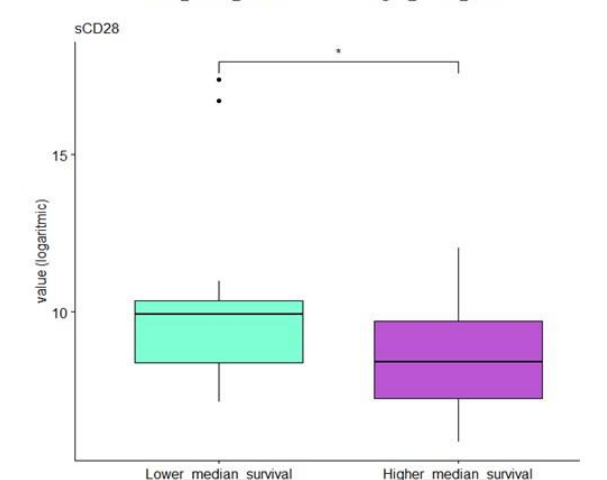
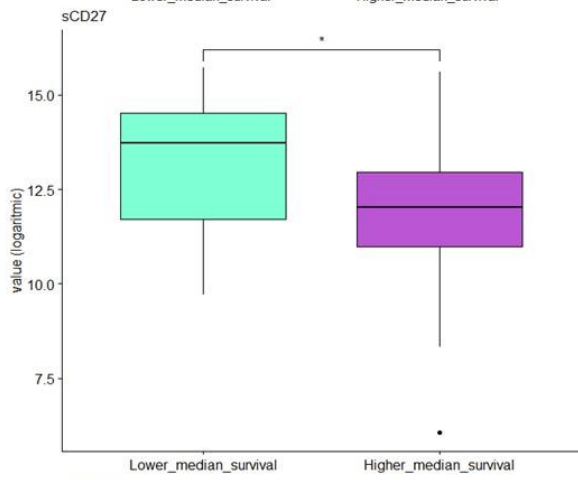
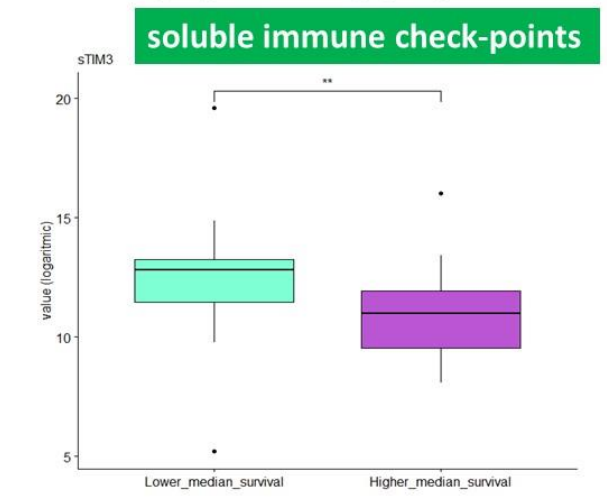
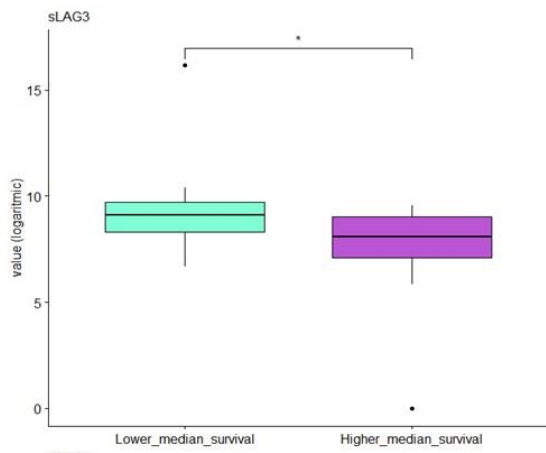
B**C**

Figure 7 Statistical analysis at T0 for soluble molecules from groups of patients divided according to overall survival (OS) value. Boxplot of cytokines (A), chemokines (B), and soluble immune-checkpoints (C) molecules expression level (logarithmic scale) in 27 patients with a OS value greater than the median cut off (i.e., 11 months) (violet box), 26 patients with a survival value lower than the median cut off (water blue box) at T0. P-values were obtained by applying a Mann-Whitney test for unpaired samples. Legend: * p-value ≤ 0.05 ; ** p-value ≤ 0.01 ; *** p-value ≤ 0.001 .

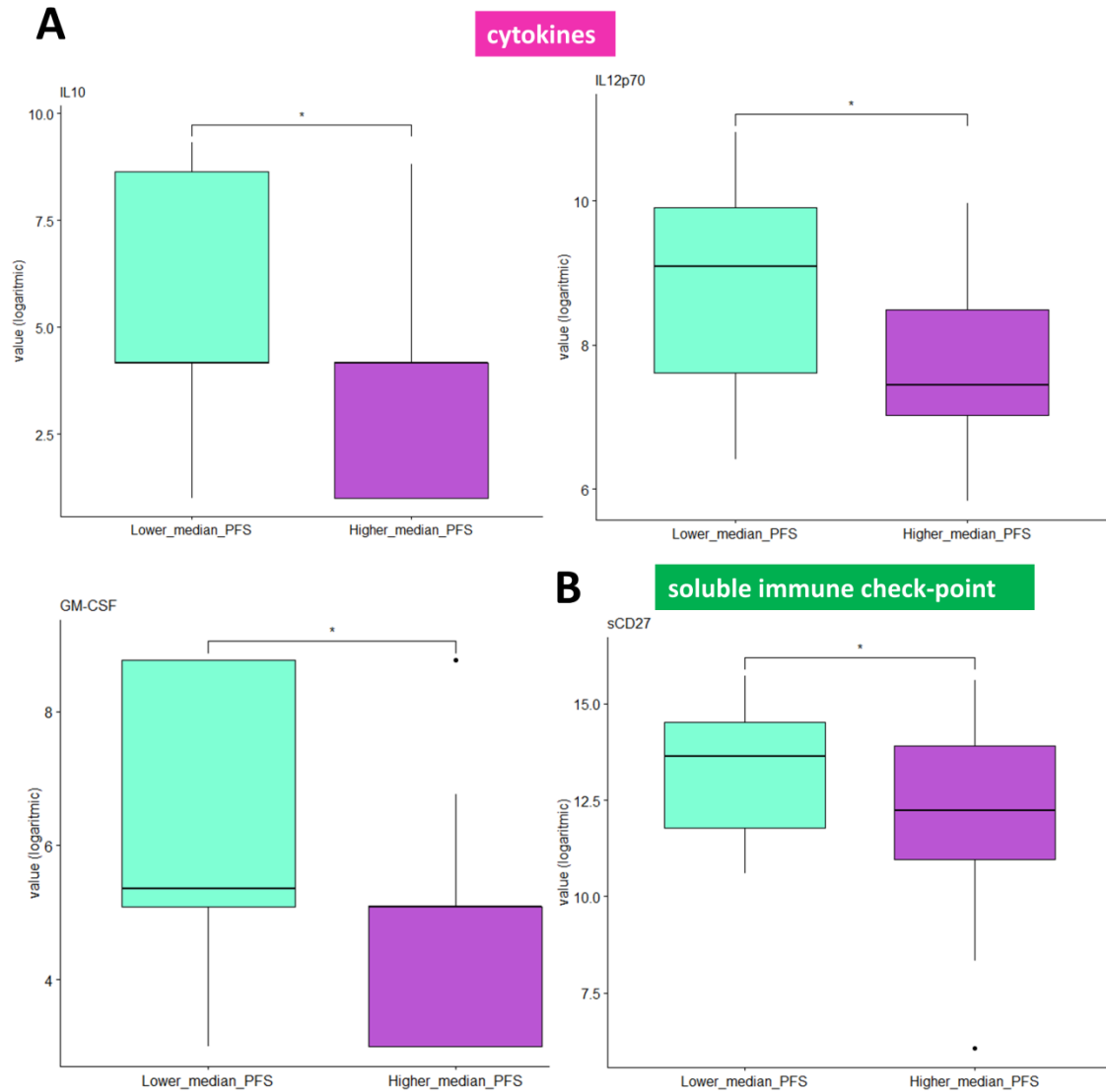
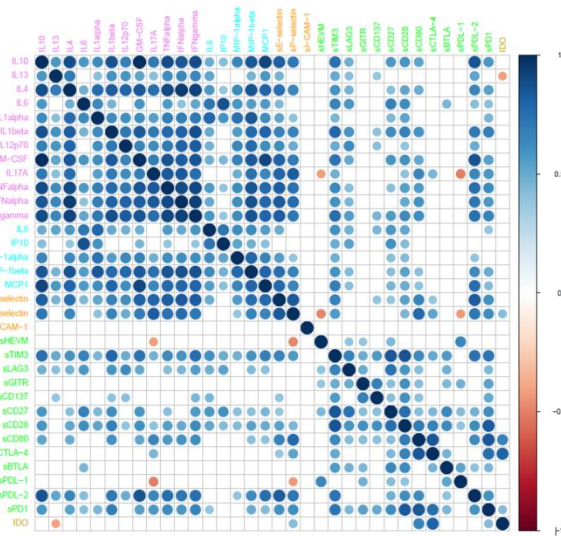


Figure 8 Statistical analysis at T0 for soluble molecules from groups of patients divided according to progression-free survival (PFS) value. Boxplot of cytokines (A) and soluble immune-checkpoints (B) molecules expression level (logarithmic scale) in 34 patients with a PFS value greater than the median cutoff (i.e., 4 months) (violet box) and 19 patients with a PFS value lower than the median cutoff (water blue box) at T0. P-values were obtained by applying a Mann-Whitney test for unpaired samples. Legend: * p-value ≤ 0.05 ; ** p-value ≤ 0.01 ; *** p-value ≤ 0.001 .

A

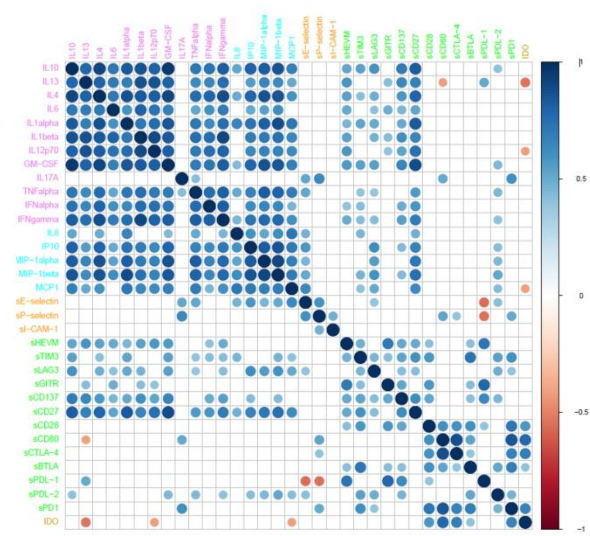
Higher OS



- cytokines
- chemokines
- adhesion molecules
- soluble immune check-points
- others

B

Lower OS

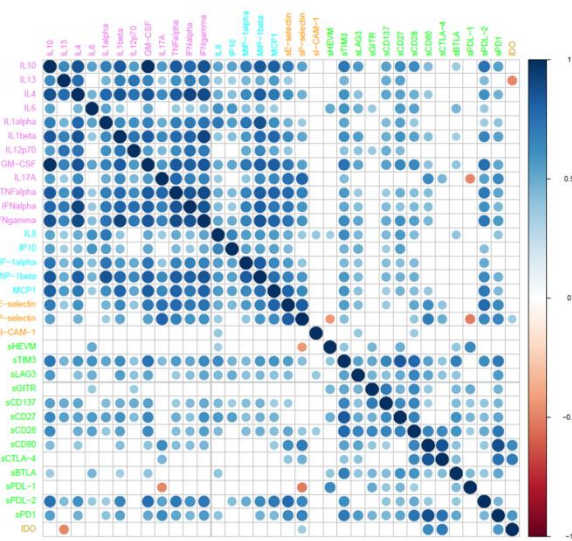


- cytokines
- chemokines
- adhesion molecules
- soluble immune check-points
- others

Figure 9 Connectivity map between molecules in patients with a value of overall survival (OS) that is higher (A) and lower (B) of the selected cut-off (i.e., the median of overall survival in the entire cohort of patients) at T0. Statistically significant Spearman correlations ($p\text{-value} \leq 0.05$) are reported. In the plot, circles are scaled and coloured according to the correlation values, increasing from red (negative correlation) to blue (positive correlation). Molecules are grouped and ordered according to the functional group reported in the legend.

A

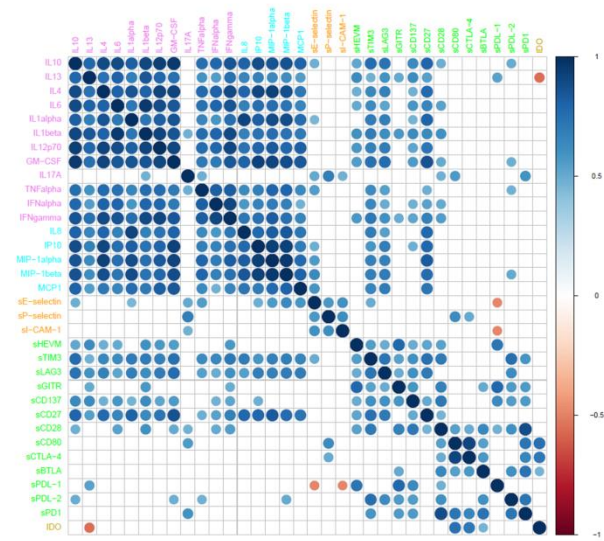
Higher PFS



- cytokines
- chemokines
- adhesion molecules
- soluble immune check-points
- others

B

Lower PFS



- cytokines
- chemokines
- adhesion molecules
- soluble immune check-points
- others

Figure 10 Connectivity map between molecules in patients with a value of progression-free survival (PFS) that is higher (A) and lower (B) of the selected cut-off (i.e., the median of progression free survival in the entire cohort of patients) at T0. Statistically significant Spearman correlations ($p\text{-value} \leq 0.05$) are reported. In the plot, circles are scaled and coloured according to the correlation values, increasing from red (negative correlation) to blue (positive correlation). Molecules are grouped and ordered according to the functional group reported in the legend.

Discussion

In this study, we evidenced that the connectivity between the circulating molecules analyzed can change in responder and non responder patients in presence or not of immune-related toxicity. Biological systems respond to multiple inputs that can vary and interact simultaneously - i.e., these are complex systems that form molecular networks [224]. The investigation of these networks is essential for understanding the true bases for phenotype and pathophenotype since each molecular entities does not exert its effect on phenotype in isolation, rather a disease is driven by complex interactions among a variety of molecular mediators [225]. To construct these networks, we chose to exploit a quantitative approach based on the co-expression between molecules, quantifying the relationship between two molecules (connectivity) via the correlation between their expression profiles. Even if correlation does not imply causation, molecules that are co-expressed can be functionally coordinated in response to an external stimulus, implying a common way of functioning or the influence by a shared underlying mechanism [226].

The immunological status of 4 different groups of patients with peculiar clinical and prognostic features requiring targeted therapeutic choices and personalized strategies were defined. By calculating the Spearman correlation coefficients and p-values among each pair of molecules for each group of analysed patients, a specific connectivity network was constructed according to the occurrence of cumulative toxicity, detecting a specific immune condition in patients susceptible to developing toxicity during treatment. These results confirm the findings of a previous study, including 79 patients with solid tumours treated with immunotherapy, which showed a specific connectivity network between circulating molecules in the presence of cumulative toxicity, suggesting a dysregulation of the immune system leading to the loss of self-tolerance mechanisms [179]. In addition, peculiar connectivity network characteristics in the non-responder with toxicity subgroup were also identified. This result is particularly significant considering that patients in this subgroup had high grade G2-G3 toxicity. Moreover, this set of patients that will develop the worst clinical condition requires a targeted and personalised management by the oncologist. The identification of patients who are resistant to immunotherapy and more prone to develop toxicities may direct the physician towards alternative treatment choices, such as chemotherapy, target therapy or best supportive care, depending on the patient clinico-pathological characteristics in according to the site of the primary tumor. Furthermore, this subset of difficult-to-manage patients should be discussed in molecular tumor board and candidates for molecular profiling to allow access to innovative, personalized and safe treatments based on the specific molecular alterations that may be

highlighted. Thus, the opportunity to identify baseline immune biomarkers predictive of this poor outcome and toxicity is of paramount importance and deserves further investigation.

The heatmap showing molecule expression levels in different groups (Figure 2A), revealed the presence of two distinct subgroups in non-responder patients without toxicities, one of which is characterised by high cytokine and chemokine concentrations, and consists exclusively of NSCLC patients. Furthermore, considering the distribution of the primary tumor types in the 4 groups, a higher concentration of HNSCC can be observed in the non-responder with toxicity group, whereas UMs are exclusively present in the responder/non-responder without cumulative toxicity groups. These evidences suggest the existence of an organ-specific immunity beyond common clinical behaviour. Indeed, HNSCC, as known in the literature, are tumours characterised by an extremely immunosuppressive microenvironment, in which dysregulation of the immune system plays a central role in carcinogenesis and tumour progression [227]. On the other hand, UMs constitute a peculiar pathological entity with respect to cutaneous melanomas, with specific immune regulatory mechanisms still to be fully understood.

In non-responder patients with toxicity, higher level of IL17A and adhesion molecules (sICAM-1, sP-selectin and sE-selectine) were detected compared to other subgroups (Figure 2B). Moreover, in this subgroup higher levels of sCTLA-4 compared to both responder and non-responder without toxicity and higher sCD80 level compared to both responder with toxicity and non-responder without toxicity were found. On the other hand, sHVEM and sPDL-1 were lower in non responder with toxicity group compared to non-responder without toxicities. IL-17A plays a key role in fostering the creation of an ideal tumour microenvironment through its ability to induce the production of inflammatory mediators and mobilise MDSC cells. Indeed, IL-17A through binding to its receptor (IL-17Ra) is able to promote tumourigenesis and angiogenesis; thus it has been associated with a poor prognosis in colon rectal cancer patients [228, 229]. Furthermore, IL-17A promotes the recruitment of MDSC cells in mouse colon tumours [230] and promotes the immunosuppressive activity of Tregs, resulting in tumour progression [231].

Recently in the literature, IL17A has been associated with the failure of anti-PD-1 therapy in patients with MSS colon-rectal cancer (CRC). Although growing evidence suggests that IL-17A activity may drive resistance to antitumour immunity and contribute to therapeutic failure, it is still unclear whether blocking IL-17A can improve sensitivity to ICIs [232]. IL17A is implicated in the pathogenesis of some autoimmune diseases, including ankylosing spondylitis for which an IL17A inhibitor (secukinumab) is approved [233]. Therefore, IL17A might play a key role as a driver of immune dysregulation in the subgroup of non-responder patients with toxicity. Similarly, the

presence of high circulating levels of soluble adhesion molecules also confirms the loss of immune balance in patients of this subgroup. In literature high level of soluble adhesion molecules are associated with sepsis, autoimmune disease, such as rheumatoid arthritis and other inflammatory and vascular disease [234-236]. Moreover, sICAM-1 may have predictive clinical value in transplanted patients with acute renal allograft rejection, as it is present in serum in high concentrations prior to the occurrence of the acute event [237]. Recently, it was shown that hepatocellular carcinoma (HCC) patients with elevated serum levels of sICAM-1 had a worse OS than those with low levels of sICAM-1 who were more likely to benefit from immune checkpoint blockade therapy [238]. Furthermore, in a recent study including patients with different primary tumours treated with immunotherapy, the worst prognosis cluster was characterised by elevated serum levels of cytokines/chemokines and adhesion molecules, confirming the possible predictive significance of immune imbalance of these molecules [153]. These findings were confirmed in the connectivity map (Figure 4), which shows that in the non-responder with toxicity group there are specific negative correlations between ICAM-1 and sP-selectins and different cytokines/chemokines.

On the other hand, the soluble form of CTLA-4, capable of binding CD80, is implicated in the pathogenesis of several autoimmune diseases, in which sCTLA-4 is able to inhibit early T-cell activation by blocking the interaction between CD80 and the costimulatory receptor CD28. Furthermore, high levels of sCTLA-4 could compete for binding of the membrane form of CTLA-4 causing a reduction in inhibitory signalling [239]. The potent immunoregulatory activities of sCTLA-4 are confirmed by the high concentrations in the sera of patients with melanoma who develop toxicity during immunotherapy [240]. The biological functions of the soluble forms of HVEM and PDL1 are still largely unknown, but some evidence suggests an important immunoregulatory role [241]. Therefore, their function should be interpreted in the immunological context of the individual patient. The 4 connectivity maps obtained showed that in patients who develop toxicity there is a specific and peculiar connectivity pattern. In patients with toxicities we observed a loss of connectivity of mostly of sIC and the cytokines/chemokines correlations suggesting that the immune system is in equilibrium when there is a well-organised crosstalk between the different molecules, whereas it is dysregulated and more 'inflamed' when molecules act chaotically losing connections with each other.

Although toxicity has the greatest impact on the connectivity pattern, it is possible to observe peculiarities in the connectivity map of non-responder patients with toxicity, in which a reversal of correlation is observed for certain adhesion molecules, whose correlation sign from positive or null has become negative comparing with the other 3 groups. These negative correlations involve, above all, two soluble adhesion molecules (s-Pselectin and sICAM-1 with a negative correlation with many cytokines/chemokines) and IDO (with the occurrence of a negative correlation with IL13, MIP-alpha

and sPDL1). These findings might suggest that the non-responder group with toxicity is more inflamed than the other 3 with greater dysregulation and loss of immune fitness.

The differences in the 4 groups of patients are confirmed by the connectivity networks, which show the presence of specific connections for each subgroup, with a relatively small number (14) of connections common to all 4 networks. In addition, each network has a distinct molecule with the role of leading player in the greatest number of interactions, defined as the first hub. Significantly, INF α is the first hub in the connectivity network of responder patients without toxicity, who represent the best prognosis group, benefiting most from immunotherapy. The importance of IFN α in cancer control has been known for a long time, since it was the first drug approved in the treatment of certain solid tumours such as melanoma and kidney cancer [242]. As a central immunomodulatory agent, IFN α has an important immunomodulatory function and is able to mediate pro-apoptotic, anti-proliferative functions favouring cancer elimination. However, chronic activation of the IFN α pathway may lead to an immunosuppressive action due to depletion of the immune activity involved in tumour escape mechanisms [243]. In non-responder with toxicity group, first hubs were sGITR and sICAM-1. As already mentioned, soluble adhesion molecules should play an important role in this subgroup of patients, given their pro-inflammatory action. On the other hand, the GITR/GITR ligand pathway induces a positive costimulatory signal on effector T cells, promoting their activation and proliferation, while inhibiting the immunosuppressive activity of Treg cells [244, 245]. GITR activation has been associated with anti-tumor activity, with anti-viral activity, but with aggravation of autoimmune diseases [246]. Elevated serum levels of the soluble form of GITRL and/or GITR have been reported in some autoimmune disorders such as Sjögren's syndrome and Hashimoto's thyroiditis [247, 248].

Preclinical data on GITR-agonist monoclonal antibodies demonstrated in vitro and in vivo antitumor activity that enhances the CD8⁺ and CD4⁺ effector T cells and decreases tumour-infiltrating Tregs [249]. However, the functions of the soluble form of GITR are not fully understood to date.

The first hub in responder with toxicity group was GM-CSF, a cytokine able to promote the differentiation of myeloid cells, with immunostimulatory effects in inducing antitumor immunity. Furthermore, GM-CSF is capable of inducing the differentiation of DCs, which are responsible for the presentation of tumor antigens for the priming of cytotoxic T lymphocytes [250]. In non-responder patients without toxicities first hub was MIP1-alpha, an interesting chemokine, capable both of inducing leukocyte chemotaxis, carrying out a pro-inflammatory activity, and of inhibiting the proliferation of hematopoietic stem cells in vitro and in vivo [251].

Overall, a specific signature in terms of network connectivity of the molecules characterizing the different groups of responder and non-responder patients with and without toxicity has been

highlighted. Each network had a precise number of significant and specific connections. In particular, it is of interest to note that the highest number of both significant connections (143) and specific connections (80) was recorded in non-responder patients with toxicity. Furthermore, it is the only group in which IDO is involved in 4 specific and significant connections; conversely IDO is absent in the specific connections of the other 3 networks. Among the specific connections of non-responder patients with toxicity, there are as many as 15 involving I-CAM1 and 18 involving sGITR, confirming what was previously observed. IDO, an enzyme involved in tryptophan catabolism, represents an important mechanism of immunosuppression and tumor immune escape, and it could be involved in the development of primary resistance to treatment with ICIs. In a recent work including different solid tumors, the activity of IDO was evaluated by the serum kyn/trp ratio through modified liquid chromatography – tandem mass spectrometry (LC–MS/MS) method. A high baseline kyn/trp ratio was associated with worse outcomes to immunotherapy in terms of PFS and OS [183]. Considering that tryptophan catabolism is the result of the activity of several enzymes in addition to IDO, in future research, liquid chromatography might be a more reliable method than the multiplex assay to study IDO activity, expressed as a kyn/trp ratio.

There were no statistically significant differences in either PFS or OS based on the presence of toxicity. Instead, a statistically significant difference in terms of PFS and OS was highlighted in responder or non-responder patients. This data suggests that in our study the presence of toxicity does not represent a predictive factor of survival. This evidence contrasts with what is reported in the literature. In a recent meta-analysis, the onset of irAE was associated with better ICI activity and a survival benefit [252]. This association is particularly evident for some types of cancer (melanoma and NSCLC) and for specific type of irAE (endocrine and skin) [252]. Similarly, emerging evidence also suggests that patients who develop immune-related toxicities such as vitiligo, keratitis, uveitis and erythema nodosum under BRAFi/MEKi could derive lasting benefits from these therapies [253]. Moreover, a peculiar skin toxicity, mainly consisting of an acneiform eruption, is predictive of good response to the anti EGFR monoclonal antibody in CRC [254].

By evaluating the serum levels of different molecules in patients with OS and PFS above or below the median, we found that patients with better OS and PFS had several molecules down-regulated. This data confirms what has been highlighted in a recent work, in which patients with values of sTIM3, IFN α , IFN γ , IL1 β , IL1 α , IL12p70, MIP1 β and TNF α below the median had longer OS and patients with values below the median of sCD28, sGITR, sPDL1, IL10 and IL13 had longer PFS [153]. Furthermore, in a recent study, Zizzari et al reported that low levels of sPDL1, sPDL2, sTim3, sCD137 and sBTLA4 were also correlated with a long response to immunotherapy in patients with NSCLC [155].

The high rates of progressive disease (64.1%) and patients in second-line treatment (66%) explain the short OS and PFS reported by our study population in all tumour subtypes. No statistically significant differences were reported in the connectivity maps for patients with OS and PFS above or below the median. This lack of significance can be explained in several ways: first of all, the small size of the series, the heterogeneity of the study population in terms of primary tumor, previous treatments, lines of treatment (first or second line), and lines of subsequent treatment received. The size and heterogeneity of the patient sample represent the main limitations of the study. Therefore, any conclusion or finding should be confirmed on a larger and more homogeneous population. However, this study provides some important research insights that deserve further investigation. The possibility of early identification of patient resistant to immunotherapy and at risk of developing dangerous toxicities, affecting the QoL, would have a significant impact on clinical practice.

Conclusion

In conclusion, these results allowed to define a specific connectivity pattern for each of the 4 clinical situations: responder with toxicity, responder without toxicity, non-responder with toxicity and non-responder without toxicity. In particular, in patients who will develop irAEs, a peculiar pattern of immune dysregulation has been identified. The analysis of the connectivity network has shown that patients with the worst prognosis (non-responders who will develop toxicity) have peculiar connectivity and network characteristics, which could favor their early and timely identification so as to be able to modulate the therapeutic strategy based on the patient immune status. Furthermore, our findings suggest the existence of an organ-dependent immunity reflecting in a specific clinical behaviour for each type of primary tumour.

A poorly modulated and highly "inflamed" immune system could ultimately affect both immune tolerance with the onset of irAE and response to treatment. The identification of a baseline soluble immune profile, predicting both the risk of developing immune-related toxicities and the response to treatment, represents a new challenge for precision medicine in order to design a personalized therapeutic strategy, for each patient, preferably based on the molecular profiling in the patients with the worst prognosis, to prevent life-threatening irAEs and improve outcomes.

Institutional Review Board Statement: This study was approved by local ethics committee of Sapienza University of Rome, RIF. CE: 4421

Informed Consent Statement: Informed consent was obtained from all subjects involved in the study

Acknowledgements: Special thanks to Prof. Silvia Mezi for teaching me so much during these years of training. Thanks to Prof. Giulia D'amati for her support and advice.

Thanks to Prof. Andrea Botticelli, Prof. Paolo Marchetti and Prof. Marianna Nuti for making this project possible and for giving me the opportunity to work on it.

References

1. Drake CG, Jaffee E, Pardoll DM. Mechanisms of immune evasion by tumors. *Adv Immunol* 2006;90:51–81.
2. Vesely MD, Kershaw MH, Schreiber RD, Smyth MJ. Natural innate and adaptive immunity to cancer. *Annu Rev Immunol* 2011;29:235–71.
3. Mellman I, Coukos G, Dranoff G. Cancer Immunotherapy comes of age. *Nature* 2011;480:21–9.
4. Corthay A. Does the immune system naturally protect against cancer? *Front Immunol* 2014;5:197.
5. Mellman I, Coukos G, Dranoff G. Cancer Immunotherapy comes of age. *Nature* 2011;480:21–9.
6. Corthay A. Does the immune system naturally protect against cancer? *Front Immunol* 2014;5:197.
7. Ozga AJ, Chow MT, Luster AD. Chemokines and the immune response to cancer. *Immunity*. 2021;54(5):859-874. doi:10.1016/j.immuni.2021.01.012
8. Thommen DS, Schreiner J, Müller P, et al. Progression of Lung Cancer Is Associated with Increased Dysfunction of T Cells Defined by Coexpression of Multiple Inhibitory Receptors. *Cancer Immunol Res*. 2015;3(12):1344-1355. doi:10.1158/2326-6066.CIR-15-0097
9. Hanna GJ, Lizotte P, Cavanaugh M, et al. Frameshift events predict anti-PD-1/L1 response in head and neck cancer. *JCI Insight*. 2018;3(4):e98811. Published 2018 Feb 22. doi:10.1172/jci.insight.98811
10. Chen Y, Wang Q, Shi B, et al. Development of a sandwich ELISA for evaluating soluble PD-L1 (CD274) in human sera of different ages as well as supernatants of PD-L1+ cell lines. *Cytokine*. 2011;56(2):231-238. doi:10.1016/j.cyto.2011.06.004
11. Briukhovetska D, Dörr J, Endres S, Libby P, Dinarello CA, Kobold S. Interleukins in cancer:

- from biology to therapy. *Nat Rev Cancer*. 2021;21(8):481-499. doi:10.1038/s41568-021-00363-z
12. Nagarsheth N, Wicha MS, Zou W. Chemokines in the cancer microenvironment and their relevance in cancer immunotherapy. *Nat Rev Immunol*. 2017;17(9):559-572. doi:10.1038/nri.2017.49
 13. Guerrouahen BS, Maccalli C, Cugno C, Rutella S, Akporiaye ET. Reverting Immune Suppression to Enhance Cancer Immunotherapy. *Front Oncol*. 2020;9:1554. Published 2020 Jan 21. doi:10.3389/fonc.2019.01554
 14. Lipson EJ, Forde PM, Hammers HJ, Emens LA, Taube JM, Topalian SL. Antagonists of PD-1 and PD-L1 in Cancer Treatment. *Semin Oncol*. 2015;42(4):587-600. doi:10.1053/j.seminoncol.2015.05.013
 15. Peggs KS, Quezada SA, Korman AJ, Allison JP. Principles and use of anti-CTLA4 antibody in human cancer immunotherapy. *Curr Opin Immunol*. 2006;18(2):206-213. doi:10.1016/j.coi.2006.01.011
 16. Schadendorf D, Hodi FS, Robert C, et al. Pooled Analysis of Long-Term Survival Data From Phase II and Phase III Trials of Ipilimumab in Unresectable or Metastatic Melanoma. *J Clin Oncol*. 2015;33(17):1889-1894. doi:10.1200/JCO.2014.56.2736
 17. Hodi FS, O'Day SJ, McDermott DF, et al. Improved survival with ipilimumab in patients with metastatic melanoma [published correction appears in *N Engl J Med*. 2010 Sep 23;363(13):1290]. *N Engl J Med*. 2010;363(8):711-723. doi:10.1056/NEJMoa1003466
 18. Abdou Y, Pandey M, Sarma M, Shah S, Baron J, Ernstoff MS. Mechanism-based treatment of cancer with immune checkpoint inhibitor therapies. *Br J Clin Pharmacol*. 2020;86(9):1690-1702. doi:10.1111/bcp.14316
 19. Kraehenbuehl L, Weng CH, Eghbali S, Wolchok JD, Merghoub T. Enhancing immunotherapy in cancer by targeting emerging immunomodulatory pathways. *Nat Rev Clin Oncol*. 2022;19(1):37-50. doi:10.1038/s41571-021-00552-7
 20. Hossain MA, Liu G, Dai B, et al. Reinvigorating exhausted CD8⁺ cytotoxic T lymphocytes in the tumor microenvironment and current strategies in cancer immunotherapy. *Med Res Rev*. 2021;41(1):156-201. doi:10.1002/med.21727
 21. Basu A, Ramamoorthi G, Albert G, et al. Differentiation and Regulation of TH Cells: A Balancing Act for Cancer Immunotherapy. *Front Immunol*. 2021;12:669474. Published 2021 May 3. doi:10.3389/fimmu.2021.669474
 22. Reck M, Rodríguez-Abreu D, Robinson AG, et al. Pembrolizumab versus Chemotherapy for PD-L1-Positive Non-Small-Cell Lung Cancer. *N Engl J Med*. 2016;375(19):1823-1833.

doi:10.1056/NEJMoa1606774

23. Herbst RS, Baas P, Kim DW, et al. Pembrolizumab versus docetaxel for previously treated, PD-L1-positive, advanced non-small-cell lung cancer (KEYNOTE-010): a randomised controlled trial. *Lancet*. 2016;387(10027):1540-1550. doi:10.1016/S0140-6736(15)01281-7
24. Pelster MS, Gruschkus SK, Bassett R, et al. Nivolumab and Ipilimumab in Metastatic Uveal Melanoma: Results From a Single-Arm Phase II Study. *J Clin Oncol*. 2021;39(6):599-607. doi:10.1200/JCO.20.00605
25. Kaštelan S, Antunica AG, Oresković LB, Pelčić G, Kasun E, Hat K. Immunotherapy for Uveal Melanoma - Current Knowledge and Perspectives. *Curr Med Chem*. 2020;27(8):1350-1366. doi:10.2174/0929867326666190704141444
26. Ferris RL, Blumenschein G Jr, Fayette J, et al. Nivolumab for Recurrent Squamous-Cell Carcinoma of the Head and Neck. *N Engl J Med*. 2016;375(19):1856-1867. doi:10.1056/NEJMoa1602252
27. Burtneß B, Harrington KJ, Greil R, et al. Pembrolizumab alone or with chemotherapy versus cetuximab with chemotherapy for recurrent or metastatic squamous cell carcinoma of the head and neck (KEYNOTE-048): a randomised, open-label, phase 3 study [published correction appears in *Lancet*. 2020 Jan 25;395(10220):272] [published correction appears in *Lancet*. 2020 Feb 22;395(10224):564] [published correction appears in *Lancet*. 2021 Jun 12;397(10291):2252]. *Lancet*. 2019;394(10212):1915-1928. doi:10.1016/S0140-6736(19)32591-7
28. Powles T, Plimack ER, Soulières D, et al. Pembrolizumab plus axitinib versus sunitinib monotherapy as first-line treatment of advanced renal cell carcinoma (KEYNOTE-426): extended follow-up from a randomised, open-label, phase 3 trial [published correction appears in *Lancet Oncol*. 2020 Dec;21(12):e553]. *Lancet Oncol*. 2020;21(12):1563-1573. doi:10.1016/S1470-2045(20)30436-8
29. AIOM-AiRTUM 2018. I numeri del cancro in Italia 2018. Intermedia Editore 2018
30. Fuhrman SA, Lasky LC, Limas C. Prognostic significance of morphologic parameters in renal cell carcinoma. *Am J Surg Pathol*. 1982;6(7):655-663. doi:10.1097/00000478-198210000-00007
31. Elson, P.J. (2000). Prognostic Factors in Metastatic Renal Cell Carcinoma. In: Bukowski, R.M., Novick, A.C. (eds) *Renal Cell Carcinoma. Current Clinical Oncology*. Humana Press, Totowa, NJ. https://doi.org/10.1007/978-1-59259-229-6_9
32. Hanna KS. A Review of Immune Checkpoint Inhibitors for the Management of Locally Advanced or Metastatic Urothelial Carcinoma. *Pharmacotherapy*. 2017;37(11):1391-1405.

doi:10.1002/phar.2033

33. Alikhan MB, Pease G, Watkin W, Grogan R, Krausz T, Antic T. Primary epithelioid sarcoma of the kidney and adrenal gland: report of 2 cases with immunohistochemical and molecular cytogenetic studies. *Hum Pathol.* 2017;61:158-163. doi:10.1016/j.humpath.2016.09.024
34. Kidney Cancer Update. The year in review in kidney cancer. *Clinical Advances in Hematology & Oncology: H&O.* 2015;13(5):327-329. PubMed PMID: 26352778
35. Florek M, Haase M, Marzesco AM, et al. Prominin-1/CD133, a neural and hematopoietic stem cell marker, is expressed in adult human differentiated cells and certain types of kidney cancer. *Cell Tissue Res.* 2005;319(1):15-26. doi:10.1007/s00441-004-1018-z
36. Santoni M, Berardi R, Amantini C, et al. Role of natural and adaptive immunity in renal cell carcinoma response to VEGFR-TKIs and mTOR inhibitor. *Int J Cancer.* 2014;134(12):2772-2777. doi:10.1002/ijc.28503
37. Murphy KA, James BR, Guan Y, Torry DS, Wilber A, Griffith TS. Exploiting natural anti-tumor immunity for metastatic renal cell carcinoma. *Hum Vaccin Immunother.* 2015;11(7):1612-1620. doi:10.1080/21645515.2015.1035849
38. Daurkin I, Eruslanov E, Stoffs T, et al. Tumor-associated macrophages mediate immunosuppression in the renal cancer microenvironment by activating the 15-lipoxygenase-2 pathway. *Cancer Res.* 2011;71(20):6400-6409. doi:10.1158/0008-5472.CAN-11-1261
39. Hemmerlein B, Johanns U, Halbfass J, et al. The balance between MMP-2/-9 and TIMP-1/-2 is shifted towards MMP in renal cell carcinomas and can be further disturbed by hydrogen peroxide. *Int J Oncol.* 2004;24(5):1069-1076.
40. O'Hayre M, Salanga CL, Handel TM, Allen SJ. Chemokines and cancer: migration, intracellular signalling and intercellular communication in the microenvironment. *Biochem J.* 2008;409(3):635-649. doi:10.1042/BJ20071493
41. Hembruff SL, Cheng N. Chemokine signaling in cancer: Implications on the tumor microenvironment and therapeutic targeting. *Cancer Ther.* 2009;7(A):254-267.
42. Ross K, Jones RJ. Immune checkpoint inhibitors in renal cell carcinoma. *Clin Sci (Lond).* 2017;131(21):2627-2642. Published 2017 Oct 27. doi:10.1042/CS20160894
43. Chan JY, Choudhury Y, Tan MH. Predictive molecular biomarkers to guide clinical decision making in kidney cancer: current progress and future challenges. *Expert Rev Mol Diagn.* 2015;15(5):631-646. doi:10.1586/14737159.2015.1032261
44. Motzer RJ, Escudier B, McDermott DF, et al. Nivolumab versus Everolimus in Advanced Renal-Cell Carcinoma. *N Engl J Med.* 2015;373(19):1803-1813.

doi:10.1056/NEJMoa1510665

45. Cella D, Grünwald V, Nathan P, et al. Quality of life in patients with advanced renal cell carcinoma given nivolumab versus everolimus in CheckMate 025: a randomised, open-label, phase 3 trial [published correction appears in *Lancet Oncol*. 2016 Jul;17 (7):e270]. *Lancet Oncol*. 2016;17(7):994-1003. doi:10.1016/S1470-2045(16)30125-5
46. Shah R, Botteman M, Solem CT, et al. A Quality-adjusted Time Without Symptoms or Toxicity (Q-TWiST) Analysis of Nivolumab Versus Everolimus in Advanced Renal Cell Carcinoma (aRCC). *Clin Genitourin Cancer*. 2019;17(5):356-365.e1. doi:10.1016/j.clgc.2019.05.010
47. Motzer RJ, Escudier B, George S, et al. Nivolumab versus everolimus in patients with advanced renal cell carcinoma: Updated results with long-term follow-up of the randomized, open-label, phase 3 CheckMate 025 trial. *Cancer*. 2020;126(18):4156-4167. doi:10.1002/cncr.33033
48. Motzer RJ, Tannir NM, McDermott DF, et al. Nivolumab plus Ipilimumab versus Sunitinib in Advanced Renal-Cell Carcinoma. *N Engl J Med*. 2018;378(14):1277-1290. doi:10.1056/NEJMoa1712126
49. Larkin J, Chiarion-Sileni V, Gonzalez R, et al. Five-Year Survival with Combined Nivolumab and Ipilimumab in Advanced Melanoma. *N Engl J Med*. 2019;381(16):1535-1546. doi:10.1056/NEJMoa1910836
50. Albiges L, Tannir NM, Burotto M, et al. Nivolumab plus ipilimumab versus sunitinib for first-line treatment of advanced renal cell carcinoma: extended 4-year follow-up of the phase III CheckMate 214 trial. *ESMO Open*. 2020;5(6):e001079. doi:10.1136/esmoopen-2020-001079
51. Tannir NM, Signoretti S, Choueiri TK, et al. Efficacy and Safety of Nivolumab Plus Ipilimumab versus Sunitinib in First-line Treatment of Patients with Advanced Sarcomatoid Renal Cell Carcinoma. *Clin Cancer Res*. 2021;27(1):78-86. doi:10.1158/1078-0432.CCR-20-2063
52. Rini BI, Plimack ER, Stus V, et al. Pembrolizumab plus Axitinib versus Sunitinib for Advanced Renal-Cell Carcinoma. *N Engl J Med*. 2019;380(12):1116-1127. doi:10.1056/NEJMoa1816714
53. Rini BI, Plimack ER, Stus V, et al: Pembrolizumab (pembro) plus axitinib (axi) versus sunitinib as first-line therapy for advanced clear cell renal cell carcinoma (ccRCC): Results from 42-month follow-up of KEYNOTE-426. *J Clin Oncol* 39, 2021 39:15_suppl, 4500-4500
54. Motzer RJ, Penkov K, Haanen J, et al. Avelumab plus Axitinib versus Sunitinib for Advanced Renal-Cell Carcinoma. *N Engl J Med*. 2019;380(12):1103-1115.

doi:10.1056/NEJMoa1816047

55. Rini BI, Powles T, Atkins MB, et al. Atezolizumab plus bevacizumab versus sunitinib in patients with previously untreated metastatic renal cell carcinoma (IMmotion151): a multicentre, open-label, phase 3, randomised controlled trial. *Lancet*. 2019;393(10189):2404-2415. doi:10.1016/S0140-6736(19)30723-8
56. Motzer RJ, Powles T, Atkins MB, et al. Final Overall Survival and Molecular Analysis in IMmotion151, a Phase 3 Trial Comparing Atezolizumab Plus Bevacizumab vs Sunitinib in Patients With Previously Untreated Metastatic Renal Cell Carcinoma. *JAMA Oncol*. 2022;8(2):275-280. doi:10.1001/jamaoncol.2021.5981
57. Choueiri TK, Powles T, Burotto M, et al. Nivolumab plus Cabozantinib versus Sunitinib for Advanced Renal-Cell Carcinoma. *N Engl J Med*. 2021;384(9):829-841. doi:10.1056/NEJMoa2026982
58. Cella D, Motzer RJ, Suarez C, et al. Patient-reported outcomes with first-line nivolumab plus cabozantinib versus sunitinib in patients with advanced renal cell carcinoma treated in CheckMate 9ER: an open-label, randomised, phase 3 trial. *Lancet Oncol*. 2022;23(2):292-303. doi:10.1016/S1470-2045(21)00693-8
59. Motzer RJ, Powles T, Burotto M, et al. Nivolumab plus cabozantinib versus sunitinib in first-line treatment for advanced renal cell carcinoma (CheckMate 9ER): long-term follow-up results from an open-label, randomised, phase 3 trial [published correction appears in *Lancet Oncol*. 2022 Jul;23(7):e319] [published correction appears in *Lancet Oncol*. 2022 Sep;23(9):e404]. *Lancet Oncol*. 2022;23(7):888-898. doi:10.1016/S1470-2045(22)00290-X
60. Motzer R, Alekseev B, Rha SY, et al. Lenvatinib plus Pembrolizumab or Everolimus for Advanced Renal Cell Carcinoma. *N Engl J Med*. 2021;384(14):1289-1300. doi:10.1056/NEJMoa2035716
61. Choueiri T, Powles TB, Albiges L et al. Phase 3 study of cabozantinib (C) in combination with nivolumab (N) and ipilimumab (I) in previously untreated advanced renal cell carcinoma (aRCC) of IMDC intermediate or poor risk (COSMIC-313). *Annals of Oncology* (2022) 33 (suppl_7): S808-S869. 10.1016/annonc/annonc1089
62. Ferris RL. Immunology and Immunotherapy of Head and Neck Cancer. *J Clin Oncol*. 2015;33(29):3293-3304. doi:10.1200/JCO.2015.61.1509
63. Seiwert TY, Burtness B, Mehra R, et al. Safety and clinical activity of pembrolizumab for treatment of recurrent or metastatic squamous cell carcinoma of the head and neck (KEYNOTE-012): an open-label, multicentre, phase 1b trial. *Lancet Oncol*. 2016;17(7):956-965. doi:10.1016/S1470-2045(16)30066-3

64. Cancer Genome Atlas Network. Comprehensive genomic characterization of head and neck squamous cell carcinomas. *Nature*. 2015;517(7536):576-582. doi:10.1038/nature14129
65. Lui VW, Hedberg ML, Li H, et al. Frequent mutation of the PI3K pathway in head and neck cancer defines predictive biomarkers. *Cancer Discov*. 2013;3(7):761-769. doi:10.1158/2159-8290.CD-13-0103
66. Rischin D, Harrington KJ, Greil R, et al. Pembrolizumab alone or with chemotherapy for recurrent or metastatic head and neck squamous cell carcinoma: Health-related quality-of-life results from KEYNOTE-048. *Oral Oncol*. 2022;128:105815. doi:10.1016/j.oraloncology.2022.105815
67. Guigay J, Aupérin A, Fayette J, et al. Cetuximab, docetaxel, and cisplatin versus platinum, fluorouracil, and cetuximab as first-line treatment in patients with recurrent or metastatic head and neck squamous-cell carcinoma (GORTEC 2014-01 TPExtreme): a multicentre, open-label, randomised, phase 2 trial. *Lancet Oncol*. 2021;22(4):463-475. doi:10.1016/S1470-2045(20)30755-5
68. Harrington KJ, Burtneß B, Greil R, et al. Pembrolizumab With or Without Chemotherapy in Recurrent or Metastatic Head and Neck Squamous Cell Carcinoma: Updated Results of the Phase III KEYNOTE-048 Study [published online ahead of print, 2022 Oct 11]. *J Clin Oncol*. 2022;JCO2102508. doi:10.1200/JCO.21.02508
69. Tahara M, Greil R, Rischin D et al. Pembrolizumab with or without chemotherapy for first-line treatment of recurrent/metastatic (R/M) head and neck squamous cell carcinoma (HNSCC): 5-year results from KEYNOTE-048. *Annals of Oncology* (2022) 33 (suppl_7): S295-S322. 10.1016/annonc/annonc1056
70. Argiris A, Harrington K, Tehara M et al. Nivolumab (N) + ipilimumab (I) vs EXTREME as first-line (1L) treatment (tx) for recurrent/metastatic squamous cell carcinoma of the head and neck (R/M SCCHN): Final results of CheckMate 651. *Ann Oncol* 2021;32 Suppl_5:s1283-s1346.
71. Cohen EE, Machiels JP, Harrington KJ et al. KEYNOTE-040: a phase III randomized trial of pembrolizumab (MK-3475) versus standard treatment in patients with recurrent or metastatic head and neck cancer. *J Clin Oncol* 2015; 33 (Suppl 15): TPS6084 – TPS6084.
72. Soulieres D, Harrington KJ, Le Tourneau C et al. Pembrolizumab (pembro) vs standard-of-care (SOC) in previously treated recurrent/metastatic (R/M) head and neck squamous cell carcinoma (HNSCC): 6-year follow-up of KEYNOTE-040 *Annals of Oncology* 33:S843

DOI:10.1016/j.annonc.2022.07.782

73. Dzienis MR, Cundom JE, Fuentes Cs et al. Pembrolizumab (pembro) + carboplatin (carbo) + paclitaxel (pacli) as first-line (1L) therapy in recurrent/metastatic (R/M) head and neck squamous cell carcinoma (HNSCC): Phase VI KEYNOTE-B10 study. *Annals of Oncology* (2022) 33 (suppl_7): S295-S322. 10.1016/annonc/annonc1056
74. Ferris RL, Blumenschein G Jr, Fayette J, et al. Nivolumab vs investigator's choice in recurrent or metastatic squamous cell carcinoma of the head and neck: 2-year long-term survival update of CheckMate 141 with analyses by tumor PD-L1 expression. *Oral Oncol.* 2018;81:45-51. doi:10.1016/j.oraloncology.2018.04.008
75. Zandberg DP, Algazi AP, Jimeno A, et al. Durvalumab for recurrent or metastatic head and neck squamous cell carcinoma: Results from a single-arm, phase II study in patients with $\geq 25\%$ tumour cell PD-L1 expression who have progressed on platinum-based chemotherapy. *Eur J Cancer.* 2019;107:142-152. doi:10.1016/j.ejca.2018.11.015
76. Siu LL, Even C, Mesía R, et al. Safety and Efficacy of Durvalumab With or Without Tremelimumab in Patients With PD-L1-Low/Negative Recurrent or Metastatic HNSCC: The Phase 2 CONDOR Randomized Clinical Trial. *JAMA Oncol.* 2019;5(2):195-203. doi:10.1001/jamaoncol.2018.4628
77. Ferris RL, Haddad R, Even C, et al. Durvalumab with or without tremelimumab in patients with recurrent or metastatic head and neck squamous cell carcinoma: EAGLE, a randomized, open-label phase III study. *Ann Oncol.* 2020;31(7):942-950. doi:10.1016/j.annonc.2020.04.001
78. Haddad RI, Harrington K, Tahara M, et al. Nivolumab Plus Ipilimumab Versus EXTREME Regimen as First-Line Treatment for Recurrent/Metastatic Squamous Cell Carcinoma of the Head and Neck: The Final Results of CheckMate 651 [published online ahead of print, 2022 Dec 6]. *J Clin Oncol.* 2022;JCO2200332. doi:10.1200/JCO.22.00332
79. Saba NF, Ekpenyong A, McCook-Veal A et al. A phase II trial of pembrolizumab and cabozantinib in patients (pts) with recurrent metastatic head and neck squamous cell carcinoma (RMHNSCC). DOI: 10.1200/JCO.2022.40.16_suppl.6008 *Journal of Clinical Oncology* 40, no. 16_suppl (June 01, 2022) 6008-6008
80. Travis WD, Brambilla E, Nicholson AG, et al. The 2015 World Health Organization Classification of lung tumors. Impact of genetic, clinical and radiologic advances since the the 2004 classification. *J Thorac Oncol.* 2015;10:1243-1260.
81. Cancer Genome Atlas Research Network. Comprehensive molecular profiling of lung adenocarcinoma [published correction appears in *Nature*. 2014 Oct 9;514(7521):262. Rogers,

- K [corrected to Rodgers, K]] [published correction appears in Nature. 2018 Jul;559(7715):E12]. Nature. 2014;511(7511):543-550. doi:10.1038/nature13385
82. Cancer Genome Atlas Research Network. Comprehensive genomic characterization of squamous cell lung cancers [published correction appears in Nature. 2012 Nov 8;491(7423):288. Rogers, Kristen [corrected to Rodgers, Kristen]]. Nature. 2012;489(7417):519-525. doi:10.1038/nature11404
83. Brahmer JR. Harnessing the immune system for the treatment of non-small-cell lung cancer. *J Clin Oncol*. 2013;31(8):1021-1028. doi:10.1200/JCO.2012.45.8703
84. Forde PM, Reiss KA, Zeidan AM, Brahmer JR. What lies within: novel strategies in immunotherapy for non-small cell lung cancer. *Oncologist*. 2013;18(11):1203-1213. doi:10.1634/theoncologist.2013-0171
85. Woo EY, Chu CS, Goletz TJ, et al. Regulatory CD4(+)CD25(+) T cells in tumors from patients with early-stage non-small cell lung cancer and late-stage ovarian cancer. *Cancer Res*. 2001;61(12):4766-4772.
86. Zhang Y, Huang S, Gong D, Qin Y, Shen Q. Programmed death-1 upregulation is correlated with dysfunction of tumor-infiltrating CD8+ T lymphocytes in human non-small cell lung cancer. *Cell Mol Immunol*. 2010;7(5):389-395. doi:10.1038/cmi.2010.28.
87. Mu CY, Huang JA, Chen Y, Chen C, Zhang XG. High expression of PD-L1 in lung cancer may contribute to poor prognosis and tumor cells immune escape through suppressing tumor infiltrating dendritic cells maturation. *Med Oncol*. 2011;28(3):682-688. doi:10.1007/s12032-010-9515-2
88. Konishi J, Yamazaki K, Azuma M, Kinoshita I, Dosaka-Akita H, Nishimura M. B7-H1 expression on non-small cell lung cancer cells and its relationship with tumor-infiltrating lymphocytes and their PD-1 expression. *Clin Cancer Res*. 2004;10(15):5094-5100. doi:10.1158/1078-0432.CCR-04-0428
89. Korkolopoulou P, Kaklamanis L, Pezzella F, Harris AL, Gatter KC. Loss of antigen-presenting molecules (MHC class I and TAP-1) in lung cancer. *Br J Cancer*. 1996;73(2):148-153. doi:10.1038/bjc.1996.28
90. Domagala-Kulawik J, Osinska I, Hoser G. Mechanisms of immune response regulation in lung cancer. *Transl Lung Cancer Res*. 2014;3(1):15-22. doi:10.3978/j.issn.2218-6751.2013.11.03
91. Brahmer J, Reckamp KL, Baas P, et al. Nivolumab versus Docetaxel in Advanced Squamous-Cell Non-Small-Cell Lung Cancer. *N Engl J Med*. 2015;373(2):123-135.

doi:10.1056/NEJMoa1504627

92. Borghaei H, Paz-Ares L, Horn L, et al. Nivolumab versus Docetaxel in Advanced Nonsquamous Non-Small-Cell Lung Cancer. *N Engl J Med.* 2015;373(17):1627-1639. doi:10.1056/NEJMoa1507643
93. Rittmeyer A, Barlesi F, Waterkamp D, et al. Atezolizumab versus docetaxel in patients with previously treated non-small-cell lung cancer (OAK): a phase 3, open-label, multicentre randomised controlled trial [published correction appears in *Lancet.* 2017 Apr 8;389(10077):e5]. *Lancet.* 2017;389(10066):255-265. doi:10.1016/S0140-6736(16)32517-X
94. Reck M, Rodríguez-Abreu D, Robinson AG, et al. Five-Year Outcomes With Pembrolizumab Versus Chemotherapy for Metastatic Non-Small-Cell Lung Cancer With PD-L1 Tumor Proportion Score \geq 50. *J Clin Oncol.* 2021;39(21):2339-2349. doi:10.1200/JCO.21.00174
95. Sezer A, Kilickap S, Gümüş M, et al. Cemiplimab monotherapy for first-line treatment of advanced non-small-cell lung cancer with PD-L1 of at least 50%: a multicentre, open-label, global, phase 3, randomised, controlled trial. *Lancet.* 2021;397(10274):592-604. doi:10.1016/S0140-6736(21)00228-2
96. Langer CJ, Gadgeel SM, Borghaei H, et al. Carboplatin and pemetrexed with or without pembrolizumab for advanced, non-squamous non-small-cell lung cancer: a randomised, phase 2 cohort of the open-label KEYNOTE-021 study. *Lancet Oncol.* 2016;17(11):1497-1508. doi:10.1016/S1470-2045(16)30498-3
97. Gandhi L, Rodríguez-Abreu D, Gadgeel S, et al. Pembrolizumab plus chemotherapy in metastatic non-small-cell lung cancer. *N Engl J Med.* 2018;378(22):2078-92.
98. Gadgeel S, Rodríguez-Abreu D, Speranza G et al., Updated Analysis From KEYNOTE-189: Pembrolizumab or Placebo Plus Pemetrexed and Platinum for Previously Untreated Metastatic Nonsquamous Non-Small-Cell Lung Cancer. *J Clin Oncol.* 2020 May 10;38(14):1505-1517. doi: 10.1200/JCO.19.03136. Epub 2020 Mar 9. 375.
99. Nishio M, Barlesi F, West H, et al. Atezolizumab Plus Chemotherapy for First-Line Treatment of Nonsquamous NSCLC: Results From the Randomized Phase 3 IMpower132 Trial. *J Thorac Oncol.* 2021;16(4):653-664. doi:10.1016/j.jtho.2020.11.025
100. Reck M, Mok TSK, Nishio M, et al. Atezolizumab plus bevacizumab and chemotherapy in non-small-cell lung cancer (IMpower150): key subgroup analyses of patients with EGFR mutations or baseline liver metastases in a randomised, open-label phase 3 trial. *Lancet Respir Med.* 2019;7(5):387-401. doi:10.1016/S2213-2600(19)30084-0
101. Socinski MA, Nishio M, Jotte RM, et al. IMpower150 Final Overall Survival Analyses for Atezolizumab Plus Bevacizumab and Chemotherapy in First-Line Metastatic Nonsquamous

- NSCLC. *J Thorac Oncol*. 2021;16(11):1909-1924. doi:10.1016/j.jtho.2021.07.009
102. West H, McCleod M, Hussein M, et al. Atezolizumab in combination with carboplatin plus nab-paclitaxel chemotherapy compared with chemotherapy alone as first-line treatment for metastatic non-squamous non-small-cell lung cancer (IMpower130): a multicentre, randomised, open-label, phase 3 trial. *Lancet Oncol*. 2019;20(7):924-97
103. Paz-Ares L, Luft A, Vicente D, et al. Pembrolizumab plus Chemotherapy for Squamous Non-Small-Cell Lung Cancer. *N Engl J Med*. 2018;379(21):2040-2051. doi:10.1056/NEJMoa1810865
104. Robinson AG, Vicente D, Tafreshi A, et al. First-Line Pembrolizumab Plus Chemotherapy for Patients With Advanced Squamous NSCLC: 3-Year Follow-up From KEYNOTE-407. *Journal of Thoracic Oncology* (2021) 16 (suppl_4): S748-S802.
105. Jotte R, Capuzzo F, Vynnychenko I, et al. Atezolizumab in combination with carboplatin and nab-paclitaxel in advanced squamous NSCLC (IMpower131): results from a randomized phase III trial. *J Thorac Oncol* 2020; 15(8):1351-60
106. Paz-Ares LG, Ciuleanu TE, Lee JS et al. Nivolumab (NIVO) plus ipilimumab (IPI) versus chemotherapy (chemo) as first-line (1L) treatment for advanced non-small cell lung cancer (NSCLC): 4-year update from CheckMate 227. *Journal of Clinical Oncology* 2021 39:15_suppl, 9016-9016
107. Brahmer JR, Lee JS, Ciuleanu TE, et al. Five-Year Survival Outcomes With Nivolumab Plus Ipilimumab Versus Chemotherapy as First-Line Treatment for Metastatic Non-Small Cell Lung Cancer in CheckMate 227 [published online ahead of print, 2022 Oct 12]. *J Clin Oncol*. 2022;101200JCO2201503. doi:10.1200/JCO.22.01503
108. Reck M, Ciuleanu TE, Cobo M et al. First-line nivolumab (NIVO) plus ipilimumab (IPI) plus two cycles of chemotherapy (chemo) versus chemo alone (4 cycles) in patients with advanced non-small cell lung cancer (NSCLC): Two-year update from CheckMate 9LA. *Journal of Clinical Oncology* 2021 39:15_suppl, 9000-9000
109. Paz-Ares LG, Ciuleanu TE, Cobo-Dols M et al. First-line (1L) nivolumab (NIVO) + ipilimumab (IPI) + 2 cycles of chemotherapy (chemo) versus chemo alone (4 cycles) in patients (pts) with metastatic non-small cell lung cancer (NSCLC): 3-year update from CheckMate 9LA. *Journal of Clinical Oncology* 40, no. 17_suppl (June 10, 2022) LBA9026-LBA9026. DOI: 10.1200/JCO.2022.40.17_suppl.LBA9026
110. M. Johnson, B.C. Cho, A. Luft, J. Alatorre-Alexander, et al. PL02.01 Durvalumab ± Tremelimumab + Chemotherapy as First-line Treatment for mNSCLC: Results from the Phase 3 POSEIDON Study, *Journal of Thoracic Oncology*, Volume 16, Issue 10, Supplement, 2021,

111. M. Johnson, B.C. Cho, A. Luft, et al. Durvalumab (D) ± tremelimumab (T) + chemotherapy (CT) in 1L metastatic (m) NSCLC: Overall survival (OS) update from POSEIDON after median follow-up (mFU) of approximately 4 years (y) *Annals of Oncology* (2022) 33 (suppl_7): S808-S869. [10.1016/annonc/annonc1089](https://doi.org/10.1016/annonc/annonc1089)
112. Horn L, Spigel DR, Vokes EE, et al. Nivolumab Versus Docetaxel in Previously Treated Patients With Advanced Non-Small-Cell Lung Cancer: Two-Year Outcomes From Two Randomized, Open-Label, Phase III Trials (CheckMate 017 and CheckMate 057). *J Clin Oncol*. 2017;35(35):3924-3933. doi:10.1200/JCO.2017.74.3062
113. Herbst RS, Garon EB, Kim DW, et al. Long-Term Outcomes and Retreatment Among Patients With Previously Treated, Programmed Death-Ligand 1–Positive, Advanced Non–Small-Cell Lung Cancer in the KEYNOTE-010 Study. *J Clin Oncol*. 2020 May 10;38(14):1580-1590.
114. Von Pawel J, Bordoni R, Satouchi M, et al. Long-term survival in patients with advanced non-small-cell lung cancer treated with atezolizumab versus docetaxel: Results from the randomised phase III OAK study. *Eur J Cancer*. 2019;107:124-32.
115. Albert DM, Ryan LM, Borden EC. Metastatic ocular and cutaneous melanoma: a comparison of patient characteristics and prognosis. *Arch Ophthalmol*. 1996;114:107-8
116. Inskip PD, Devesi SS, Fraumeni JF. Trends in the incidence of ocular melanoma in the United States, 1974-1998. *Cancer Causes Control*. 2003;14:251-7.
117. Heppt MV, Heinzerling L, Kähler KC, et al. Prognostic factors and outcomes in metastatic uveal melanoma treated with programmed cell death-1 or combined PD-1/cytotoxic T-lymphocyte antigen-4 inhibition. *Eur J Cancer*. 2017;82:56-65. doi:10.1016/j.ejca.2017.05.038
118. Algazi AP, Tsai KK, Shoushtari AN, et al. Clinical outcomes in metastatic uveal melanoma treated with PD-1 and PD-L1 antibodies. *Cancer*. 2016;122(21):3344-53.
119. Kottschade LA, McWilliams RR, Markovic SN, et al. The use of pembrolizumab for the treatment of metastatic uveal melanoma. *Melanoma Res*. 2016;26(3):300-3.
120. Maio M, Danielli R, Chiarion-Sileni V, et al. Efficacy and safety of ipilimumab in patients with pre-treated, uveal melanoma. *Ann Oncol*. 2013;24(11):2911-5.
121. Mignard C, Deschamps Huvier A, Gillibert A, et al. Efficacy of immunotherapy in patients with metastatic mucosal or uveal melanoma. *J Oncol*. 2018;2018:1908065.
122. Sharma P, Hu-Lieskovan S, Wargo JA, Ribas A. Primary, Adaptive, and Acquired Resistance to Cancer Immunotherapy. *Cell*. 2017;168(4):707–723. doi:10.1016/j.cell.2017.01.017

123. Gubin MM, Zhang X, Schuster H, et al. Checkpoint blockade cancer immunotherapy targets tumour-specific mutant antigens. *Nature*. 2014;515(7528):577-581. doi:10.1038/nature13988
124. Liu C, Peng W, Xu C, et al. BRAF inhibition increases tumor infiltration by T cells and enhances the antitumor activity of adoptive immunotherapy in mice. *Clin Cancer Res*. 2013;19(2):393-403. doi:10.1158/1078-0432.CCR-12-1626
125. Peng W, Chen JQ, Liu C, et al. Loss of PTEN Promotes Resistance to T Cell-Mediated Immunotherapy. *Cancer Discov*. 2016;6(2):202-216. doi:10.1158/2159-8290.CD-15-0283
126. Spranger S, Bao R, Gajewski TF. Melanoma-intrinsic β -catenin signalling prevents anti-tumour immunity. *Nature*. 2015;523(7559):231-235. doi:10.1038/nature14404
127. Benci JL, Xu B, Qiu Y, et al. Tumor Interferon Signaling Regulates a Multigenic Resistance Program to Immune Checkpoint Blockade. *Cell*. 2016;167(6):1540-1554.e12. doi:10.1016/j.cell.2016.11.022
128. Shankaran V, Ikeda H, Bruce AT, et al. IFN γ and lymphocytes prevent primary tumour development and shape tumour immunogenicity. *Nature*. 2001;410(6832):1107-1111. doi:10.1038/35074122
129. Li C, Jiang P, Wei S, Xu X, Wang J. Regulatory T cells in tumor microenvironment: new mechanisms, potential therapeutic strategies and future prospects. *Mol Cancer*. 2020;19(1):116. Published 2020 Jul 17. doi:10.1186/s12943-020-01234-1
130. Yu X, Harden K, Gonzalez LC, et al. The surface protein TIGIT suppresses T cell activation by promoting the generation of mature immunoregulatory dendritic cells. *Nat Immunol*. 2009;10(1):48-57. doi:10.1038/ni.1674
131. Park HJ, Park JS, Jeong YH, et al. PD-1 upregulated on regulatory T cells during chronic virus infection enhances the suppression of CD8⁺ T cell immune response via the interaction with PD-L1 expressed on CD8⁺ T cells [published correction appears in *J Immunol*. 2015 Dec 15;195(12):5841-2]. *J Immunol*. 2015;194(12):5801-5811. doi:10.4049/jimmunol.1401936
132. Liang B, Workman C, Lee J, et al. Regulatory T cells inhibit dendritic cells by lymphocyte activation gene-3 engagement of MHC class II. *J Immunol*. 2008;180(9):5916-5926. doi:10.4049/jimmunol.180.9.5916
133. Pandiyan P, Zheng L, Ishihara S, Reed J, Lenardo MJ. CD4⁺CD25⁺Foxp3⁺ regulatory T cells induce cytokine deprivation-mediated apoptosis of effector CD4⁺ T cells. *Nat Immunol*. 2007;8(12):1353-1362. doi:10.1038/ni1536
134. Togashi Y, Shitara K, Nishikawa H. Regulatory T cells in cancer immunosuppression - implications for anticancer therapy. *Nat Rev Clin Oncol*. 2019;16(6):356-371.

doi:10.1038/s41571-019-0175-7

135. Zhou G, Levitsky HI. Natural regulatory T cells and de novo-induced regulatory T cells contribute independently to tumor-specific tolerance. *J Immunol*. 2007;178(4):2155-2162. doi:10.4049/jimmunol.178.4.2155
136. Chaudhary B, Elkord E. Regulatory T Cells in the Tumor Microenvironment and Cancer Progression: Role and Therapeutic Targeting. *Vaccines (Basel)*. 2016;4(3):28. Published 2016 Aug 6. doi:10.3390/vaccines4030028
137. Viehl CT, Moore TT, Liyanage UK, et al. Depletion of CD4+CD25+ regulatory T cells promotes a tumor-specific immune response in pancreas cancer-bearing mice. *Ann Surg Oncol*. 2006;13(9):1252-1258. doi:10.1245/s10434-006-9015-y
138. Quezada SA, Peggs KS, Curran MA, Allison JP. CTLA4 blockade and GM-CSF combination immunotherapy alters the intratumor balance of effector and regulatory T cells. *J Clin Invest*. 2006;116(7):1935-1945. doi:10.1172/JCI27745
139. Yang L, DeBusk LM, Fukuda K, et al. Expansion of myeloid immune suppressor Gr⁺CD11b⁺ cells in tumor-bearing host directly promotes tumor angiogenesis. *Cancer Cell*. 2004;6(4):409-421. doi:10.1016/j.ccr.2004.08.031
140. Solito S, Falisi E, Diaz-Montero CM, et al. A human promyelocytic-like population is responsible for the immune suppression mediated by myeloid-derived suppressor cells. *Blood*. 2011;118(8):2254-2265. doi:10.1182/blood-2010-12-325753
141. Meyer C, Cagnon L, Costa-Nunes CM, et al. Frequencies of circulating MDSC correlate with clinical outcome of melanoma patients treated with ipilimumab. *Cancer Immunol Immunother*. 2014;63(3):247-257. doi:10.1007/s00262-013-1508-5
142. Chanmee T, Ontong P, Konno K, Itano N. Tumor-associated macrophages as major players in the tumor microenvironment. *Cancers*. 2014;6:1670–1690.
143. Hu W, Li X, Zhang C, Yang Y, Jiang J, Wu C. Tumor-associated macrophages in cancers. *Clin Transl Oncol*. 2016;18(3):251-258. doi:10.1007/s12094-015-1373-0
144. Boutilier AJ, ElSawa SF. Macrophage Polarization States in the Tumor Microenvironment. *Int J Mol Sci*. 2021;22(13):6995. Published 2021 Jun 29. doi:10.3390/ijms22136995
145. Allavena P, Sica A, Solinas G, Porta C, Mantovani A. The inflammatory micro-environment in tumor progression: the role of tumor-associated macrophages. *Crit Rev Oncol Hematol*. 2008;66(1):1-9. doi:10.1016/j.critrevonc.2007.07.004
146. Wynn TA, Chawla A, Pollard JW. Macrophage biology in development, homeostasis and disease. *Nature*. 2013;496(7446):445-455. doi:10.1038/nature12034

147. Fritz JM, Tennis MA, Orlicky DJ, et al. Depletion of tumor-associated macrophages slows the growth of chemically induced mouse lung adenocarcinomas [published correction appears in *Front Immunol.* 2015;6:88]. *Front Immunol.* 2014;5:587. Published 2014 Nov 25. doi:10.3389/fimmu.2014.00587
148. Kuang DM, Zhao Q, Peng C, et al. Activated monocytes in peritumoral stroma of hepatocellular carcinoma foster immune privilege and disease progression through PD-L1. *J Exp Med.* 2009;206(6):1327-1337. doi:10.1084/jem.20082173
149. Chen PL, Roh W, Reuben A, et al. Analysis of Immune Signatures in Longitudinal Tumor Samples Yields Insight into Biomarkers of Response and Mechanisms of Resistance to Immune Checkpoint Blockade. *Cancer Discov.* 2016;6(8):827-837. doi:10.1158/2159-8290.CD-15-1545
150. Dong H, Strome SE, Salomao DR, et al. Tumor-associated B7-H1 promotes T-cell apoptosis: a potential mechanism of immune evasion [published correction appears in *Nat Med* 2002 Sep;8(9):1039]. *Nat Med.* 2002;8(8):793-800. doi:10.1038/nm730
151. Gajewski TF, Schreiber H, Fu YX. Innate and adaptive immune cells in the tumor microenvironment. *Nat Immunol.* 2013;14(10):1014-1022. doi:10.1038/ni.2703.
152. Wang Q, Zhang J, Tu H, et al. Soluble immune checkpoint-related proteins as predictors of tumor recurrence, survival, and T cell phenotypes in clear cell renal cell carcinoma patients. *J Immunother Cancer.* 2019;7(1):334. Published 2019 Nov 29. doi:10.1186/s40425-019-0810-y.
153. Botticelli A, Pomati G, Cirillo A, et al. The role of immune profile in predicting outcomes in cancer patients treated with immunotherapy. *Front Immunol.* 2022;13:974087. Published 2022 Nov 3. doi:10.3389/fimmu.2022.974087
154. Rodrigues M, Mobuchon L, Houy A, et al. Outlier response to anti-PD1 in uveal melanoma reveals germline MBD4 mutations in hypermutated tumors. *Nat Commun.* 2018;9(1):1866. Published 2018 May 14. doi:10.1038/s41467-018-04322-5
155. Zizzari IG, Di Filippo A, Scirocchi F, et al. Soluble Immune Checkpoints, Gut Metabolites and Performance Status as Parameters of Response to Nivolumab Treatment in NSCLC Patients. *J Pers Med.* 2020;10(4):208. Published 2020 Nov 4. doi:10.3390/jpm10040208
156. Daassi D, Mahoney KM, Freeman GJ. The importance of exosomal PDL1 in tumour immune evasion. *Nat Rev Immunol.* 2020;20:209–15. doi: 10.1038/s41577-019-0264-y.
157. Gu D, Ao X, Yang Y, Chen Z, Xu X. Soluble immune checkpoints in cancer: production, function and biological significance. *J Immunother Cancer.* 2018;6:132. doi: 10.1186/s40425-018-0449-0.
158. Ugurel S, Schadendorf D, Horny K, et al. Elevated baseline serum PD-1 or PD-L1 predicts poor

- outcome of PD-1 inhibition therapy in metastatic melanoma. *Ann Oncol.* 2020;31(1):144-152. doi:10.1016/j.annonc.2019.09.005
- 159.Zizzari IG, Di Filippo A, Botticelli A, et al. Circulating CD137+ T Cells Correlate with Improved Response to Anti-PD1 Immunotherapy in Patients with Cancer. *Clin Cancer Res.* 2022;28(5):1027-1037. doi:10.1158/1078-0432.CCR-21-2918
- 160.Machiraju D, Wiecken M, Lang N, et al. Soluble immune checkpoints and T-cell subsets in blood as biomarkers for resistance to immunotherapy in melanoma patients. *Oncoimmunology.* 2021;10(1):1926762. Published 2021 May 25. doi:10.1080/2162402X.2021.1926762
- 161.Lim SY, Lee JH, Gide TN, et al. Circulating Cytokines Predict Immune-Related Toxicity in Melanoma Patients Receiving Anti-PD-1-Based Immunotherapy. *Clin Cancer Res.* 2019;25(5):1557-1563. doi:10.1158/1078-0432.CCR-18-2795.
- 162.Kang JH, Bluestone JA, Young A. Predicting and Preventing Immune Checkpoint Inhibitor Toxicity: Targeting Cytokines. *Trends Immunol.* 2021 Apr;42(4):293-311. doi: 10.1016/j.it.2021.02.006.
- 163.Wang M, Zhai X, Li J, et al. The Role of Cytokines in Predicting the Response and Adverse Events Related to Immune Checkpoint Inhibitors. *Front Immunol.* 2021;12:670391. Published 2021 Jul 22. doi:10.3389/fimmu.2021.670391
- 164.Propper DJ, Balkwill FR. Harnessing cytokines and chemokines for cancer therapy. *Nat Rev Clin Oncol.* 2022 Jan 7. doi: 10.1038/s41571-021-00588-9.
- 165.Mollica Poeta V, Massara M, Capucetti A, Bonocchi R. Chemokines and Chemokine Receptors: New Targets for Cancer Immunotherapy. *Front Immunol.* 2019;10:379. Published 2019 Mar 6. doi:10.3389/fimmu.2019.00379
- 166.Chen AY, Wolchok JD, Bass AR. TNF in the era of immune checkpoint inhibitors: friend or foe? *Nat Rev Rheumatol.* 2021 Apr;17(4):213-223. doi: 10.1038/s41584-021-00584-4
- 167.Wanhai Ke, Li Zhang, Yan Dai. The role of IL-6 in immunotherapy of non-small cell lung cancer (NSCLC) with immune-related adverse events (irAEs). *Thorac Cancer.* 2020 Apr;11(4):835-839. doi: 10.1111/1759-7714.13341.
- 168.Azadeh H, Alizadeh-Navaei R, Rezaeiemanesh A, Rajabinejad M. Immune-related adverse events (irAEs) in ankylosing spondylitis (AS) patients treated with interleukin (IL)-17 inhibitors: a systematic review and meta-analysis. *Inflammopharmacology.* 2022;30(2):435-451. doi:10.1007/s10787-022-00933-z
- 169.Croft M, Benedict CA, Ware CF. Clinical Targeting of the TNF and TNFR Superfamilies. *Nat Rev Drug Discov* (2013) 12:147–68.

170. Arida A, Fragiadaki K, Giavri E, Sfikakis PP. Anti-TNF agents for Behçet's disease: analysis of published data on 369 patients. *Semin Arthritis Rheum.* 2011;41(1):61-70. doi:10.1016/j.semarthrit.2010.09.002
171. Perez-Ruiz E, Minute L, Otano I, et al. Prophylactic TNF blockade uncouples efficacy and toxicity in dual CTLA-4 and PD-1 immunotherapy. *Nature.* 2019;569(7756):428-432. doi:10.1038/s41586-019-1162-y
172. Minor DR, Chin K, Kashani-Sabet M. Infliximab in the treatment of anti-CTLA4 antibody (ipilimumab) induced immune-related colitis. *Cancer Biother Radiopharm.* 2009;24(3):321-325. doi:10.1089/cbr.2008.0607
173. Hirashima T, Kanai T, Suzuki H, et al. The Levels of Interferon-gamma Release as a Biomarker for Non-small-cell Lung Cancer Patients Receiving Immune Checkpoint Inhibitors. *Anticancer Res.* 2019;39(11):6231-6240. doi:10.21873/anticancer.13832
174. Bromberg J, Wang TC. Inflammation and cancer: IL-6 and STAT3 complete the link. *Cancer Cell.* 2009;15(2):79-80. doi:10.1016/j.ccr.2009.01.009
175. Tanaka R, Okiyama N, Okune M, et al. Serum level of interleukin-6 is increased in nivolumab-associated psoriasiform dermatitis and tumor necrosis factor- α is a biomarker of nivolumab reactivity. *J Dermatol Sci.* 2017;86(1):71-73. doi:10.1016/j.jdermsci.2016.12.019
176. Okiyama N, Tanaka R. *Nihon Rinsho Meneki Gakkai Kaishi.* 2017;40(2):95-101. doi:10.2177/jsci.40.95
177. Tanaka R, Okiyama N, Okune M, et al. Serum level of interleukin-6 is increased in nivolumab-associated psoriasiform dermatitis and tumor necrosis factor- α is a biomarker of nivolumab reactivity. *J Dermatol Sci.* 2017;86(1):71-73. doi:10.1016/j.jdermsci.2016.12.019
178. Ozawa Y, Amano Y, Kanata K, et al. Impact of early inflammatory cytokine elevation after commencement of PD-1 inhibitors to predict efficacy in patients with non-small cell lung cancer. *Med Oncol.* 2019;36(4):33. Published 2019 Mar 1. doi:10.1007/s12032-019-1255-3
179. Botticelli A, Cirillo A, Pomati G et al. Immune-related toxicity and soluble profile in patients affected by solid tumours: a network approach, *Cancer Immunology, Immunotherapy.* 2023 accepted January 2023
180. Platten M, Wick W, Van den Eynde BJ. Tryptophan catabolism in cancer: beyond IDO and tryptophan depletion. *Cancer Res.* 2012;72(21):5435-5440. doi:10.1158/0008-5472.CAN-12-0569

181. Botticelli A, Cerbelli B, Lionetto L, et al. Can IDO activity predict primary resistance to anti-PD-1 treatment in NSCLC?. *J Transl Med.* 2018;16(1):219. Published 2018 Aug 6. doi:10.1186/s12967-018-1595-3
182. Wang Y, Hu GF, Wang ZH. The status of immunosuppression in patients with stage IIIB or IV non-small-cell lung cancer correlates with the clinical characteristics and response to chemotherapy. *Onco Targets Ther.* 2017;10:3557-3566. Published 2017 Jul 19. doi:10.2147/OTT.S136259
183. Botticelli A, Mezi S, Pomati G, et al. Tryptophan Catabolism as Immune Mechanism of Primary Resistance to Anti-PD-1. *Front Immunol.* 2020;11:1243. Published 2020 Jul 7. doi:10.3389/fimmu.2020.01243
184. Munn DH, Shafizadeh E, Attwood JT, Bondarev I, Pashine A, Mellor AL. Inhibition of T cell proliferation by macrophage tryptophan catabolism. *J Exp Med.* 1999;189(9):1363-1372. doi:10.1084/jem.189.9.1363
185. Hwu P, Du MX, Lapointe R, Do M, Taylor MW, Young HA. Indoleamine 2,3-dioxygenase production by human dendritic cells results in the inhibition of T cell proliferation. *J Immunol.* 2000;164(7):3596-3599. doi:10.4049/jimmunol.164.7.3596
186. Chen W, Liang X, Peterson AJ, Munn DH, Blazar BR. The indoleamine 2,3-dioxygenase pathway is essential for human plasmacytoid dendritic cell-induced adaptive T regulatory cell generation. *J Immunol.* 2008;181(8):5396-5404. doi:10.4049/jimmunol.181.8.5396
187. Holmgaard RB, Zamarin D, Munn DH, Wolchok JD, Allison JP. Indoleamine 2,3-dioxygenase is a critical resistance mechanism in antitumor T cell immunotherapy targeting CTLA-4. *J Exp Med.* 2013;210(7):1389-1402. doi:10.1084/jem.20130066
188. Botticelli A, Cirillo A, Scagnoli S, et al. The Agnostic Role of Site of Metastasis in Predicting Outcomes in Cancer Patients Treated with Immunotherapy. *Vaccines (Basel).* 2020;8(2):203. Published 2020 Apr 28. doi:10.3390/vaccines8020203
189. Botticelli A, Zizzari IG, Scagnoli S, et al. The Role of Soluble LAG3 and Soluble Immune Checkpoints Profile in Advanced Head and Neck Cancer: A Pilot Study. *J Pers Med.* 2021;11(7):651. Published 2021 Jul 10. doi:10.3390/jpm11070651
190. Le DT, Durham JN, Smith KN, et al. Mismatch repair deficiency predicts response of solid tumors to PD-1 blockade. *Science.* 2017;357(6349):409-413. doi:10.1126/science.aan6733
191. Le DT, Uram JN, Wang H, et al. PD-1 Blockade in Tumors with Mismatch-Repair Deficiency.

- N Engl J Med. 2015;372(26):2509-2520. doi:10.1056/NEJMoa1500596
192. Goodman A.M., Kato S., Bazhenova L., et al. Tumor mutational burden as an independent predictor of response to immunotherapy in diverse cancers. *Mol Cancer Ther.* 2017;16(11):2598–2608
193. Marabelle A., Fakih M., Lopez J., et al. Association of tumour mutational burden with outcomes in patients with advanced solid tumours treated with pembrolizumab: prospective biomarker analysis of the multicohort, open-label, phase 2 KEYNOTE-158 study. *Lancet Oncol.* 2020;21(10):1353–1365.
194. Carbone DP, Reck M, Paz-Ares L, et al. First-line nivolumab in stage IV or recurrent non–small-cell lung cancer. *N Engl J Med* 2017;376:2415-26.
195. Fourcade J, Sun Z, Benallaoua M, et al. Upregulation of Tim-3 and PD-1 expression is associated with tumor antigen-specific CD8+ T cell dysfunction in melanoma patients. *J Exp Med.* 2010;207(10):2175-2186. doi:10.1084/jem.20100637
196. Kurtulus S, Sakuishi K, Ngiow SF, et al. TIGIT predominantly regulates the immune response via regulatory T cells. *J Clin Invest.* 2015;125(11):4053-4062. doi:10.1172/JCI81187
197. Koyama S, Akbay EA, Li YY, et al. Adaptive resistance to therapeutic PD-1 blockade is associated with upregulation of alternative immune checkpoints. *Nat Commun.* 2016;7:10501. Published 2016 Feb 17. doi:10.1038/ncomms10501
198. Haddad RE, Blumenschein G, Fayette J Jr et al. Treatment beyond progression with nivolumab in patients with recurrent or metastatic (R/M) squamous cell carcinoma of the head and neck (SCCHN) in the phase 3 checkmate 141 study: a biomarker analysis and updated clinical outcomes. *Ann Oncol* 2017; 28(Suppl 5):mdx374.001.
199. Tawbi HA, Schadendorf D, Lipson EJ, et al. Relatlimab and Nivolumab versus Nivolumab in Untreated Advanced Melanoma. *N Engl J Med.* 2022;386(1):24-34. doi:10.1056/NEJMoa2109970
200. Routy B, Le Chatelier E, Derosa L, et al. Gut microbiome influences efficacy of PD-1-based immunotherapy against epithelial tumors. *Science.* 2018;359(6371):91-97. doi:10.1126/science.aan3706
201. Darnell EP, Mooradian MJ, Baruch EN, Yilmaz M, Reynolds KL. Immune-Related Adverse Events (irAEs): Diagnosis, Management, and Clinical Pearls. *Curr Oncol Rep.* 2020;22(4):39. Published 2020 Mar 21. doi:10.1007/s11912-020-0897-9

202. Sullivan RJ, Weber JS. Immune-related toxicities of checkpoint inhibitors: mechanisms and mitigation strategies. *Nat Rev Drug Discov.* 2021 Jul 27. doi: 10.1038/s41573-021-00259-5
203. Choi J, Lee SY. Clinical Characteristics and Treatment of Immune-Related Adverse Events of Immune Checkpoint Inhibitors. *Immune Netw.* 2020 Feb 17;20(1):e9. doi: 10.4110/in.2020.20.
204. Postow MA, Sidlow R, Hellmann MD. Immune-Related Adverse Events Associated with Immune Checkpoint Blockade. *N Engl J Med.* 2018;378(2):158-168. doi:10.1056/NEJMra1703481
205. Puzanov I, Diab A, Abdallah K, et al. Managing toxicities associated with immune checkpoint inhibitors: consensus recommendations from the Society for Immunotherapy of Cancer (SITC) Toxicity Management Working Group. *J Immunother Cancer.* 2017;5(1):95. Published 2017 Nov 21. doi:10.1186/s40425-017-0300-z
206. Voon PJ, Cella D, Hansen AR. Health-related quality-of-life assessment of patients with solid tumors on immuno-oncology therapies. *Cancer.* 2021;127(9):1360-1368. doi:10.1002/cncr.33457
207. Wang DY, Salem JE, Cohen JV, et al. Fatal Toxic Effects Associated With Immune Checkpoint Inhibitors: A Systematic Review and Meta-analysis [published correction appears in *JAMA Oncol.* 2018 Dec 1;4(12):1792]. *JAMA Oncol.* 2018;4(12):1721-1728. doi:10.1001/jamaoncol.2018.3923
208. Daly LE, Power DG, O'Reilly Á, et al. The impact of body composition parameters on ipilimumab toxicity and survival in patients with metastatic melanoma. *Br J Cancer.* 2017;116(3):310-317. doi:10.1038/bjc.2016.431
209. Haik L, Gonthier A, Quivy A, et al. The impact of sarcopenia on the efficacy and safety of immune checkpoint inhibitors in patients with solid tumours. *Acta Oncol.* 2021;60(12):1597-1603. doi:10.1080/0284186X.2021.1978540
210. Ramos-Casals M, Brahmer JR, Callahan MK, et al. Immune-related adverse events of checkpoint inhibitors. *Nat Rev Dis Primers.* 2020;6(1):38. Published 2020 May 7. doi:10.1038/s41572-020-0160-6
211. Kronzer VL, Crowson CS, Sparks JA, Myasoedova E, Davis J 3rd. Family History of Rheumatic, Autoimmune, and Nonautoimmune Diseases and Risk of Rheumatoid Arthritis. *Arthritis Care Res (Hoboken).* 2021;73(2):180-187. doi:10.1002/acr.24115
212. Shah NJ, Al-Shbool G, Blackburn M, et al. Safety and efficacy of immune checkpoint inhibitors (ICIs) in cancer patients with HIV, hepatitis B, or hepatitis C viral infection. *J Immunother Cancer.* 2019;7(1):353. Published 2019 Dec 17. doi:10.1186/s40425-019-0771-1

213. Belluomini L, Caldart A, Avancini A, et al. Infections and Immunotherapy in Lung Cancer: A Bad Relationship?. *Int J Mol Sci.* 2020;22(1):42. Published 2020 Dec 22. doi:10.3390/ijms22010042
214. Botticelli A, Cirillo A, Pomati G, et al. The role of opioids in cancer response to immunotherapy. *J Transl Med.* 2021;19(1):119. Published 2021 Mar 23. doi:10.1186/s12967-021-02784-8
215. Buti S, Bersanelli M, Perrone F, et al. Effect of concomitant medications with immunomodulatory properties on the outcomes of patients with advanced cancer treated with immune checkpoint inhibitors: development and validation of a novel prognostic index. *Eur J Cancer.* 2021;142:18-28. doi:10.1016/j.ejca.2020.09.033.
216. Suresh K, Naidoo J, Lin CT, Danoff S. Immune Checkpoint Immunotherapy for Non-Small Cell Lung Cancer: Benefits and Pulmonary Toxicities. *Chest.* 2018;154(6):1416-1423. doi:10.1016/j.chest.2018.08.1048
217. Delaunay M, Cadranet J, Lusque A, et al. Immune-checkpoint inhibitors associated with interstitial lung disease in cancer patients [published correction appears in *Eur Respir J.* 2017 Nov 9;50(5)]. *Eur Respir J.* 2017;50(2):1700050. Published 2017 Aug 10. doi:10.1183/13993003.00050-2017
218. Schuurhuizen CS, Verheul HM, Braamse AM, et al. The predictive value of cumulative toxicity for quality of life in patients with metastatic colorectal cancer during first-line palliative chemotherapy. *Cancer Manag Res.* 2018;10:3015-3021. Published 2018 Aug 29. doi:10.2147/CMAR.S166468
219. Castellanos EH, Chen SC, Drexler H, Horn L. Making the Grade: The Impact of Low-Grade Toxicities on Patient Preference for Treatment With Novel Agents. *J Natl Compr Canc Netw.* 2015;13(12):1490-1495. doi:10.6004/jnccn.2015.0177
220. Iacovelli R, Verri E, Cossu Rocca M, et al. Prognostic role of the cumulative toxicity in patients affected by metastatic renal cells carcinoma and treated with first-line tyrosine kinase inhibitors. *Anticancer Drugs.* 2017;28(2):206-212. doi:10.1097/CAD.0000000000000439
221. Schneider BJ, Naidoo J, Santomaso BD, et al. Management of Immune-Related Adverse Events in Patients Treated With Immune Checkpoint Inhibitor Therapy: ASCO Guideline Update [published correction appears in *J Clin Oncol.* 2022 Jan 20;40(3):315]. *J Clin Oncol.* 2021;39(36):4073-4126. doi:10.1200/JCO.21.01440
222. Dine J, Gordon R, Shames Y, Kasler MK, Barton-Burke M. Immune Checkpoint Inhibitors: An Innovation in Immunotherapy for the Treatment and Management of Patients with Cancer. *Asia Pac J Oncol Nurs.* 2017;4(2):127-135. doi:10.4103/apjon.apjon_4_17

223. Rich JT, Neely JG, Paniello RC, Voelker CC, Nussenbaum B, Wang EW. A practical guide to understanding Kaplan-Meier curves. *Otolaryngol Head Neck Surg.* 2010;143(3):331-336. doi:10.1016/j.otohns.2010.05.007
224. Silverman EK, Schmidt HHHW, Anastasiadou E, et al. Molecular networks in Network Medicine: Development and applications. *Wiley Interdiscip Rev Syst Biol Med.* 2020;12(6):e1489. doi:10.1002/wsbm.1489
225. Barabási AL, Gulbahce N, Loscalzo J. Network medicine: a network-based approach to human disease. *Nat Rev Genet.* 2011;12(1):56-68. doi:10.1038/nrg2918.
226. Paci P, Fiscon G, Conte F, Wang RS, Farina L, Loscalzo J. Gene co-expression in the interactome: moving from correlation toward causation via an integrated approach to disease module discovery. *NPJ Syst Biol Appl.* 2021;7(1):3. Published 2021 Jan 21. doi:10.1038/s41540-020-00168-0
227. Botticelli A, Mezi S, Pomati G, et al. The 5-Ws of immunotherapy in head and neck cancer. *Crit Rev Oncol Hematol.* 2020;153:103041. doi:10.1016/j.critrevonc.2020.103041
228. Tosolini M, Kirilovsky A, Mlecnik B, et al.. Clinical impact of different classes of infiltrating T cytotoxic and helper cells (Th1, Th2, Treg, Th17) in patients with colorectal cancer. *Cancer Res* 2011;71:1263–71. 10.1158/0008-5472.CAN-10-2907,
229. Razi S, Baradaran Noveiry B, Keshavarz-Fathi M, et al.. IL-17 and colorectal cancer: from carcinogenesis to treatment. *Cytokine* 2019;116:7–12. 10.1016/j.cyto.2018.12.021
230. Wu P, Wu D, Ni C, et al.. $\gamma\delta$ T17 cells promote the accumulation and expansion of myeloid-derived suppressor cells in human colorectal cancer. *Immunity* 2014;40:785–800. 10.1016/j.immuni.2014.03.013
231. Chen J, Ye X, Pitmon E, et al.. IL-17 inhibits CXCL9/10-mediated recruitment of CD8+ cytotoxic T cells and regulatory T cells to colorectal tumors. *J Immunother Cancer* 2019;7:324. 10.1186/s40425-019-0757-z
232. Liu C, Liu R, Wang B, et al. Blocking IL-17A enhances tumor response to anti-PD-1 immunotherapy in microsatellite stable colorectal cancer [published correction appears in *J Immunother Cancer.* 2021 Oct;9(10):]. *J Immunother Cancer.* 2021;9(1):e001895. doi:10.1136/jitc-2020-001895
233. Blair HA. Secukinumab: A Review in Ankylosing Spondylitis [published correction appears in *Drugs.* 2019 Mar 11;:]. *Drugs.* 2019;79(4):433-443. doi:10.1007/s40265-019-01075-3
234. Ono E, Uede T. Implication of Soluble Forms of Cell Adhesion Molecules in Infectious Disease and Tumor: Insights from Transgenic Animal Models. *Int J Mol Sci.* 2018;19(1):239.

Published 2018 Jan 13. doi:10.3390/ijms19010239

235. Volin MV. Soluble adhesion molecules in the pathogenesis of rheumatoid arthritis. *Curr Pharm Des.* 2005;11(5):633-53. doi: 10.2174/1381612053381972.
236. Giddings JC. Soluble adhesion molecules in inflammatory and vascular diseases. *Biochem Soc Trans.* 2005 Apr;33(Pt 2):406-8. doi: 10.1042/BST0330406.
237. Bricio T, Rivera M, Molina A, Martin A, Burgos J, Mampaso F. Soluble adhesion molecules in renal transplantation. *Ren Fail.* 1996;18(1):75-83. doi:10.3109/08860229609052776.
238. Cao W, Chen Y, Han W, et al. Potentiality of α -fetoprotein (AFP) and soluble intercellular adhesion molecule-1 (sICAM-1) in prognosis prediction and immunotherapy response for patients with hepatocellular carcinoma. *Bioengineered.* 2021;12(2):9435-9451. doi:10.1080/21655979.2021.1990195
239. Saverino D, Simone R, Bagnasco M, Pesce G. The soluble CTLA-4 receptor and its role in autoimmune diseases: an update. *Auto Immun Highlights.* 2010;1(2):73-81. Published 2010 Nov 4. doi:10.1007/s13317-010-0011-7.
240. Pistillo MP, Fontana V, Morabito A, et al. Soluble CTLA-4 as a favorable predictive biomarker in metastatic melanoma patients treated with ipilimumab: an Italian melanoma intergroup study. *Cancer Immunol Immunother.* 2019;68(1):97-107. doi:10.1007/s00262-018-2258-1
241. Zhu X, Lang J. Soluble PD-1 and PD-L1: predictive and prognostic significance in cancer. *Oncotarget.* 2017;8(57):97671-97682. Published 2017 May 31. doi:10.18632/oncotarget.18311
242. Belardelli F, Ferrantini M, Proietti E, Kirkwood JM. Interferon-alpha in tumor immunity and immunotherapy. *Cytokine Growth Factor Rev.* 2002;13(2):119-134. doi:10.1016/s1359-6101(01)00022-3
243. Vidal P. Interferon α in cancer immunoediting: From elimination to escape. *Scand J Immunol.* 2020;91(5):e12863. doi:10.1111/sji.12863
244. Tone M, Tone Y, Adams E, et al. Mouse glucocorticoid-induced tumor necrosis factor receptor ligand is costimulatory for T cells. *Proc Natl Acad Sci U S A.* 2003;100(25):15059-15064. doi:10.1073/pnas.2334901100
245. Shimizu J, Yamazaki S, Takahashi T, Ishida Y, Sakaguchi S. Stimulation of CD25(+)CD4(+) regulatory T cells through GITR breaks immunological self-tolerance. *Nat Immunol.* 2002;3(2):135-142. doi:10.1038/ni759
246. Nocentini G, Riccardi C. GITR: a multifaceted regulator of immunity belonging to the tumor necrosis factor receptor superfamily. *Eur J Immunol.* 2005;35(4):1016-1022.

doi:10.1002/eji.200425818

247. Gan X, Feng X, Gu L, et al. Correlation of increased blood levels of GITR and GITRL with disease severity in patients with primary Sjögren's syndrome. *Clin Dev Immunol.* 2013;2013:340751. doi:10.1155/2013/340751
248. Liu Y, Tang X, Tian J, et al. Th17/Treg cells imbalance and GITRL profile in patients with Hashimoto's thyroiditis. *Int J Mol Sci.* 2014;15(12):21674-21686. Published 2014 Nov 25. doi:10.3390/ijms151221674
249. Buzzatti G, Dellepiane C, Del Mastro L. New emerging targets in cancer immunotherapy: the role of GITR. *ESMO Open.* 2020;4(Suppl 3):e000738. doi:10.1136/esmoopen-2020-000738
250. Yan WL, Shen KY, Tien CY, Chen YA, Liu SJ. Recent progress in GM-CSF-based cancer immunotherapy. *Immunotherapy.* 2017;9(4):347-360. doi:10.2217/imt-2016-0141
251. Cook DN. The role of MIP-1 alpha in inflammation and hematopoiesis. *J Leukoc Biol.* 1996;59(1):61-66. doi:10.1002/jlb.59.1.61
252. Zhou X, Yao Z, Yang H, Liang N, Zhang X, Zhang F. Are immune-related adverse events associated with the efficacy of immune checkpoint inhibitors in patients with cancer? A systematic review and meta-analysis. *BMC Med.* 2020;18(1):87. Published 2020 Apr 20. doi:10.1186/s12916-020-01549-2
253. Ben-Betzalel G, Baruch EN, Boursi B, et al. Possible immune adverse events as predictors of durable response to BRAF inhibitors in patients with BRAF V600-mutant metastatic melanoma. *Eur J Cancer.* 2018;101:229-235. doi:10.1016/j.ejca.2018.06.030
254. Li T, Perez-Soler R. Skin toxicities associated with epidermal growth factor receptor inhibitors. *Target Oncol.* 2009;4(2):107-119. doi:10.1007/s11523-009-0114-0